

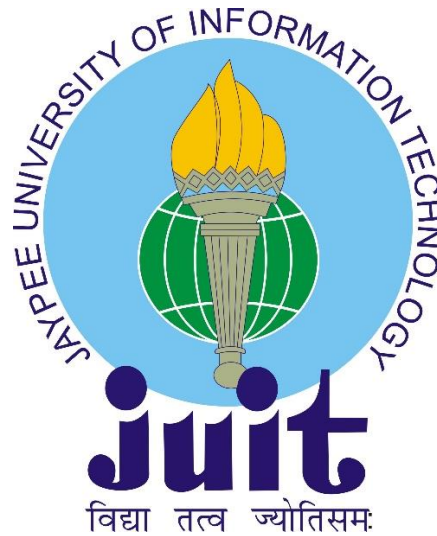
# **DESIGN OF SHARED APERTURE MICROSTRIP PATCH ANTENNAS AND ARRAY FOR L/S-BAND**

*Thesis submitted in fulfilment for the requirement of the Degree of*

**Doctor of Philosophy**

By

**JONNY DHIMAN**



DEPARTMENT OF PHYSICS AND MATERIALS SCIENCE

JAYPEE UNIVERSITY OF INFORMATION TECHNOLOGY

WAKNAGHAT, H.P. (INDIA)

SEPTEMBER 2019

@Copyright JAYPEE UNIVERSITY OF INFORMATION TECHNOLOGY,  
WAKNAGHAT  
SEPTEMBER 2019

ALL RIGHTS RESERVED



# JAYPEE UNIVERSITY OF INFORMATION TECHNOLOGY

(Established by H.P. State Legislature vide Act No. 14 of 2002,  
P.O. Wagnaghat, Teh. Kandaghat, Distt. Solan - 173234 (H.P.) INDIA

Website : [www.juit.ac.in](http://www.juit.ac.in)

Phone No. +91-01792-257999 (30 Lines)

Fax : +91-01792-245362

## SUPERVISOR'S CERTIFICATE

This is to certify that the work reported in the Ph.D. thesis entitled "**DESIGN OF SHARED APERTURE MICROSTRIP PATCH ANTENNAS AND ARRAY FOR L/S-BAND**", submitted by **Jonny Dhiman** at **Jaypee University of Information of Information Technology Wagnaghat, Solan (HP), India** is a bonafide record of his original work carried out under my supervision. This work has not been submitted elsewhere for any other degree diploma.

Prof. Sunil Kumar Khah

Physics and Materials Science

Jaypee University of Information Technology, Wagnaghat, Solan

(HP), India

Date: 30<sup>th</sup> Sept 2019



# JAYPEE UNIVERSITY OF INFORMATION TECHNOLOGY

(Established by H.P. State Legislature vide Act No. 14 of 2002)  
P.O. Wagnaghat, Teh. Kandaghat, Distt. Solan - 173234 (H.P.) INDIA

Website : [www.juit.ac.in](http://www.juit.ac.in)

Phone No. +91-01792-257999 (30 Lines)

Fax : +91-01792-245362

## DECLARATION BY THE SCHOLAR

I hereby declare that the work reported in the Ph.D. thesis entitled "**DESIGN OF SHARED APERTURE MICROSTRIP PATCH ANTENNAS AND ARRAY FOR L/S-BAND**", submitted at Jaypee University of Information Technology, Wagnaghat, India is an authentic record of my work carried out under the supervision of **Prof. Sunil Kumar Khah**. I have not submitted this work elsewhere for any other degree or diploma. I am fully responsible for the contents of my Ph.D. thesis.

  
Jonny Dhiman

Enrolment No.: 146953

Physics and Materials Science

Jaypee University of Information Technology, Wagnaghat, Solan

(HP), India

Date: 30th Sept 2018

*Dedicated*

*To*

*My*

*Parents*



## ACKNOWLEDGMENT

Before acknowledging anyone I would like to thank My Lord and My Parents (Mr. Tara Chand and Mrs. Neelam Devi) for making me who I am today, for always believing in me and supporting me. My gratitude and regard for them are worth more than I can express in words. I thank **Prof. Sunil Kumar Khah**, my supervisor for giving me the opportunity to do Ph.D. under his supervision. I am very thankful to him for his constant support throughout my research work. I would like to thank HOD, Department of Physics and Materials Science, **Prof. P. B. Barman** for his excellent monitoring which always energized me to work hard.

Besides my supervisor, I would like to thank the rest of my doctoral committee: **Prof. Sudhir Kumar Syal, Dr. Vineet Sharma, Dr. Pankaj Sharma**, and for their insightful comments and encouragement, and also for their feedback which incentivized me to widen my research from various perspectives. I also convey my thanks to Dr. Ragini Raj Singh, Dr. Rajesh Kumar, Dr. Surajit Hazra, Dr. Sanjiv Tiwari & Dr. Dheeraj Sharma, and for their cooperation and valuable suggestions.

I extend my gratitude to the founder of Jaypee University of Information Technology Shri Jaiprakash Gaur Ji, Prof. Vinod Kumar (VC JUIT), Maj. Gen. Rakesh Bassi (Registrar JUIT), Prof. Samir Dev Gupta (Director & Academic Head JUIT) for providing me all kinds of facilities to carry out my research work.

I am very thankful to my dear friends **Dr. Neha Kondal, Dr. Priyam Dhani, Dr. Rohit Sharma** and **Dr. Prashant Thakur** for their support and motivation during my entire research work. I am thankful to my seniors Dr. Bandna, Dr. Sarita, Dr. Dikshita, Dr. Hitanshu, Dr. Rajinder Singh, and Dr. Rajender Kumar. I am also thankful to my colleagues Dr. Sampan Attri, Dr. Geetanjali Rathi, Mr. Prince Sharma, Subhash Chand, Pooja Bhardwaj, Dipti Rawat, Anuradha, Shikha Sinha, Ekta, Priyanka Sharma, Neha Luhakhra, Kanchan, Smita Hooda, Sweta Singh, Swati Sharma, Neha, Achyut Sharma, Rajan Sharma, Sanjay Kumar, Raj Kumar, Shiv Kumar & Deepak Sharma for their kind support and help during my Ph.D. work. I would also like to thank our technical staff members Er. Kamlesh Mishra, Mr. Ravendra Tiwari and Mr. Deepak Singh for their cooperation.

I am very much thankful to my parents, my elder sister Ruby and her husband Ajay, my younger sisters Vishakha, Shalini and especially to my life lines Vanshika and Pranvi for their support and motivation during my Doctorate degree. Dear Mom & Dad, you have been there every moment, to make sure my life turned out this way. It is actually impossible to thank you adequately for everything you've done, from loving me unconditionally to raising me to this day.

I wish to express my sincere appreciation to all those who have contributed to this thesis and supported me in one way or the other during this amazing journey.

Lastly, I want to state for any errors that may remain in this work, the responsibility is entirely my own while the expertise in this study belongs to those acknowledged above.

***Jonny Dhiman***

## ABSTRACT

In this thesis, research has been carried out to the study of shared aperture based antenna design for L and S-band. “Cavity model”, being the simplest model that also leads to reactive input impedance, is used for the exploration of “Microstrip Patch Antenna (MPA)” to calculate the resonating frequency, input impedance & other important parameters of various configurations based on aperture sharing of two adjacent bands i.e. L and S bands. First of all, a simple structure using “Dollar” shape is developed to check the feasibility of the two adjacent bands i.e L and S bands on the same aperture. Then, effect of coupling is analysed on two “Dollar” shaped patched antennas placed by each other on the same aperture. This work is presented as a preliminary work in the introduction chapter. To further study, two different configurations of patch antennas are developed based on standard Y-shape. Again the structure is designed using the same surface and placed by each other. After studying the effect of placement of two different configurations i.e. dollar shaped and Y shaped patch antenna, a study is undertaken to investigate the influence of parasitic elements on “Swastika” shaped and “parasitic” antenna based structures using different configurations while using aperture sharing for L/S-band. Next, the aperture sharing method is executed and the influence of notch formation on the resonating frequencies of the patch antenna is deliberated. Finally, analysis of the MPA array based on aperture sharing, again for L/S bands, is presented along with the effect of array formation on the overall antenna parameters such as dimensions, resonating frequency and other properties wherein an attempt has been made to reduce the isolation between two patched antennas while improving the overall bandwidth of the structure.



## TABLE OF CONTENTS

<b>Table of Contents</b>	<b>Page No.</b>
COVER PAGE	i
COPYRIGHT	ii
TABLE OF CONTENTS	iii-iv
DECLARATION BY THE SCHOLAR	v
SUPERVISOR'S CERTIFICATE	vii
ACKNOWLEDGEMENT	ix-xii
ABSTRACT	xiii
LIST OF ABBREVIATIONS	xv
LIST OF FIGURES	xvii-xxi
LIST OF TABLES	xxii
<b>CHAPTER 1 INTRODUCTION</b>	<b>1-28</b>
1.1 Microstrip Patch Antenna	
1.2 Excitation Methods of Microstrip Patches	
1.2.1. Microstrip Line Feed or Edge fed Patches	
1.2.2. Co-Axial Feed	
1.2.3. Aperture Coupled Feed	
1.2.4. Proximity Coupled Feed	
1.3 Methods of Analysis	
1.3.1. Transmission Line Model	
1.3.2. Cavity Model	
1.3.3. Method of Moments (MoM)	
1.3.4. Finite Element Method (FEM)	
1.3.5. Finite Difference Time Domain (FDTD) Method	
1.4 Advantages and Disadvantages	
1.5 Shared Aperture Antenna	
1.6 Statement of Problem	

1.7 Preliminary Work Done	
1.7.1 Feed Point Location of the Designed Antennas	
1.7.2 Dollar Shaped Shared Aperture Antenna	
1.7.3 Results and Discussion	
<b>CHAPTER 2 NON-CONVENTIONAL SHAPED PATCH ANTENNAS</b>	<b>29-78</b>
2.1 Introduction	
2.2 Y-Shaped Patch Antennas	
2.2.1 Results and Discussion	
2.3 Swastika Shaped Patch Antenna	
2.3.1 Results and Discussion	
2.4 Parasitic Patch Antenna	
2.4.1 Results and Discussion	
2.5 Conclusion	
<b>CHAPTER 3 CONVENTIONAL SHAPED PATCH ANTENNAS</b>	<b>79-94</b>
3.1 Introduction	
3.2 Notch loaded square-shaped MPA	
3.2.1 Results and Discussion	
3.3 Plus shape-based shorted MPA	
3.3.1 Results and Discussion	
3.4 Conclusion	
<b>CHAPTER 4 MICROSTRIP ANTENNA ARRAY</b>	<b>95-106</b>
4.1 Introduction	
4.2 Antenna Design	
4.2 Antenna Design	
4.3 Conclusion	
<b>CHAPTER 5 CONCLUSION</b>	<b>107-110</b>
<b>REFERENCES</b>	<b>111-124</b>

## LIST OF FIGURES

Figure No.	Caption	Page No.
Figure 1.1	Schematic view of the microstrip patch antenna	4
Figure 1.2	Common shapes of microstrip patch elements	6
Figure 1.3	Co-axial feed of microstrip patch antenna	7
Figure 1.4	Aperture coupled feed	8
Figure 1.5	Geometry of proximity coupled feed	9
Figure 1.6	Rectangular microstrip patch antenna	11
Figure 1.7.	Basic geometry of Dollar shape-based microstrip patch antenna	23
Figure 1.8	Scattering Parameters for Dollar shape-based patch antenna	25
Figure 1.9	Isolation for Dollar shape-based patch antenna	25
Figure 1.10 (a)	Co-Polar plot for E-Plane	26
Figure 1.10 (b)	Co-Polar plot for H-Plane	26
Figure 1.11 (a)	Cross-polarization plot for E-Plane	27
Figure 1.11 (b)	Cross-polarization plot for H-Plane	27
Figure 2.1	Basic configuration of horizontally placed Y-shapes	33
Figure 2.2	Basic configuration of vertically placed Y-shapes	33
Figure 2.3	Equivalent rectangular patch of Y-shapes	34
Figure 2.4 (a)	Scattering parameters (S11) for horizontally placed Y-shapes	35
Figure 2.4 (b)	Scattering parameters (S22) for horizontally placed Y-shapes	36
Figure 2.5 (a)	Scattering parameters (S11) for vertically placed Y-shapes	36
Figure 2.5 (b)	Scattering parameters (S22) for vertically placed Y-shapes	37
Figure 2.6 (a)	Isolation of horizontally placed Y-shapes	37
Figure 2.6 (b)	Isolation of vertically placed Y-shapes	38

Figure 2.7 (a)	E-plane Co-polarization of horizontal arrangement	38
Figure 2.7 (b)	H-plane Co-polarization of horizontal arrangement	39
Figure 2.7 (c)	E-plane Co-polarization of vertical arrangement	39
Figure 2.7 (d)	H-plane Co-polarization of vertical arrangement	40
Figure 2.8 (a)	E-plane cross-polarization of horizontal arrangement	40
Figure 2.8 (b)	H-plane cross-polarization of horizontal arrangement	41
Figure 2.8 (c)	E-plane cross-polarization of vertical arrangement	41
Figure 2.8 (d)	H-plane cross-polarization of vertical arrangement	42
Figure 2.9 (a)	Basic configuration of Swastika shape-based MPA without parasitic	45
Figure 2.9 (b)	Swastika shape-based MPA with parasitic element	45
Figure 2.10 (a)	Layout of fabricated Swastika shape-based MPA without parasitic	46
Figure 2.10 (b)	Layout of fabricated MPA with a parasitic element ( $L_b + L_v = 113.84$ mm)	46
Figure 2.10 (c)	Layout of fabricated MPA with a parasitic element ( $L_b + L_v = 117.94$ mm)	47
Figure 2.11 (a)	Scattering parameters (S11) of MPA (without parasitic element)	48
Figure 2.11 (b)	Scattering parameters (S22) of MPA (without parasitic element)	49
Figure 2.11 (c)	Scattering parameters of MPA (S11) (parasitic length = 113.84 mm)	49
Figure 2.11 (d)	Scattering parameters of MPA (S22) (parasitic length = 113.84 mm)	50
Figure 2.11 (e)	Scattering parameters (S11) of MPA (parasitic length = 117.94 mm)	50
Figure 2.11 (f)	Scattering parameters (S22) of MPA (parasitic length = 117.94 mm)	51
Figure 2.12 (a)	Isolation between two MPA (without parasitic element)	51
Figure 2.12 (b)	Isolation between two MPA (parasitic length = 113.84 mm)	52
Figure 2.12 (c)	Isolation between two MPA (parasitic length = 117.94 mm)	52
Figure 2.13 (a)	Co-polar data of E-plane (without parasitic element)	53
Figure 2.13 (b)	Co-polar data of H-plane (without parasitic element)	53

Figure 2.13 (c)	Co-polar data of E-plane (parasitic length =113.84 mm)	54
Figure 2.13 (d)	Co-polar data of H-plane (parasitic length =113.84 mm)	54
Figure 2.13 (e)	Co-polar data of E-plane (parasitic length =117.94 mm)	55
Figure 2.13 (f)	Co-polar data of H-plane (parasitic length =117.94 mm)	55
Figure 2.14 (a)	Cross-polar data of E-plane (without parasitic element)	56
Figure 2.14 (b)	Cross-polar data of H-plane (without parasitic element)	56
Figure 2.14 (c)	Cross-polar data of E-plane (parasitic length =113.84 mm)	57
Figure 2.14 (d)	Cross-polar data of H-plane (parasitic length =113.84 mm)	57
Figure 2.14 (e)	Cross-polar data of E-plane (parasitic length =117.94 mm)	58
Figure 2.14 (f)	Cross-polar data of H-plane (parasitic length =117.94 mm)	58
Figure 2.15 (a)	Configuration 1 & 2 of the designed structure	61
Figure 2.15 (b)	Configuration 3 & 4 of the designed structure	61
Figure 2.15 (c)	Configuration 5 & 6 of the designed structure	61
Figure 2.15 (d)	Configuration 7 & 8 of the designed structure	62
Figure 2.16	Basic configuration of the proposed parasitic patch antenna	62
Figure 2.17 (a)	Scattering parameters for configuration_1	64
Figure 2.17 (b)	Scattering parameters for configuration_2	65
Figure 2.17 (c)	Scattering parameters for configuration_3	65
Figure 2.17 (d)	Scattering parameters for configuration_4	66
Figure 2.17 (e)	Scattering parameters for configuration_5	66
Figure 2.17 (f)	Scattering parameters for configuration_6	67
Figure 2.17 (g)	Scattering parameters for configuration_7	67
Figure 2.17 (h)	Scattering parameters for configuration_8	68
Figure 2.18 (a)	Realized gain for configuration_1	68

Figure 2.18 (b)	Realized gain for configuration_2	69
Figure 2.18 (c)	Realized gain for configuration_3	69
Figure 2.18 (d)	Realized gain for configuration_4	70
Figure 2.18 (e)	Realized gain for configuration_5	70
Figure 2.18 (f)	Realized gain for configuration_6	71
Figure 2.18 (g)	Realized gain for configuration_7	71
Figure 2.18 (h)	Realized gain for configuration_8	72
Figure 2.19 (a)	Scattering parameters (S11) of MPA	72
Figure 2.19 (b)	Scattering parameters (S22) of MPA	73
Figure 2.20	Isolation between two MPA	73
Figure 2.21 (a)	Co/Cross polar plot for E-Plane	74
Figure 2.21 (b)	Co polar plot for H-Plane	74
Figure 2.21 (c)	Cross polar plot for E-Plane	75
Figure 2.21 (d)	Cross polar plot for H-Plane	75
Figure 3.1	Basic geometry of notch loaded patch antenna (a) simulated (b) fabricated	83
Figure 3.2	S11 parameters of notch loaded patch antenna in L-band	84
Figure 3.3	S22 parameters of notch loaded patch antenna in S-band	84
Figure 3.4	Isolation between patch antennas (S12)	85
Figure 3.5 (a)	Co-polarization for E-plane	85
Figure 3.5 (b)	Co-polarization for H-plane	86
Figure 3.6 (a)	Cross-polarization for E-plane	86
Figure 3.6 (b)	Cross-polarization for H-plane	87
Figure 3.7	Basic geometry of shorted MPA	89
Figure 3.8 (a)	Scattering parameters (S11) of shorted MPA	89

Figure 3.8 (b)	Scattering parameters ( $S_{22}$ ) of shorted MPA	90
Figure 3.9	Isolation ( $S_{12}$ ) between shorted MPA	90
Figure 3.10 (a)	Co-polarization of notch loaded MPA (E-plane)	91
Figure 3.10 (b)	Co-polarization of notch loaded MPA (H-plane)	91
Figure 3.11 (a)	Cross-polarization of notch loaded MPA (E-plane)	92
Figure 3.11 (b)	Cross-polarization of notch loaded MPA (H-plane)	92
Figure 4.1	Basic configuration of Microstrip antenna array	99
Figure 4.2 (a)	Scattering parameters of smaller/inner MPA array	100
Figure 4.2 (b)	Scattering parameters of larger/outer MPA array	101
Figure 4.3	Isolation between MPA arrays	101
Figure 4.4 (a)	Gain for smaller/inner MPA array (E-plane)	102
Figure 4.4 (b)	Gain for smaller/inner MPA array (H-plane)	102
Figure 4.5 (a)	Gain for larger/outer MPA array (E-plane)	103
Figure 4.5 (b)	Gain for larger/outer MPA array (H-plane)	103
Figure 4.6 (a)	Cross-polarization between two antennas (E-plane)	104
Figure 4.6 (b)	Cross-polarization between two antennas (H-plane)	104

## LIST OF TABLES

<b>Table No.</b>	<b>Caption</b>	<b>Page No.</b>
Table 1.1	Feed–point location of various configurations	22
Table 1.2	Basic parameters of Dollar shape-based patch antenna	24
Table 1.3	Parameters as obtained from simulated results	28
Table 2.1	Parameter values for patch antenna	34
Table 2.2	Parameters values for Y-shape patch configurations	42
Table 2.3	Description and numeric design values of the MPA	47
Table 2.4 (a)	Various parameters obtained from Swastika shaped MPA	59
Table 2.4 (b)	Various parameters obtained from Seven (7) shaped MPA	59
Table 2.5	Description and numeric design values of the MPA	63
Table 2.6	Parameter as obtained from parasitic patch based MPA	76
Table 3.1	Basic parameters of the patch antenna	82
Table 3.2	Basic parameters obtained from MPA	87
Table 3.3	Basic parameters obtained from shorted MPA	93
Table 4.1.	Basic parameters of the patch antenna	99
Table 4.2	Basic parameters obtained from MPA	105

**CHAPTER 1**  
**INTRODUCTION**



Antennas are a crucial fragment of any “wireless communication system”. In today’s situation, although, this is not new for anyone. Understanding the working of this device will certainly benefit the prospective designer to come up with the design of novel structures for the requirements of the wireless antenna/communication system. According to the “IEEE Standard Definitions (IEEE Std 145–1983)” [1], this is well-defined as “a means of radiating or receiving radio waves” [2]. The antennas can be categorized into various types depending upon the basis of material types, design properties and applications [3].

## **1.1 Microstrip Patch Antenna**

Among all antennas, “Microstrip Patch Antenna (MPA)” is becoming more and more useful because of ease of fabrication/printing directly onto a “Printed Circuit Board” (PCB). “Microstrip patch antenna” comprises a radiating element (i.e. “conducting element”) on solitary side of a “dielectric” material (e.g. “FR-4”) that has a “ground plane” (i.e. a conducting element such as “copper or Cu”) on the other side. The radiating or conducting element/patch is typically made up of a conducting substantial such as “copper” (Cu) or “gold” (Au) and can be designed using any shape e.g: “circular”; “triangular”; “rectangular”; “elliptical” etc. MPA radiate mainly due to “fringing” fields among the edges/corners of the radiating section and the ground plane. For worthy antenna concert, a dense “dielectric substrate” with low “dielectric constant” ( $<5$ ) is desired since it delivers greater “efficiency”, larger “bandwidth”, and better radiation, but such confirmation indications to superior antenna size. However, a substrate with a high dielectric constant can be used for the design of a compact MPA, which may result in lower efficiency and “narrower bandwidth”.

Hence, a negotiation must be reached among various constraints of the antenna and its overall performance. Excitation guides the “electromagnetic” energy source to the patch, producing -ve charges around the feed point and +ve charges on the other part of the patch. This variance in charges builds electric fields in the antenna that are responsible for radiations from the patch antenna. These antennas ensure abundant benefits when related to conventional antennas and hence are being used in an extensive diversity of claims approaching: “mobile communication” to “satellite”, “aircraft” and other applications. MPA is becoming very rife indoors the “mobile phone” marketplace. MPA is low cost, have a small outline and are easy to fabricate. The first MPA was proposed in “1953” [4] but didn't

## INTRODUCTION

---

become practical until it was auxiliary established through other investigators [5]. The basic MPA structure is shown below in fig. 1.1.

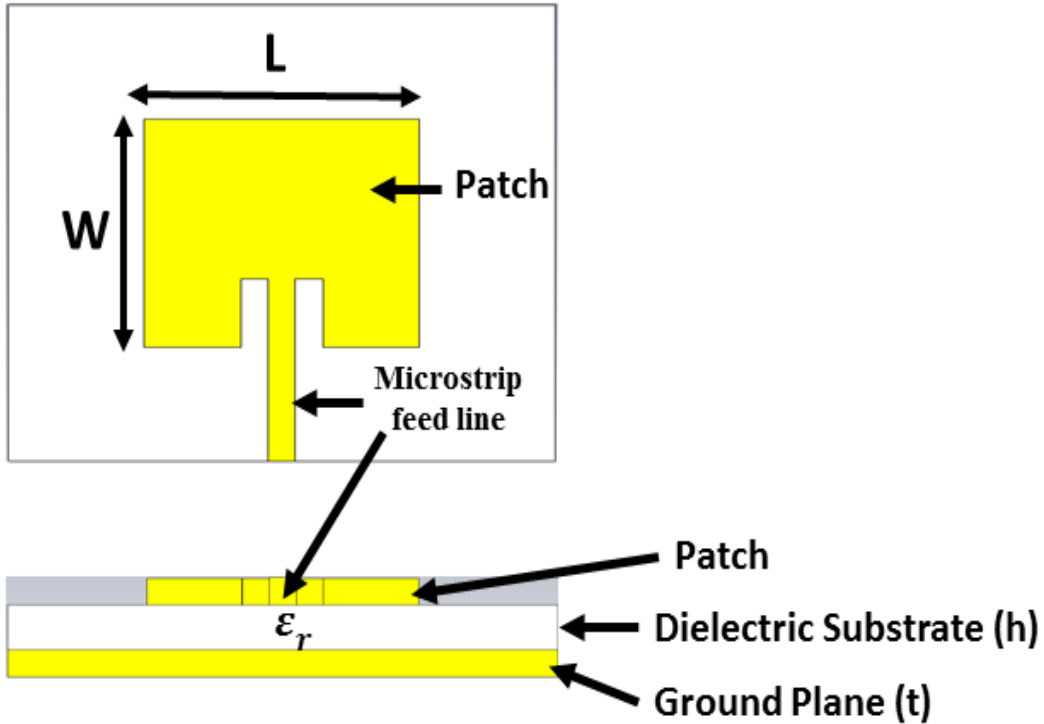


**Figure 1.1** Schematic view of the microstrip patch antenna

The size of an MPA is inversely proportional to its frequency or we can say that the “resonant frequency” of the MPA is the role of its length. The “resonating frequency” of the MPA can be calculated as shown below:

$$\text{Resonating Frequency } (f_r) = \frac{1}{2L\sqrt{\epsilon_r}\sqrt{\mu_0\epsilon_0}} \quad (1.1)$$

The above-mentioned equation does not count the fringing factor, the modified equation in the presence of the fringing factor can be written as:

$$(f_{rc}) = q \frac{1}{2L\sqrt{\epsilon_r}\sqrt{\mu_0\epsilon_0}} \quad (1.2)$$

Where ‘q’ is the fringing factor =  $\frac{f_{rc}}{f_c}$  &  $\epsilon_r$  = Relative permittivity of the substrate material

At frequencies worse than the microwave, MPA doesn't make wisdom as of the sizes essential.

MPA is a narrow band, due to the contrary relationship among the relative permittivity of the substrate being used for the antenna and the bandwidth we get.

Normally the substrate used has permittivity greater than 3.4 which causes a reduction in the bandwidth due to the surface wave propagation. A wide-beam antenna fabricated or designed by etching the antenna section pattern on metal trace attached to an insulating “dielectric substrate”, such as a “PCB”, with a continuous metal layer bonded to the opposite side of the substrate which forms a ground plane (fig. 1.1). Proposal constraints of the antenna can be obtained using formulae [6] as given below.

Width (W) of the patch:

$$W = \frac{c}{2f_o \sqrt{\frac{(\epsilon_{eff} + 1)}{2}}} \quad (1.3)$$

Actual Length (L) of the patch:

$$L = L_{eff} - 2 \Delta L \quad (1.4)$$

Effective Length ( $L_{eff}$ ):

$$L_{eff} = \frac{c}{2f_o \sqrt{\epsilon_{eff}}} \quad (1.5)$$

Length Extension ( $\Delta L$ ):

$$\Delta L = 0.412h \frac{(\epsilon_{eff} + 0.3) \left( \frac{W}{h} + 0.264 \right)}{(\epsilon_{eff} - 0.258) \left( \frac{W}{h} + 0.8 \right)} \quad (1.6)$$

$$\text{Effective Dielectric Constant } (\epsilon_{eff}) = \frac{\epsilon_r + 1}{2} + \frac{\epsilon_r - 1}{2} \left[ 1 + 12 \frac{h}{W} \right]^{1/2} \quad (1.7)$$

Where:

$f_o$  is the resonant frequency

$h$  is the height of the dielectric substrate

$\epsilon_r$  is the relative permittivity of the dielectric substrate

$c$  is the speed of light

## INTRODUCTION

---

MPA emit mainly due to “fringing fields” among the edges of the patch & the ground plane. For better antenna performance, a thick “dielectric substrate” having a low dielectric constant is desirable since this provides better “efficiency”, larger “bandwidth” and better “radiation” [2]. However, such a configuration leads to a larger antenna size. In order to design and/or fabricate a compact MPA, the higher dielectric constant must be used which are less efficient and resulting in the narrow bandwidth. Hereafter a negotiation should be grasped amid antenna “parameters” (or “dimensions”) along with its overall functioning/operation. Various shapes of the MPA are depicted below in fig. 1.2.

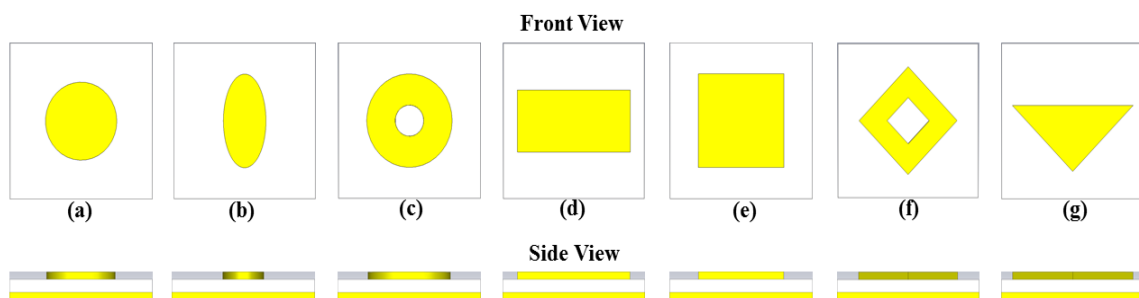


**Figure 1.2** Common shapes of microstrip patch elements

### 1.2 Excitation Methods of Microstrip Patches

The method by which a “microstrip patch antenna” is excited defines the feasible “impedance bandwidth” (ultimately), the clarity and path of the “radiated fields”, the “efficiency” of the entire antenna, the comfort of construction/building of the antenna and its validity. There are numerous means available to feed or spread electromagnetic energy to a “microstrip patch antenna”. The supreme widespread feeding approaches are the “Microstrip Line Feed”, “Co-axial-Fed”, “Aperture-Coupled” and “Proximity-Coupled” [8] and are explained below.

#### 1.2.1. Microstrip Line Feed or Edge fed Patches

Here, a “conducting strip” is coupled directly to the edge site of the MPA (fig. 1.1). The said strip is small in size (i.e. “width”) when compared with patch and has numerous benefit such as feed can be engraved on to the identical substrate to deliver a two-dimensional assembly. For “impedance matching” among the antenna input point and feeding line, sometimes we need to join feed line not at the edges but somewhere close to the midpoint of the radiating section (fig. 1.1). This is so, because, at the edges of the patch, it acts as an open circuit,

giving infinite impedance. While on the other side at mid of the patch, due to short circuit, it will behave as zero impedance. So, we connect this feed line between these two points. The reason behind inset cut with the patch is for “impedance matching” of the feed line with MPA without supplementary matching factor. This is accomplished by appropriately adjusting the inset site. Hence this is a stress-free feeding scheme, due to comfort of assembly and ease in modeling as well as impedance matching.

### 1.2.2. Co-Axial Feed

For feeding an MPA the “coaxial feed” may be a quite common practice being used. Here the innermost conductor of the “coaxial” connector is pierced/encompasses thru the “dielectric substrate” (fig. 1.3) and is coupled to the radiating section, while the external conductor is coupled to the ground surface. One of the convenience of using “co-axial feed” is that this can be placed/located at any preferred position on the patch exterior, for input impedance matching. The scheme is stress-free during fabrication along with low unauthentic radiation. However, its major shortcoming is: “narrow bandwidth” and difficulty to model due to drilling of a hole in the substrate along with the connector sticks out exterior to the ground plane, thus not building it wholly planar for dense substrates (“ $h > 0.02 \lambda_0$ ”).

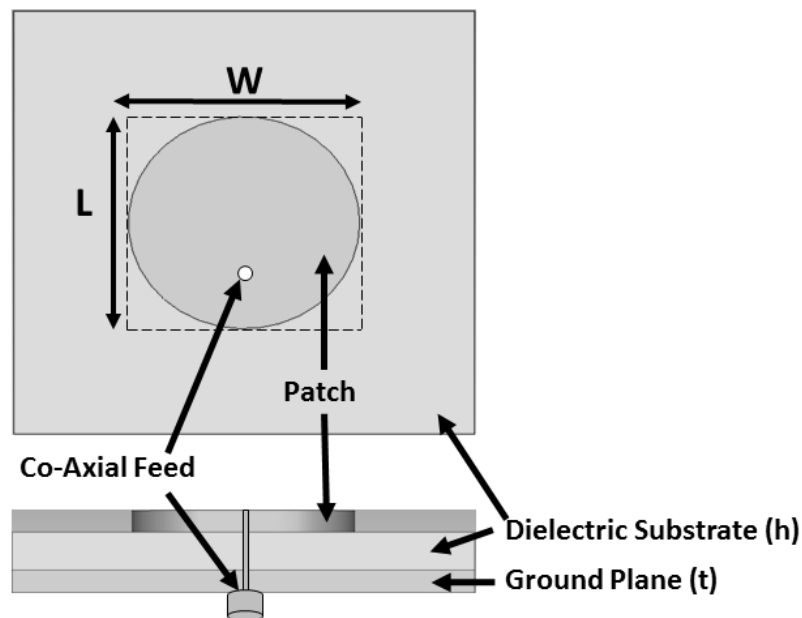


**Figure 1.3** Co-axial feed of microstrip patch antenna

## INTRODUCTION

---

### 1.2.3. Aperture Coupled Feed

Here, the “radiating patch” along with the “microstrip feed line” is disjointed by the ground plane (fig. 1.4). The twinning (or coupling) within the radiating patch and the above mentioned “feed line” is prepared thru a slot or an aperture in the said ground exterior. The twinning aperture is most often pored within the patch, consequential in less cross-polarization due to the regularity of the conformation. The twinning quantity (i.e. among “feed line” & “patch”) is estimated by the “shape”, “size” etc., along with the aperture location. As the radiating patch and the feed line are separated via ground plane, thus spurious radiation is minimalized and provides constricted bandwidth. Usually, separate “dielectric” material (having prominent “dielectric constant”) is used for the back-side substrate and another substrate (having large thickness with a low “dielectric constant”) is castoff for the upper-side substrate for the augmented radiation from the said radiating section. The foremost shortcoming of this feed procedure is the struggle while assembly due to numerous layers, resulting in increased thickness of the MPA.

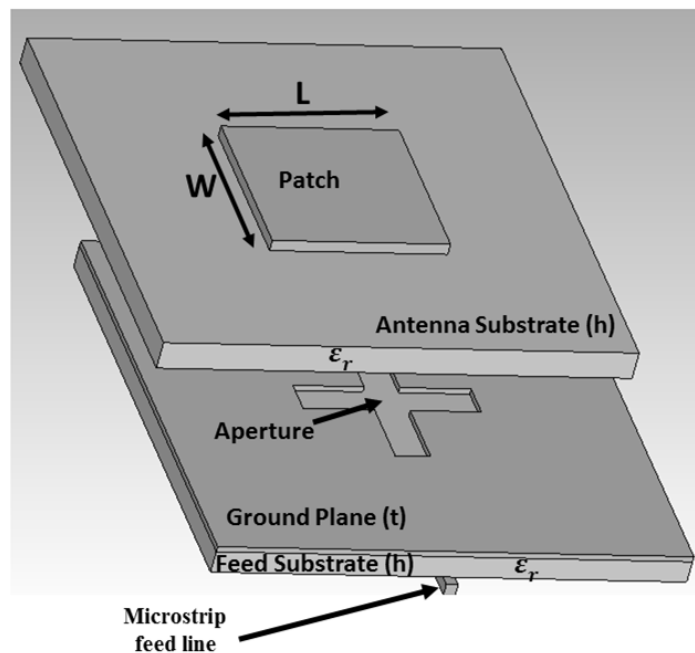


Figure 1.4 Aperture coupled feed

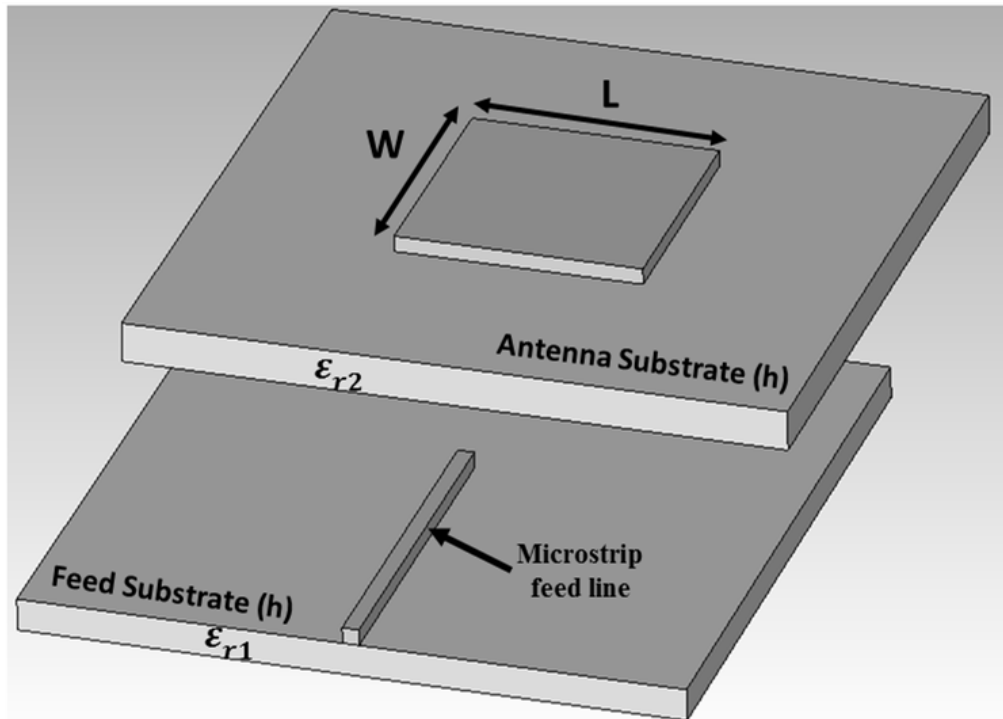


Figure 1.5 Geometry of proximity coupled feed

#### 1.2.4. Proximity Coupled Feed

Proximity coupled (or “electromagnetic coupling system”) comprises two dielectric substrates (fig. 1.5) i.e. the feed line along said 2-substrates, while the radiating section is on to the top of the upper-most substrate. It basically abolishes “spurious feed radiation” and offers larger bandwidth (as great as “13%”), due to a whole growth in the complexity of the “MPA”. This arrangement also offers varieties among dual dielectric materials, solitary for the radiating section and one for the “feed line” to improve the distinct acts.

### 1.3 Methods of Analysis

There are numerous methods of analysis for MPA. Few of them are [7]:

- Transmission-Line (TL) model
- Cavity Model
- Method of Moments (MoM)
- Finite Element Method (FEM)
- Finite-Difference Time Domain (FDTD)

## **INTRODUCTION**

---

The “transmission-line model” is the easiest among all, giving worthy physical understanding, but less precise & is more problematic to ideal twinning. The “cavity model” is more precise when equated with the “transmission-line model”, but more difficult. Though, it also gives worthy physical understanding and is somewhat problematic to model twinning. In wide-ranging, when useful appropriately, the “full-wave models” (which comprise principally “Moment Method”) are very truthful, very flexible, and can treat single elements, “finite and infinite arrays”, “stacked” elements, “arbitrarily shaped” elements, and “coupling”. Still, they remain the supreme difficult prototypes and typically contribute to fewer physical understanding.

### **1.3.1. Transmission Line Model**

The “Transmission Line (TL)” model demonstrating the “rectangular patch” as two slots, separated by a low “impedance ( $Z_c$ ) transmission line” of length  $L$ . The TL method is the easiest way to analyse the “MPA”. Results we acquire are not the finest precise associated with other methodologies but it is worthy abundant to scheme the antenna. In this model, the “rectangular microstrip antenna” comprises of a “microstrip transmission line” with a pair of loads. An “MPA” with a four-sided metallic radiating section of width (“ $W$ ”) and length (“ $L$ ”), disconnected by a distance  $h$  with a “dielectric” material between the ground plane and the patch (fig. 1.6). The radiation invents from the “fringing” electric field at either terminal of the radiating section of the antenna. These terminals are called radiating ends/terminals & the former two sides (parallel to the  $y$ -axis) are non-radiating ends/terminals. “Fringing” fields due to two radiating edges can be viewed as the two ends of the antenna of dimensions between ‘0’ and ‘ $W$ ’ and non-radiating dimensions lying between ‘0’ and ‘ $L$ ’. The patch antenna is fed with the feed point located such that it is picked to tie the antenna with desired impedance.

- Fringing Effects

The determination of the “MPA” are inadequate alongside the width & length, so the fields at the ends of the radiating section undergo “fringing”. This is demonstrated beside the length (“fig. 1.6”) for the two radiating slots of the “MPA”. The quantity of “fringing” is a role of the various constraints of the radiating section and the thickness/height of the substrate. For the primary E-plane (“ $xy$ -plane”) fringing is a function of ratio for the length of the radiating section to the height of the substrate ( $L/h$ ) and the “dielectric constant ( $\epsilon_r$ )” of the substrate. Since for MPA the “ $L/h \gg 1$ ”, thus fringing is contracted and it affects the resonant

frequency of the antenna. Due to the “fringing effect”, some of the waves travel in the substrate and some in the air, an effective dielectric constant “ $\epsilon_{\text{eff}}$ ” is familiarised to account for this influence. The effective “dielectric constant” is defined for a constant dielectric substance so that the electric field lines have the same electrical appearances, mainly propagation constant, as the authentic field line. The operative “dielectric constant” is ultimately invariant for low frequencies. At midway frequencies, its values begin to upsurge monotonically and ultimately approach the beliefs of the “dielectric constant” of the substrate.

### 1.3.2. Cavity Model

The “cavity model” is centered on the hypothesis that the section amid the radiating section and ground plane is a resonance opening constrained by ceiling and floor of electric “conductors” and magnetic parapets beside the terminal/edge of the “conductor” (fig. 1.3). The hypothesis overhead is constructed on the opinion of: a). there are only 3-field constituents in the district encircled by the opening: E-component in the z-axis (“ $E_z$ ”) and 2-constituents of “H” along the x and y-axis (“ $H_x$ ”, “ $H_y$ ”). b). since h (“height of the substrate”) is very tinny (“ $h \ll \lambda$ ”), this field in the central section do not fluctuate with “z-coordinates” for all frequencies. c). the electric current in the MPA has no section normal to the end of the radiating section at any point. This model is reasonable in learning the microstrip resonators with the end spreading somewhat to an explanation for the “fringing” field.

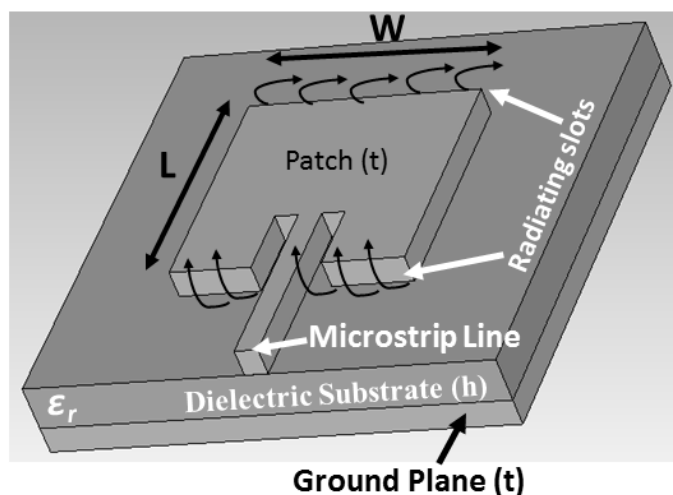


**Figure 1.6** Rectangular microstrip patch antenna

## **INTRODUCTION**

---

During coupling of MPA with a “microwave” origin, charge spreading will be recognized on the top-most as well as down-most plane/surface of the antenna. The charge spreading is typically organized by “attractive” and “repulsive” ways. The strength of attraction is amid the dissimilar charges on the radiating section and on the ground section, a “current density” is created at the lower-most side of the said radiating section and within the said dielectric. The repulsive strength amid the like charges drive the charges from the lower-most of the radiating section around the ends of the radiating section to the top of the said radiating section, this will craft the current density.

In case of MPA (“ $W \gg h$ ”) the attractive force supervises and charges focus within the dielectric below the radiating section, and the flow of current nearby the end can be abandoned as it falls as the ratio (“height to width”) falls down. This would permit the 4-sidewalls to be modeled as pure magnetic conducting sections which preferably would not disrupt the magnetic field and in turns the electric field spreading below the radiating section. This good estimate to the “cavity model” leads us to deal with the side walls as flawless magnetic conducting walls.

The “cavity model” is further realistic than the “transmission line model”. For substrate depths superior to “ $0.03 \lambda_0$ ” it is intensely endorsed not to use either estimated scheme as invalid forecasts are normal. Yet again the “cavity model” is beneficial for attaining “ball-park” figures on what material should be used and expected quantities of the radiating section. Classically we practice any of these probable means (if possible the “cavity model”) as a formerly policy iteration earlier using a supplementary demanding investigation tool. The “cavity model” does grip contactless feed radiating section solutions (e.g. “aperture coupled patch”) more precisely as associated with thru contact fed (e.g. “probe fed”) radiating section.

### **1.3.3. Method of Moments (MoM)**

In the “MoM”, the outward current is castoff to model the MPA, and volume divergence currents in the dielectric segment are castoff to model the fields in the dielectric segment. An essential equation is expressed for the unidentified currents on the MPA and the feed lines alongside with their pictures in the ground sections. The integral equations are converted into arithmetic equalities that can be certainly explained using a CPU. This

method profits into account the “fringing fields” exterior the physical boundary of the 2-dimensional radiating section, accordingly providing a supplementary precise resolution.

#### **1.3.4. Finite Element Method (FEM)**

The “FEM” is appropriate for volumetric engagements. Here the region of concern is distributed into any numeral restricted planes/volume components reliant upon the 2-D or 3-D constructions to be investigated. These discretized elements mostly denoted to as restricted fundamentals, can be any well-defined conformation frameworks such as prismatic sections for 3-D conformation and triangular sections for 2-D configurations and tetrahedral, and are proper for curved frameworks. It comprises the incorporation of approximately simple functions over the complete conducting section, which is spread into numeral subsets. The problem of resolving wave equations with inhomogeneous margin circumstances is attempted by disintegrating it into 2-edge value difficulties, one with Laplace’s equation having inhomogeneous borderline while other methodologies inhomogeneous wave equivalence beside with homogeneous margin form.

#### **1.3.5. Finite Difference Time Domain (FDTD) Method**

The “FDTD” process is well-suited for MPAs, as it can suitably model plentiful organizational inhomogeneity stumble upon in these conformations. It can also anticipate the reaction of the MPA over the widespread bandwidth thru a solitary model. Here, spatial as well as a time lattice for the electric and magnetic fields are twisted over which the resolution is mandatory. The spatial discretization besides “Cartesian coordinates” are reserved to be indistinguishable. The E-cell restrictions are conglomerated with the edge of the conformation and H-fields are acknowledged to be located at the intermediary of each E-cell. Each cell encirclements data about significant personalities and the cells incorporating the basics are whole-hearted with an appropriate excitation means, which propagates sideways the structure.

The discretized time dissimilarities of the fields are determined at anticipated points. Using a line integral of the electric field, the voltage thru the two (2) localities can be accomplished. The current is computed by a loop integral of the magnetic field immediate the conductor, where the Fourier transform produces a frequency comeback.

## **INTRODUCTION**

---

### **1.4 Advantages and Disadvantages**

Due to the low-profile structure of the MPA, it is raising in reputation for practice in wireless claims. Therefore, they are tremendously well-matched with entrenched antennas in “handheld wireless devices” such as “cellular phones”, “pagers”, etc. The telemetry & “communication antennas” on “missiles” requisite to be tinny and conformal so are MPA. MPA has been fruitfully used in “satellite communication”. Few of the benefits [2-3] and drawbacks [6-7] are given below.

#### ***Advantages:***

- Light-weight & low volume
- Low profile planar configuration
- Low cost
- Supports linear as well as circular polarization
- Ease of integration with microwave integrated circuits (MICs)
- Dual and triple frequency operations
- Mechanically robust

#### ***Disadvantages:***

- Narrow bandwidth
- Low efficiency
- Low Gain
- Extraneous radiation from feeds and junctions
- Poor end-fire radiator except tapered slot antennas
- Low power handling capacity
- Surface wave excitation

### **1.5 Shared Aperture Antenna**

The demand for progressively more sophisticated antenna has grown while space and weight restrictions have become more rigid. These two factors resulted in a strong need to diminish the number of linked antennas by aggregating the performance of multi-arrangements into a solitary antenna. The core objective is the “multifunctionality” of the antenna classifications, which led to the involvement of aperture. The “aperture sharing” has been the topic of

investigation readings in modern ages. It comprises of a gathering of fundamental radiators that can be unified simply or in an antenna array conformation. In aperture sharing, one can use alike radiators or dissimilar radiators. However, the whole design rest on our elementary necessity, i.e. approach of operation or application foundation.

As “shared aperture” scheme collaborates the functionality of a several of antennas on a solitary aperture, thus grants a sum of nominal experiments. The numeral ways can be executed for “aperture sharing” (such as “time-multiplexing” or “frequency-multiplexing”, etc.) one can elect any of these ways based on the existence of twinning/coupling amid antennas. However, if the twinning is insignificant, then the “aperture sharing” can be applied independently, i.e. we can use all antennas at the same time. For example, in “RADAR” tasks, which comprises periodic, automated broadcasts and receptions: consequently, when the “RADAR” is not functioning, the aperture could be used for other functions (time/frequency permitting). This is previously realistic in modern “RADAR’s” where single apertures performing numerous responsibilities such as searching, tracking, illumination, etc. Another straightforward methodology is to fragment a superior aperture into sub-apertures, each executing a definite part. “Shared aperture” improvement was primarily discussed in the 1990s [9]. In 1998 [10] another “dual-Frequency and Dual-polarization MPA” was presented for space-based “Synthetic Aperture Radar” (SAR) applications. Since then same technology is being used for many claims, such as “dual-polarization” [11], “broadband array antennas” [12], mobile “DBS” applications [13], “wideband” applications [14], etc. Some of which are discussed below:

“Dual-band and dual-polarized” [15-20] antenna were presented based upon shared aperture method. In [21-23] shared aperture method based antennas were presented for “Synthetic Aperture Radar” (SAR) application. The sparse antenna approach was also presented using shared aperture method for wideband applications [24] and broadband arrays [25] antennas. In [26] a cavity-backed patch shared aperture antenna array approach for mobile DBS applications was presented. In [27] differently sized elements were presented in the form of shared aperture antennas. In [28], a humble practice was unfilled to cultivate “dual-feed dual-polarization” based aperture coupled MPA for L-Band. A circularly polarized [29-30] antenna configuration was also proposed using the same technique. A unique “self-similar antenna” design for “dual-band phased array” configuration [31] is also available in the literature. Another “shared aperture” millimeter-wave antenna using “3D SIW technology”

## **INTRODUCTION**

---

[32] is also available resonating at 28 GHz and 75 GHz. A few years ago two wideband MPA arrays [33] sharing a common aperture were designed for GSM and UMTS deployments.

In 1996 Axness, T.A., et al. [9] firstly disclosed the development in the “Shared Aperture Technology” (SAT) and exposed the benefits of the same for the future purpose such as size, weight, cost, etc. The author described radiating as well as receiver module while using SAT. Where the “radiating element” is the wideband dual-polarized tapered notch element (radiate in between of 7 to 14 GHz) and the receiver module is a dual-channel monolithic microwave integrated circuit. In addition, to which, the author also described the shared aperture array-based receiver concept (arrangement of 64-element receive array for 7 to 10 GHz) resulting in maximum functionality of the “SAT” concept. In addition to that, the separate array concept was also proposed by the author for the radiating elements with some isolation in between of them (i.e. receiver and the radiator).

In 2001 Pozar, D.M., et. al., [15] represented a “shared-aperture based multilayer geometry of microstrip array structure for dual-band and dual-polarization”. The designed structure comprises aperture coupled patches for X-band (i.e. 8.0 - 12.0 GHz) along with proximity coupled perforated patches for L-band (i.e. 1.0 - 2.0 GHz). The whole structure was designed using multiple subarray based structures, resulting in a larger design. The basic layout of the antenna comprises L-band patches (“2\*2 array”) and X-band patches (“12\*16 array”).

In 2009, Meng. M., et.al. [34] represented the design of a “multilayered shared-aperture based dual-band dual-polarized (DBDP) microstrip antenna” for L and C bands. The elements for L-band are nominated as perforated sections to empower the settlement of C-band sections within them such as perforated L-band sections are enclosed by 16 C-band radiating sections, forming a unit cell. The center frequencies of the designed antennas were of the ratio of 1:4 (i.e. resonating at 1.25 GHz and 5.3 GHz respectively) along with good performance on both bands.

In 2011, Chakrabarti. S., [28] represented a “simple and broadband dual-polarized shared aperture antenna comprising a uniformly excited 4\*2 shared aperture dual-feed array antenna resonating in L-band”. The designed antenna achieved a high gain (up to 14 dBi), a high degree of isolation amid the ports beside with a great degree of cross-polarization due to which the antenna is suitable for different communication applications.

In 2012, Dastkhosh, A.R., et.al., [35] represented a “wideband high gain dual polarized slot array patch antenna for WiMAX applications resonating at 5.15–5.9 GHz frequency band”. The elementary assembly of the antenna comprises an array of the 8\*8 antenna and two four-sided slots are used for coupling the “microstrip feed lines” to the radiating section. Some optimization was accomplished with the measurements of the radiating section such as slots, feed lines, “circular patch”, and spaces amid them to attain finest radiation characteristics, wide impedance bandwidth, and high isolation between two ports. The designed antenna achieved a high gain (up to 26 dBi) and wide bandwidth (i.e. 14%).

In 2013, Naishadham, K., et.al. [36] represented a “dual-band planar array with self-similar printed folded dipoles based on shared aperture technique”. The designed antenna structure comprises a nested element printed dipole (with individual feeds) array along with “self-similar elements” for dual-band phased array job. The structure provides adequate isolation between the channels. The resonating frequencies of the designed antenna are 1GHz (with a gain of 12 dBi) and at 2 GHz (with a gain of 16 dBi) and comprises the cross-polarization superior to -25 dB.

In 2013, Sharma, D.K., et.al., [19] represented a “dual-band dual polarization microstrip patch antenna using a shared aperture technique for L&S bands”. A “square ring-shaped radiating element” is aimed for L band (1.25 GHz) and alternative square formed radiating element printed on different dielectric substrate films is retained within the square ring resonates at S-band (2.5 GHz). The performance of the intended antenna is elevated for 10 dB return loss bandwidth of 28.8% and gain of 7.22 dB for L band and return loss bandwidth of 29.4% and gain of 7.11 dB for S-band.

In 2013, A. B. Smolders, et.al., [30] represented a “dual-frequency circularly polarized microstrip array antenna using shared aperture”. The basic prototype of the antenna comprises a 2x2 array of “aperture coupled microstrip antennas (ACMAs)” with conforming feed grid functioning at 4.1 GHz (gain of 5.1 dBi) and 6 GHz (gain of 5.4 dBi) and isolation superior to 26 dB. The antenna can be cast-off as a structure block in “full-duplex wireless communication” claims e.g. wireless connectors as well as “focal-plane arrays for satellite internet (VSAT)”.

In 2013, Shi-Gang Zhou, et. al., [37] represented a “wideband, low profile P- and Ku-band shared aperture antenna with high isolation and low cross-polarization”. The basic structure

## **INTRODUCTION**

---

comprised a P-band (330-420 MHz) microstrip patch antenna along with an 8x8 aperture coupled patch array structure for Ku-band (14.27-16.20 GHz). The P-band antenna (bandwidth of 24%) was fed via L-shaped probe feeding and acted as a ground surface as well as a reflector for the Ku-band antenna, whose bandwidth is 13%. The cross-polarization was superior to -20 dB & -26 dB for P-band and Ku-band respectively. The overall gain was 6.5 dBi to 7.5 dBi for P-band and from 22.5 dBi to 23.5 dBi for Ku-band.

In 2016, Mingde, Du., and Songlin, Shuai., [38] filed a patent (US publication number: 10,003,132) which described a shared-aperture antenna and a base station, to resolve the problem of aperture sharing. The basic structure of the antenna comprising a first and second “microstrip antenna array” configurations. The first antenna array conformation comprised rows of “microstrip patch antenna” units. The second antenna array encompassed parallel placed antenna units (double-frequency antennas) and was disposed in between the first microstrip antenna array. The “microstrip patch antenna” units of the first and second array structures were configured to fit on to the surface of the dielectric substrate resulting in aperture sharing based configuration. Both the configurations were designed to resonate in two different frequencies.

In 2017, P.H. Rao, et. al., [39] represented a “multiband multi-polarization shared-aperture antenna”. The configuration comprised numerous planar antennas positioned side by side in a single footprint, such as (a) L “probe-fed”, suspended-plate and horizontally polarized antenna resonating in a 900-MHz band. (b) An “aperture-coupled”, vertically polarized, MPA resonating at 4.2 GHz. (c) a 2x2 MPA array resonating in X-band. (d) low “side-lobe level (SLL)” corporate-fed, 8x4 MPA planar array resonating in X-band for SAR. And (e) a printed “single-arm”, circularly polarized, titled-beam spiral antenna functioning at the C band were integrated into a single aperture for concurrent tasks. The antenna positions were optimized to obtain a coupling coefficient of better than -30 dB in all the cases.

In 2017, V. K. Kothapudi, and V. Kumar, [40] represented a “single layer dual-band dual-polarized (DBDP) S/X-Band series-fed shared aperture antenna for SAR applications”. A configuration comprised four-groups of 2x2 subarrays were designed to resonate in X-band. The inner element of the 2x2 subarray was etched off and the structure was transformed into a 1x2 array. Thus the space available after removing the element was further utilized to design another structure of a single square-shaped element fed with microstrip line

resonating in S-Band. The inner square-shaped antenna was resonating at 3.2 GHz with a bandwidth of 9.3% along with the gain of about 8.42 dBi and the outer structure was resonating at 9.3 GHz having a bandwidth of 1.72% along with the gain of around 10.6 dBi. The isolation was better than 30dB.

## **1.6 Statement of Problem**

Since MPA has numeral benefits when compared with conventional microwave antennas. Thus, cover many applications, i.e., broad frequency ranges from a few MHz to GHz with few advantages such as light-weight and low cost. In addition to that MPA also have some limitations if we compare with conventional microwave antennas. Such as narrow bandwidth and poor efficiency (for a substrate thru great dielectric constant), low gain, high cross-polarization and joint twinning in case of array structures. In addition to these, one more problem while working with MPA is, we need a separate antenna for separate applications, since it is not easy to use the same MPA for another application. To cover this problem, we can refer to the shared aperture technique as discussed above. Using this technique we can design a number of MPA's on the same substrate and use them simultaneously as per our requirement. Which leads to less space requirement and low cost. From literature, we come to know that MPA resonating at L/S bands were designed by few researchers [19, 22, and 31], working with L/S band simultaneously using the aperture sharing. This is due to various difficulties such as narrow bandwidth and low frequency range in the L/S band, as L-band ranges from 1-2 GHz, while the S-band from 2-4 GHz adjacent to each other.

The scope of the thesis is to design a shared aperture method based MPA for L/S Band. It first deals with the characteristics of MPA resonating in L and S-band separately. Since the range of L-band is very less (1 GHz only), giving less bandwidth. On another side, S-band is adjacent to L-band, with 2 GHz frequency range again giving less bandwidth. If we design antenna resonating in these two bands, the biggest problem is the antenna size due to adjacent frequency bands, which provides significance difference in the size of MPA. While, the same is beneficial too, because of comparative sizes, giving almost the same sized substrate area. The size of the overall patch antenna depends on the wavelength and another factor, so it is easy to design patch antenna with a larger frequency ratio. But, here we represented MPA with a frequency ratio of 1:2, which was not designed till now while using the same aperture. In literature, the stacked patch antennas were represented, which

## **INTRODUCTION**

---

are easy to design, for the resonating frequencies in two different bands. But they are not truly based on aperture sharing, because not using the same surface. In the present thesis, all the structures are using the same surface for the frequency of operation in L/S-band simultaneously and separately for different patches. The outline of the thesis comprises various chapters including the 1<sup>st</sup> chapter (named as Introduction), which represents preliminary work based on dollar shaped MPA along with other work, which is represented in the next chapters. The detailed work is represented in thesis as under.

Chapter 2<sup>nd</sup> presents the Y-shaped patch antenna designed using the same surface, which is in the continuity of the preliminary work. Further, the effect of the parasitic patch using shared-aperture method for “Swastika” shaped patch and notch loaded rotated square shapes patch antenna is also discussed in this chapter. Effect of the parasitic patch is observed on both bands.

Chapter 3<sup>rd</sup> presents analysis and study of two topics consisting of shorted MPA based on shared aperture method. One of these shorted MPA consisting of notch loaded patches, while other is without notches.

Chapter 4<sup>th</sup> present the 2x2 array-based MPA, where two different arrays are designed and analyzed for L/S bands. One array designed inside the other one following the shared aperture technique.

Chapter 5<sup>th</sup> presents the conclusion and future scope.

## 1.7 Preliminary Work Done

In this section the feed point location of the proposed antenna is described along with simulated design of a Dollar shape MPA for L & S-band.

### 1.7.1 Feed Point Location of the Designed Antennas

Feed Location plays an important role in MPA specially for impedance matching of the feeding element with the resonating structure. The normalized impedance (i.e. “50 ohm”) can be achieved by defining a proper feed location in MPA. In this thesis, the antenna feed location was calculated for an equivalent square shape based patch antenna using standard equations. In this work, we have designed all antennas using coaxial feed. The “MPA” can be fed by a diversity of means and are categorized into two types: contact-based and non-contact based. In the contact-based scheme, the RF power is fed directly to the radiating patch by means of a connecting feed. “Electromagnetic field” coupling is finished to transfer power amid the “microstrip line” and the radiating patch in the non-contact based arrangement. In this procedure, a conducting strip is straight associated with the radiating section which is reduced in measurement as associated to radiating section. It is very easy to assemble, very modest in demonstrating and matches with characteristic impedance “50 Ω”.

$$\text{Length of the substrate } (L_s) = L + 6h \quad (1.7)$$

$$\text{Width of the substrate } (W_s) = W + 6h \quad (1.8)$$

Where, L, W and h are already described in equations (1) & (2). Now, the feed point location can be calculated using formula as given below:

$$\text{Feed point location in x-axis from length of the patch } (x) = \frac{L}{2\sqrt{\epsilon_{eff}}} \quad (1.9)$$

$$\text{Feed point location in y-axis from width of the patch is } (y) = \frac{W}{3\sqrt{\epsilon_{eff}}} \quad (1.10)$$

This can accomplish by appropriately monitoring the insertion situation. “Microstrip line feed” is revealed in below fig. 1.1 & the structure of “coaxial feed” is shown in fig. 1.3. In this technique, the exterior conductor of the “coaxial” cable is associated to the ground plane, and the epicenter conductor is protracted up to the radiating section. The feed can be positioned anyplace privileged the patch to match with its input impedance. The effective length and width of the substrate can be premeditated using eq. (1) & (2). Initially, feed

## INTRODUCTION

---

location was calculated for a square as well as a circular patch antenna with defined dimensions. Later on, some optimization was performed to obtain the final desired structure and shape along with the feed point situation to obtain the final feed locality. The optimized feed location of various designed structures (as represented in the next chapters) is shown in table 1.1.

**Table 1.1** Feed–point location of various configurations

<b>Configuration</b>	<b>L-Band feed location</b>	<b>S-Band feed location</b>
Dollar-shaped (preliminary work)	x = 18.56; y = -11.5	x = -19.5; y = 6.61
Horizontally arranged Y-shapes	x = 24.05; y = -4.59	x = -24; y = -9.76
Vertically arranged Y-shapes	x = -4.61; y = 30.00	x = 3.62; y = 32.24
Swastika Shaped	x = 34.40; y = -1.14	x = 52.98; y = 54.25
Parasitic Patch Antenna	x = -12.00; y = 20.00	x = 20.83; y = -20.00
Notch loaded square shaped MPA	x = 10.95; y = 4.69	x = -5.78; y = 27.68
Plus shaped shorted MPA	x = 10.95; y = 4.69	x = -14.00; y = 39.00
Microstrip Antenna Array	x = 8.00; y = 5.00	x = 16.90; y = 15.33

### 1.7.2 Dollar Shaped Shared Aperture Antenna

While working on MPA using aperture sharing antenna size and shape need to be chosen carefully, because the frequency ratio of different bands/antennas plays an important role. Most of the design represented in literature is with the frequency ratio of 1:4 or more (while using aperture sharing), where antenna sizes are comparatively large. But while working on frequency ratio 1:2, MPA size is comparatively almost same or with little bit difference.

Which creates difficulty while designing antennas for the frequency ratio of 1:2 such as for antennas resonating L/S-Bands simultaneously. Firstly we tried to design a dollar shape-based patch antenna for study/testing purpose and to check whether it is feasible to design antennas for L-band and S-band using aperture sharing or not. Two “Dollar” shape-based patch antennas with different size were placed beside each other on the same surface to study the frequency of resonance along with coupling.

The basic design comprises “Dollar” shapes placed parallel in a horizontal arrangement on the surface of the substrate. The antenna was designed and investigated using “copper” as conducting medium and FR-4 (“ $\epsilon_r=4.3$ ”) as a dielectric substrate. The distance among two shapes directly disturbs the coupling between them, so an appropriate gap was maintained after optimization for minimum coupling. The elevated measurements of the antennas are exposed in table 1.2. The feed point location was initially calculated for annular ring-shaped patch antenna using equations 1.8 & 1.9, and then some optimization was performed to obtain the final feed point locations. The final feed point locations are. ( $x= 18.56$ ;  $y= -11.5$ ) for feed location 1 and ( $x= -19.5$ ;  $y= 6.61$ ) for feed location 2.

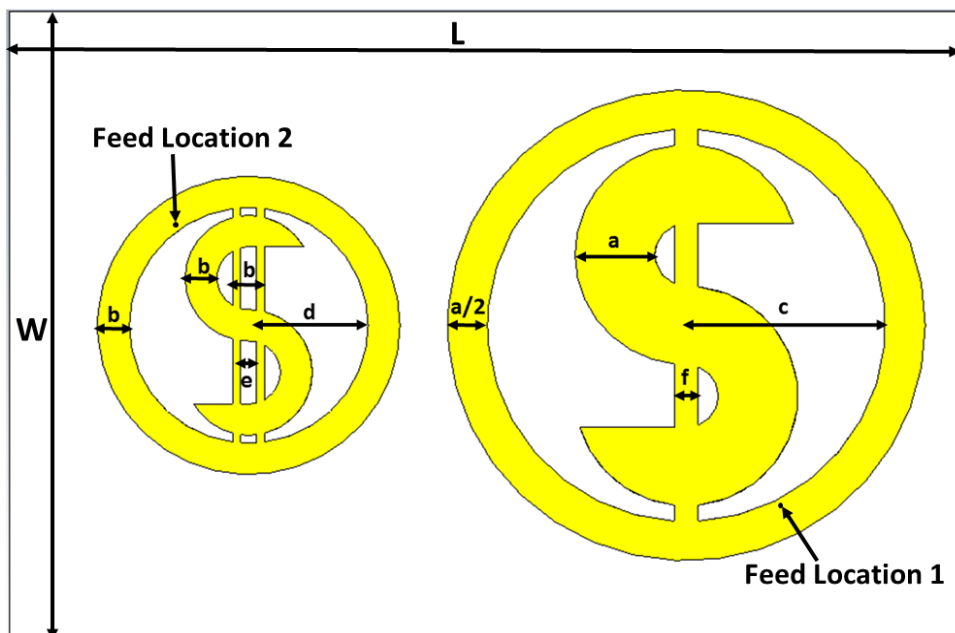


Figure 1.7. Basic geometry of Dollar shape-based microstrip patch antenna

**Table 1.2** Basic parameters of Dollar shape-based patch antenna

Sr. No.	Parameter	Value (in mm)
1.	a	5
2.	b	2
3.	c	12.5
4.	d	7.5
5.	e	$b/2$
6.	f	$e + (e/2)$
7.	L	60
8.	W	40

The inner radius for large circular shape is c mm and for small circular shape is d mm. One additional strip is placed at the center for larger dollar shaped patch antenna, to join them together and also to improve the overall results. Similarly, for small dollar shaped patch antenna two vertical strips are positioned, with some space away from the focus. The width to length ratio of the substrate is of 1:2. “Co-axial probe feed” is used for both antennas whose locations are shown in fig. 1.7 for both antennas. The right “Dollar” outline is intended to resonate in L-Band and the left one is designed for S-Band. Various parameters as obtained from simulated data are discussed in the next section.

### 1.7.3 Results and Discussion

Various parameters such as scattering, co/cross-polarization and coupling as obtained from simulated data are discussed below. Fig. 1.8 shows the scattering parameters for both the antennas giving return loss values better than 30 dB for S-band along with isolation better than 10 dB for both shapes as exposed in fig. 1.9. Fig. 1.10 (a); (b) and 1.11 (a); (b) shows co/cross-polarization values for E/H-planes. Details results are discussed in table 1.3.

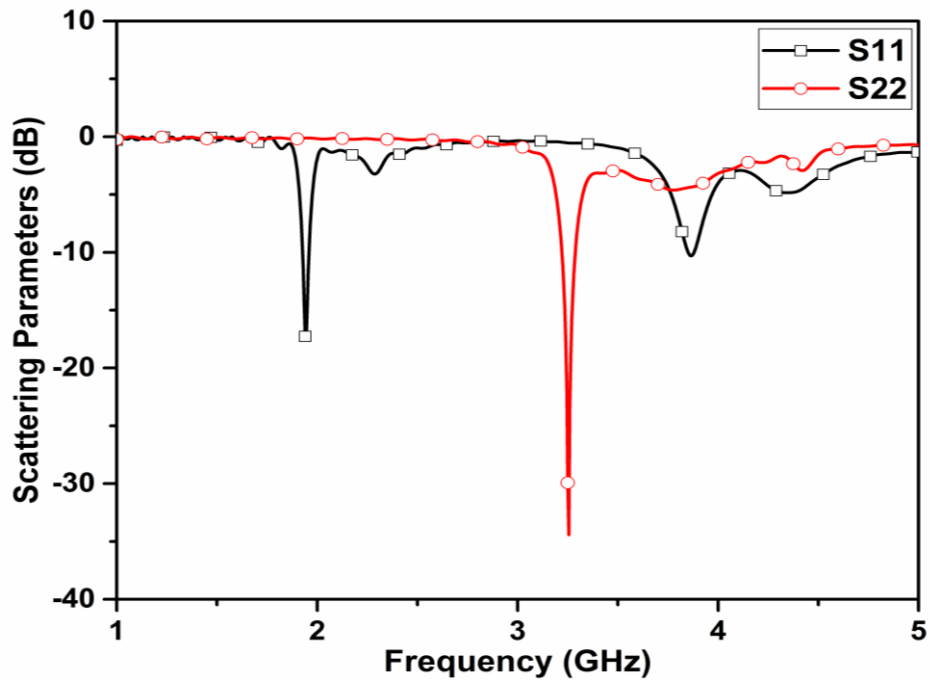


Figure 1.8 Scattering Parameters for Dollar shape-based patch antenna

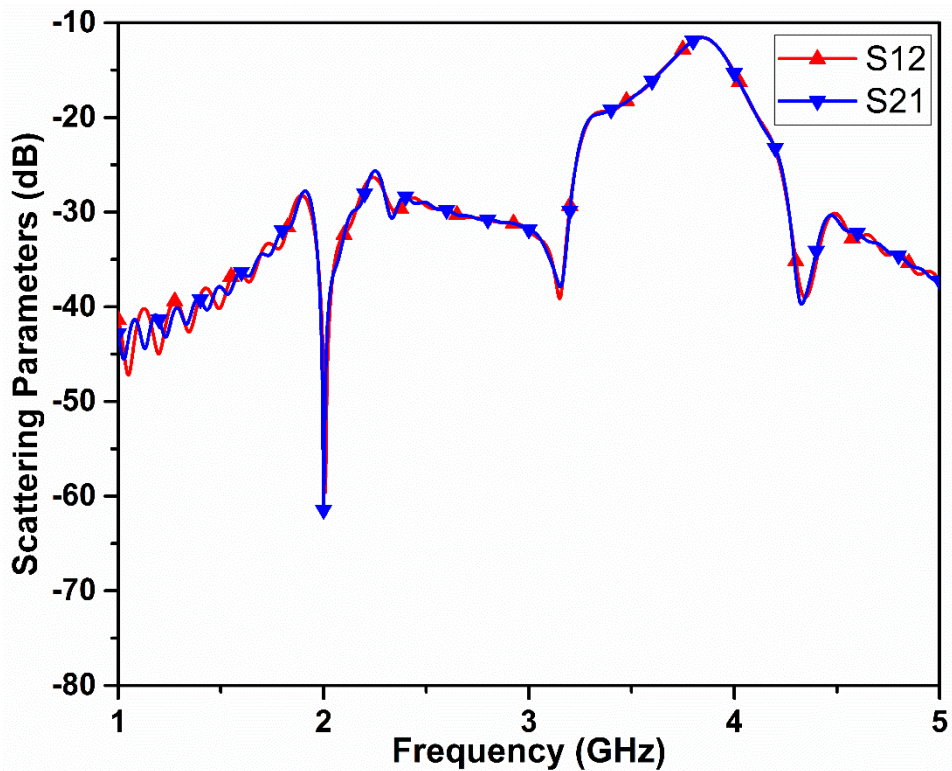


Figure 1.9 Isolation for Dollar shape-based patch antenna

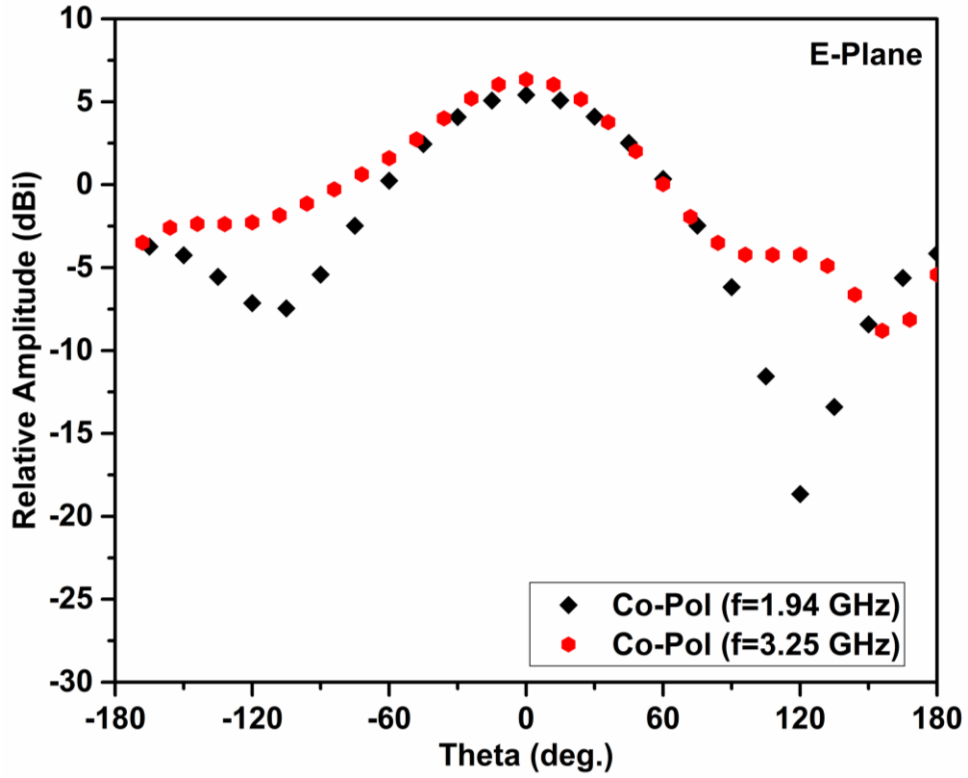


Figure 1.10 (a) Co-Polar plot for E-Plane

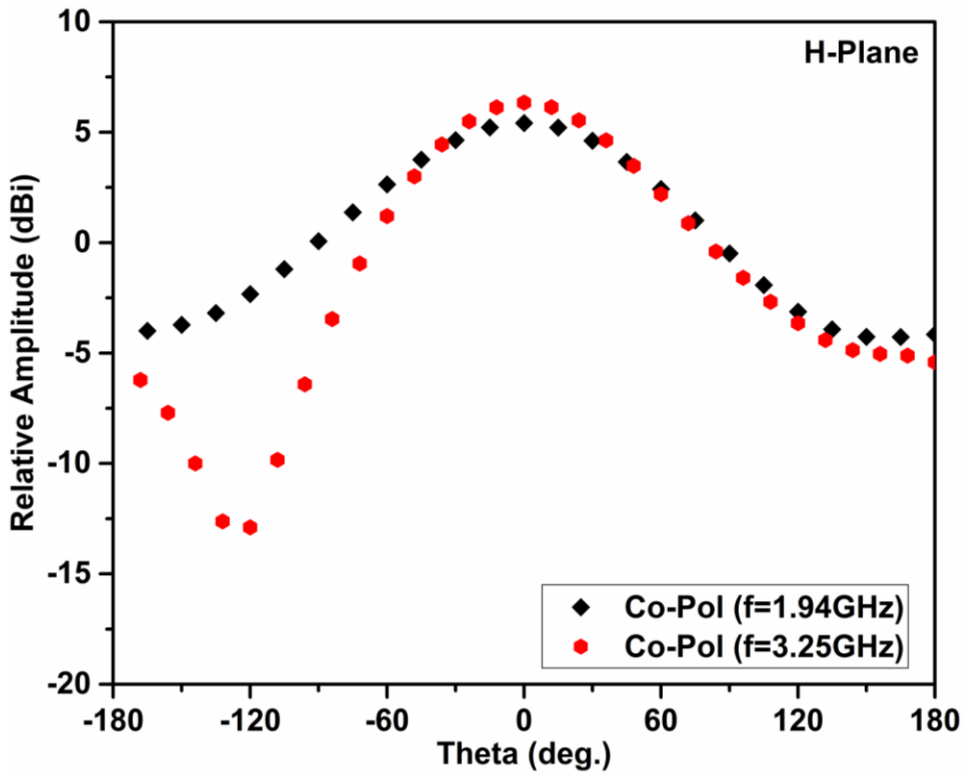


Figure 1.10 (b) Co-Polar plot for H-Plane

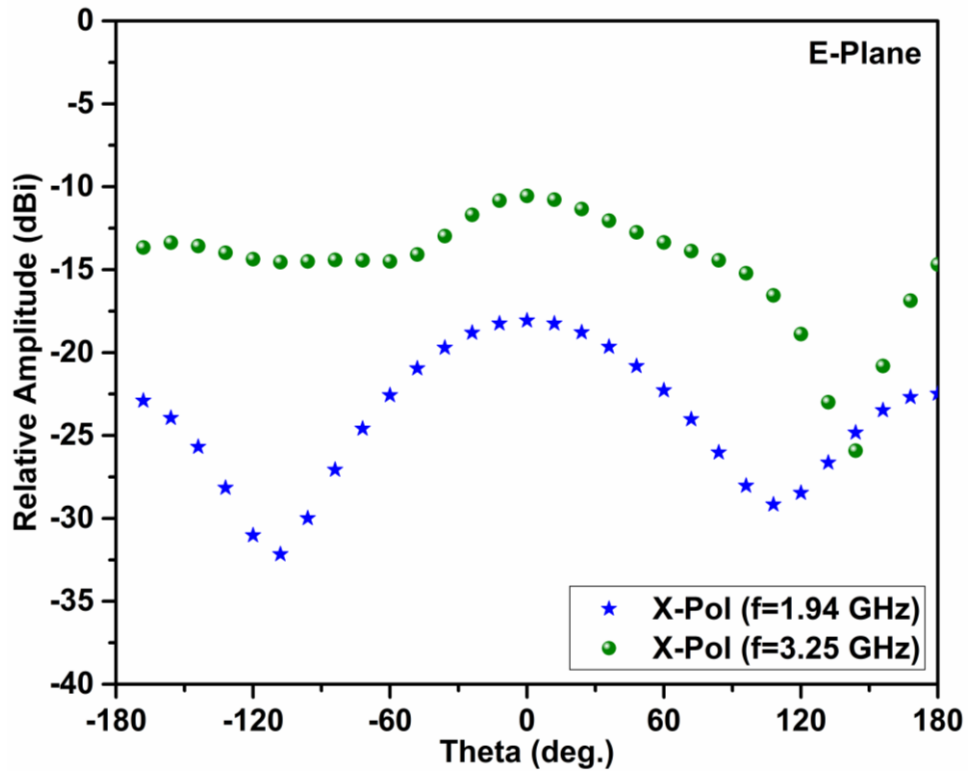


Figure 1.11 (a) Cross-polarization plot for E-Plane

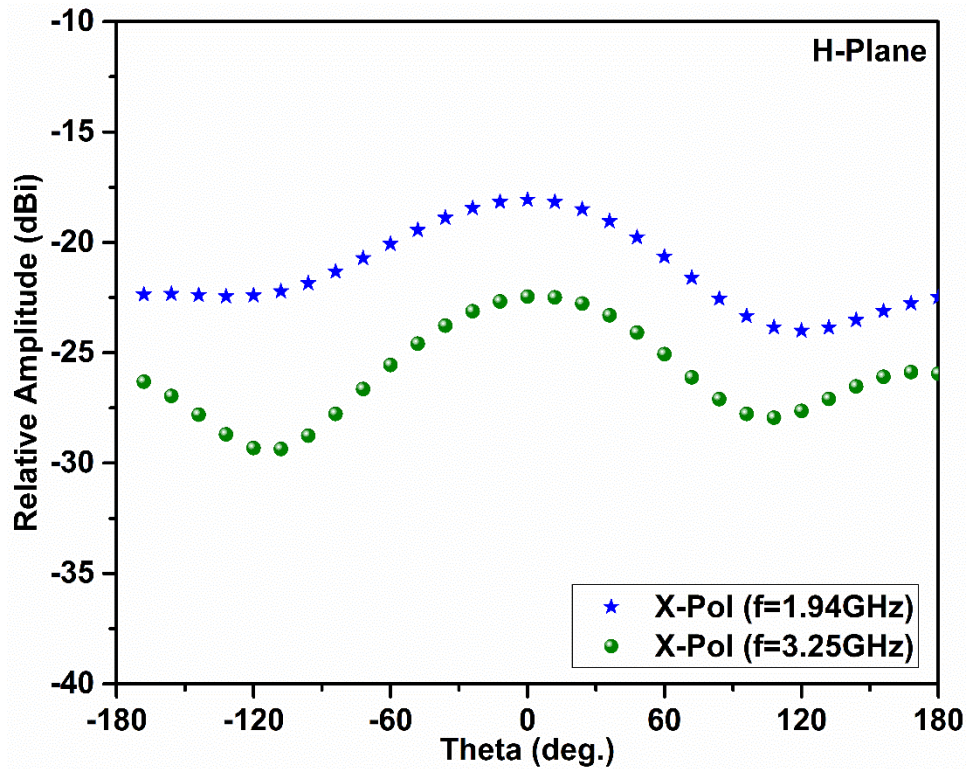


Figure 1.11 (b) Cross-polarization plot for H-Plane

## **INTRODUCTION**

---

**Table 1.3.** Parameters as obtained from simulated results

<b>Parameter</b>		<b>L-Band</b>	<b>S-Band</b>
<b>Resonating Frequency (GHz)</b>		1.94	3.25
<b>Scattering Parameters (dB)</b>		-17.56	-34.4
<b>Co-Polarization (dBi)</b>	<b>E-Plane</b>	5.41	6.34
	<b>H-Plane</b>	5.41	6.34
<b>Cross (X)-Polarization (dBi)</b>	<b>E-Plane</b>	-18.07	-10.55
	<b>H-Plane</b>	-18.07	-22.46

The “Dollar” shape-based patch antenna was successfully designed and verified for L and S-band. Two different sized Dollar shaped based structures placed beside each other were represented here, both of them were resonating in L/S-band simultaneously and separately. The preliminary proved that we can design two antennas on the same surface for both L-band and S-band simultaneously. Thus, this preliminary work was considered as the base for the design of other alternative MPA structures and the same are represented in next chapters.

**CHAPTER 2**  
**NON-CONVENTIONAL SHAPED PATCH ANTENNAS**



## 2.1 Introduction

In continuation of the preliminary work, which was described in the previous chapter, another Y-shape based patch antenna is proposed in this chapter. Although various-shaped “Microstrip Patch Antennas” (MPA) are available in literature including “rectangular” shaped [1-4], “circular Disk” shaped [5], etc. Basically, the main structure or design of MPA depends upon the resonating frequencies. However, the base of all MPA structures is a square or rectangular structure. Which is usually transformed into unique and different design after some optimization. Different unique shapes of MPA are also available [6], basically, due to ease of design of the unique shape when working on single MPA. But while working on MPA using “shared aperture” technique [7-15], antenna size and shape need to be chosen carefully, because of the frequency ratio of different bands antennas plays an important role. Most of the design present in literature are based upon shared aperture technique with frequency ratio 1:4 or more, where antenna sizes are comparatively large enough. But while working on frequency ratio 1:2, MPA size is comparatively almost same or with little bit difference. Here in this chapter, we have designed two different designs for the study/testing purpose. Each one based on aperture sharing comprised of unique and different shapes. The MPA comprises a combination of Y-shaped MPA. Two Y-shapes were placed in two different configurations i.e “horizontally” and “vertically” adjacent to each other. The effect of placement of these Y-shapes on antennas was analyzed and reported here.

The chapter further described the influence of the parasitic element on the resonating frequency using two non-conventional shape-based MPA. In literature, significant work is represented on “parasitic” elements based MPA [16-18] and “shared aperture” technique [19-21]. Although both of the above-described techniques were reported distinctly but still have extensive applications such as for the improvement of “bandwidth” and/or “gain” etc. The patch antennas with parasitic elements can be implemented in any shape or size [22-28]. This can reduce the “coupling effect” too [29]. On the other hand, the “aperture sharing” was used most of the time for the multifunctionality of the system [30, 31].

Although multifunctionality of the system can be achieved either using frequency/time multiplexing during the frequency of operation of both the antennas. Most of the literature represents patch antennas comprising interconnected structures forming an array type

assembly, thus resulting in radiation pattern for collective array assembly solitary, while in the current strategy two MPA were located individually (i.e. not coupled to each other) working independently in the existence of two parasitic patches, thus the radiation pattern is obtained separately for each of them. The selection of parasitic elements depends upon the resonating antenna and availability of space. In this chapter, we investigated both of techniques at the same time and represented the effect of parasitic elements on resonating patches using an aperture sharing method. Multifunctionality of the system is done for the utilization of space because two antennas were proposed while using the same plane/surface. Here two different configuration of MPA is described. First one consist of “Swastika” shaped patch and 7-shaped patch. Another one comprises notch loaded rotated square-shaped patch. MPA consist of Swastika shaped patch presents two different configurations, without parasitic element & with the parasitic element (having variable length). MPA with rotated square-shaped presents only with the presence of the parasitic element.

### **2.2 Y-Shaped Patch Antennas**

The basic structure consists of two Y-shaped patches placed (nearby each other) in two different orientation while using the same surface. The effect of placement of these Y-shapes on antenna performance was observed. Whole designs were investigated on “FR-4 substrate ( $\epsilon_r = 4.3$ )” and copper is used as a conducting medium for patches as well as the ground. Two different configurations of placement of Y-shapes were performed here named vertically and horizontally placed Y-shapes. While changing the orientation, some variation in resonating frequency, as well as cross/co-polarization, was observed due to the coupling effect between both of them. Two different arrangements of Y-shapes, i.e. horizontally and vertically arranged Y-shapes are exposed in fig. 2.1 and fig. 2.2 correspondingly for simulated and fabricated structures, whose dimensions were calculated using standard formula considering equivalent to a rectangular shape (fig. 2.3).

All the optimized dimension/parameters and values are shown below in table 2.1. Y-shape is equivalent to a rectangular shape & basic dimension calculation is shown in fig 2.3, whose length and width are given in equations 2.1 and 2.2. The square shape is further transformed into Y-shape after optimization. Firstly feed location was calculated for the square-shaped antenna, and later on, the feed location was optimized to attain the desired parameters. The optimized feed location for different configurations is shown in table 1.1. Results are

discussed in the next sections.

$$L = \text{Length of the Patch} = \frac{c}{2f\sqrt{\epsilon_e}} - 0.824h \frac{\left(\epsilon_e + 0.3\left(\frac{W}{h} + 0.264\right)\right)}{\left(\epsilon_e - 0.258\left(\frac{W}{h} + 0.8\right)\right)} \quad (2.1)$$

$$W = \text{Width of the Patch} = \frac{c}{2f\sqrt{\frac{\epsilon_r + 1}{2}}} \quad (2.2)$$

$$\epsilon_e = \text{effective permittivity of medium} = \frac{\epsilon_r + 1}{2} - \frac{\epsilon_r - 1}{2} \left[ \frac{1}{\sqrt{1 + 12\left(\frac{h}{W}\right)}} \right] \quad (2.3)$$

$\epsilon_r$  = dielectric constant of the medium  
 $h$  = height of substrate  
 $c$  = velocity of light ( $3 \times 10^8$  m/s)

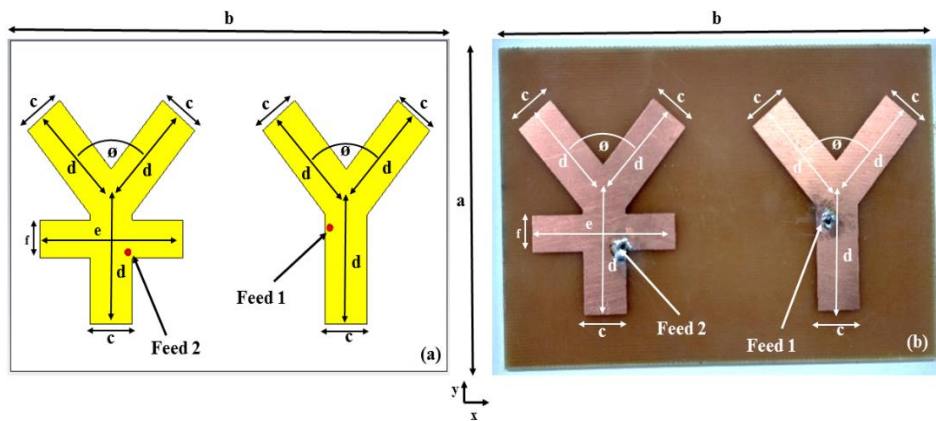


Figure 2.1 Basic configuration of horizontally placed Y-shapes

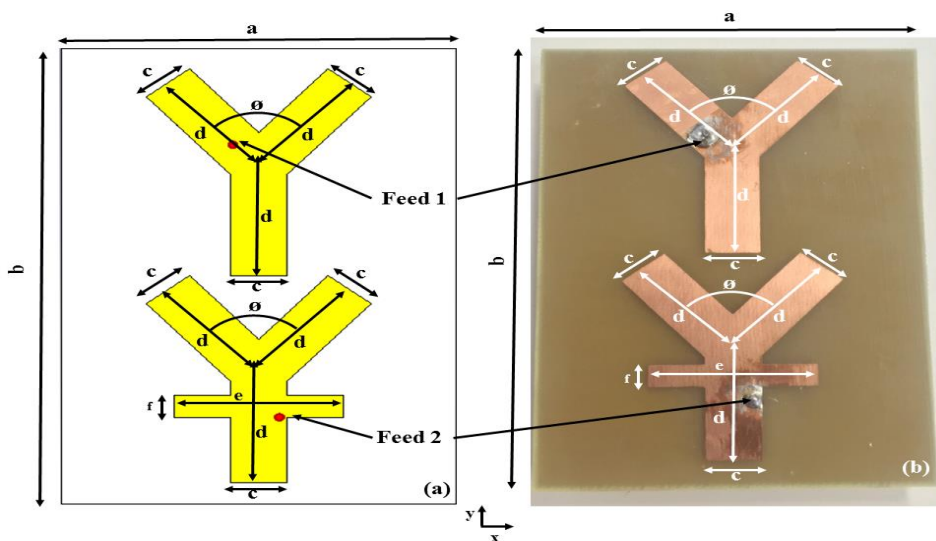
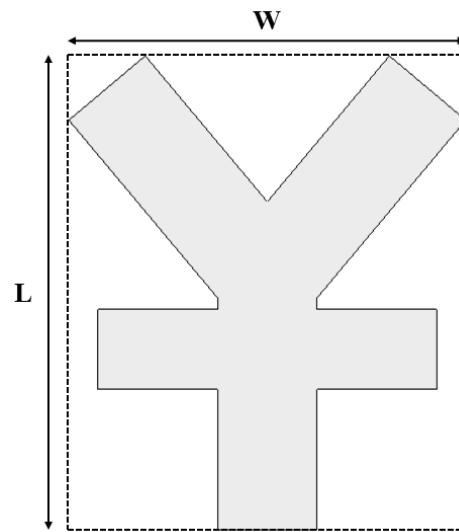


Figure 2.2 Basic configuration of vertically placed Y-shapes



**Figure 2.3** Equivalent rectangular patch of Y-shapes

**Table 2.1.** Parameter values for patch antenna

Sr. No.	Parameter	Parameter Value
1.	a	70 mm
2.	b	104 mm
3.	c	10 mm
4.	d	25 mm
5.	e	30 mm
6.	f	5 mm
7.	$\theta$	40°
8.	L	47.4 mm
9.	W	39.8 mm

### 2.2.1 Results and Discussion

Basic parameters including scattering, co-cross polarization, and isolation are shown and discussed below. Fig. 2.4 (a & b) and 2.5 (a & b) shows the “scattering parameters” for horizontally and vertically placed Y-shapes respectively, including measured and simulated data. Fig. 2.6 (a & b) giving isolation values better than 25 dB. Co/Cross-Polarization parameters for horizontal & vertical arrangements are shown in fig. 2.7 (a to d) and 2.8 (a to d) respectively. Comparative study of various parameters is given in Table 2.2 briefly.

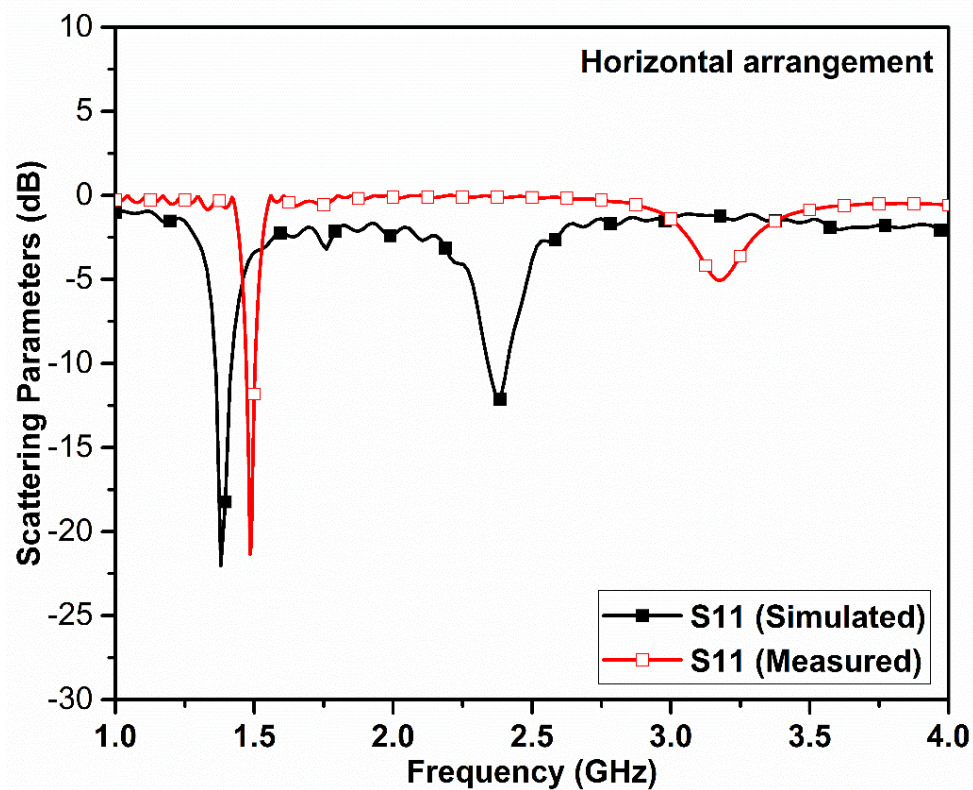


Figure 2.4 (a) Scattering parameters (S11) for horizontally placed Y-shapes

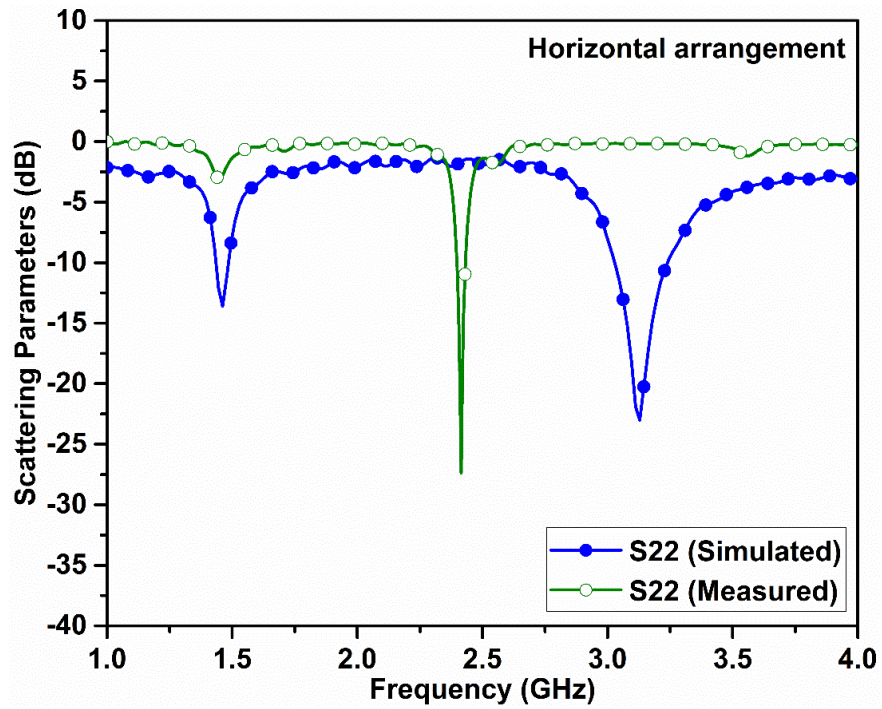


Figure 2.4 (b) Scattering parameters (S22) for horizontally placed Y-shapes

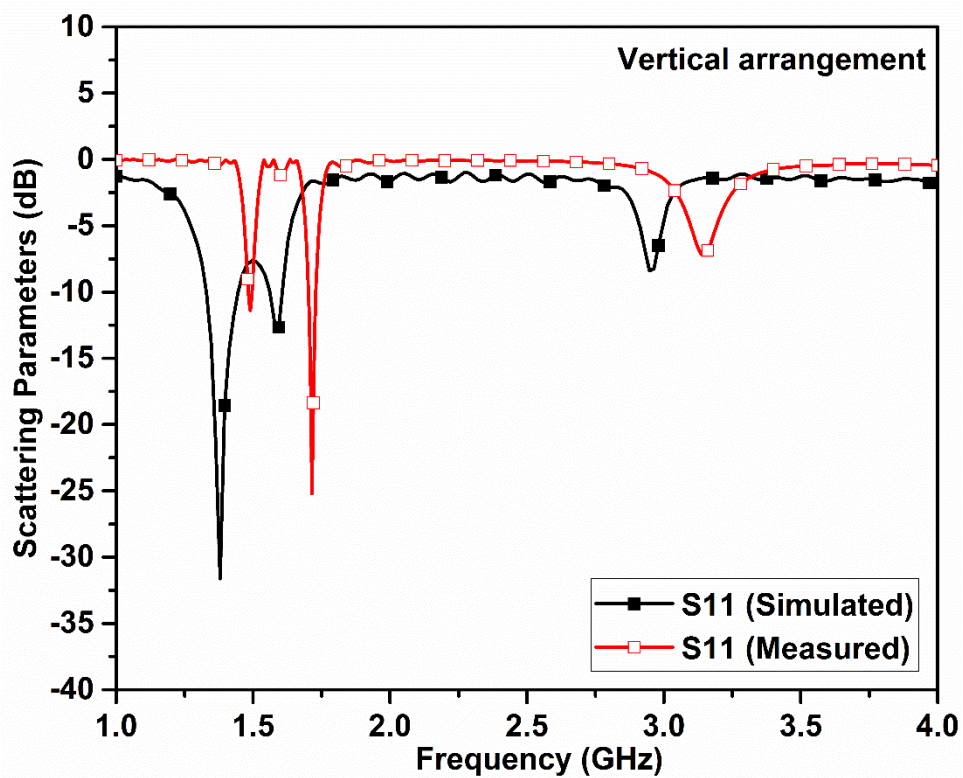


Figure 2.5 (a) Scattering parameters (S11) for vertically placed Y-shapes

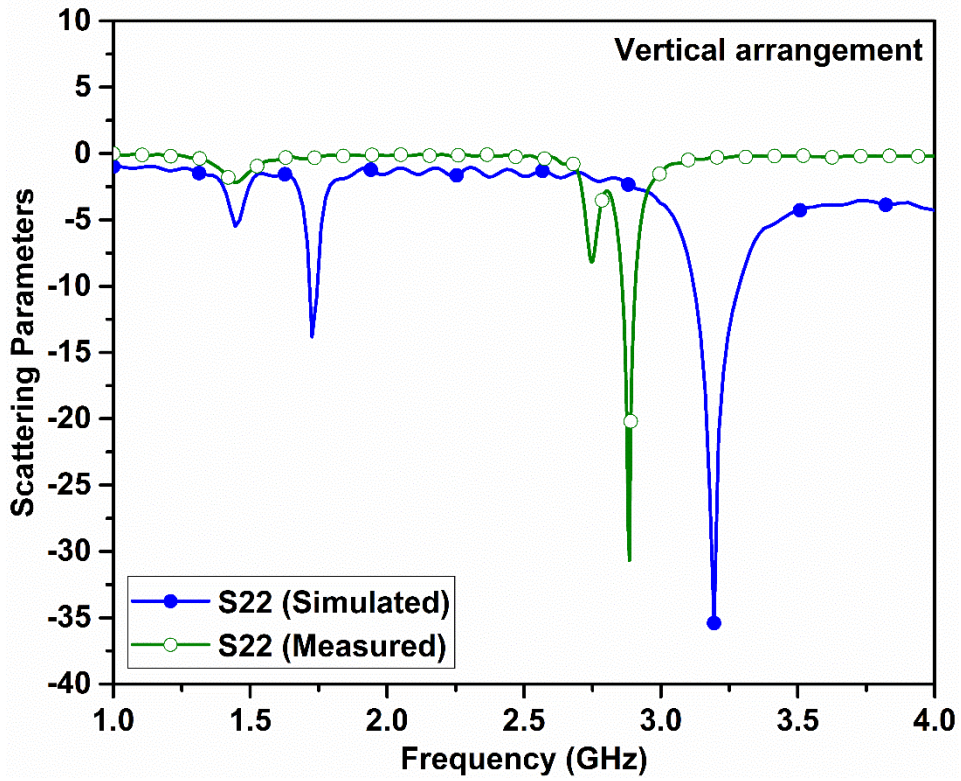


Figure 2.5 (b) Scattering parameters (S22) for vertically placed Y-shapes

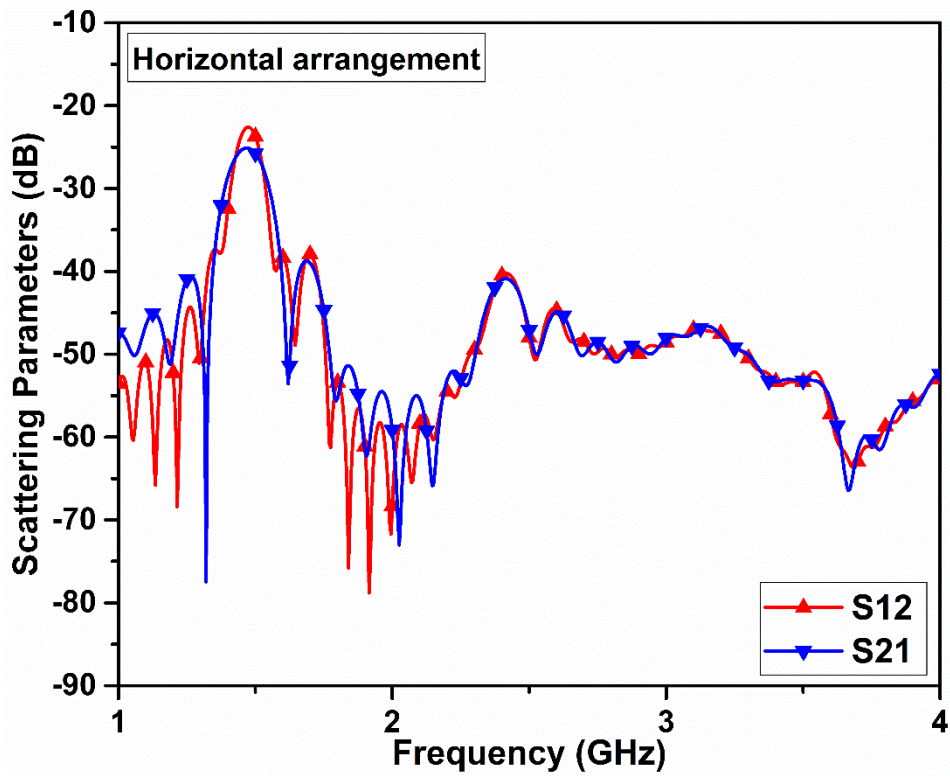


Figure 2.6 (a) Isolation of horizontally placed Y-shapes

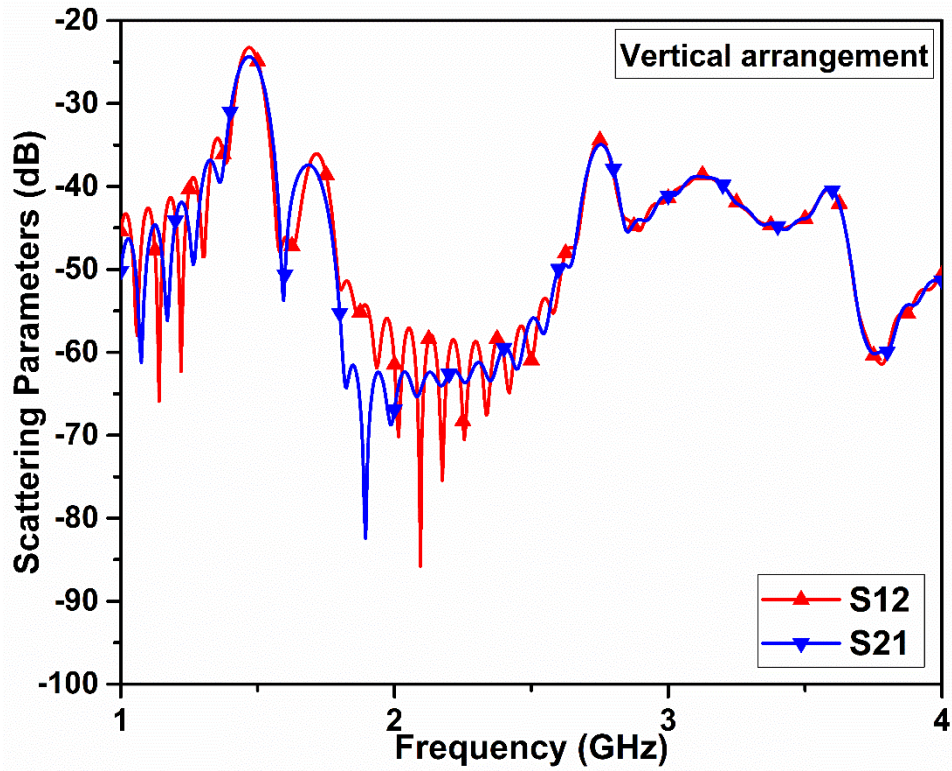


Figure 2.6 (b) Isolation of vertically placed Y-shapes

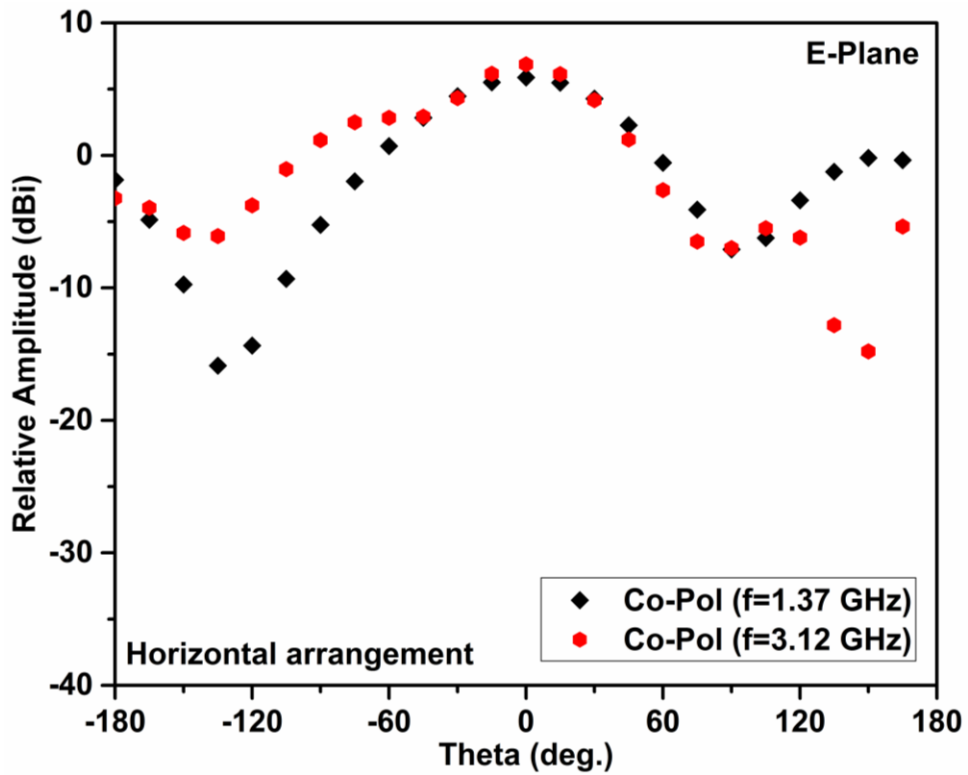


Figure 2.7 (a) E-plane Co-polarization of horizontal arrangement

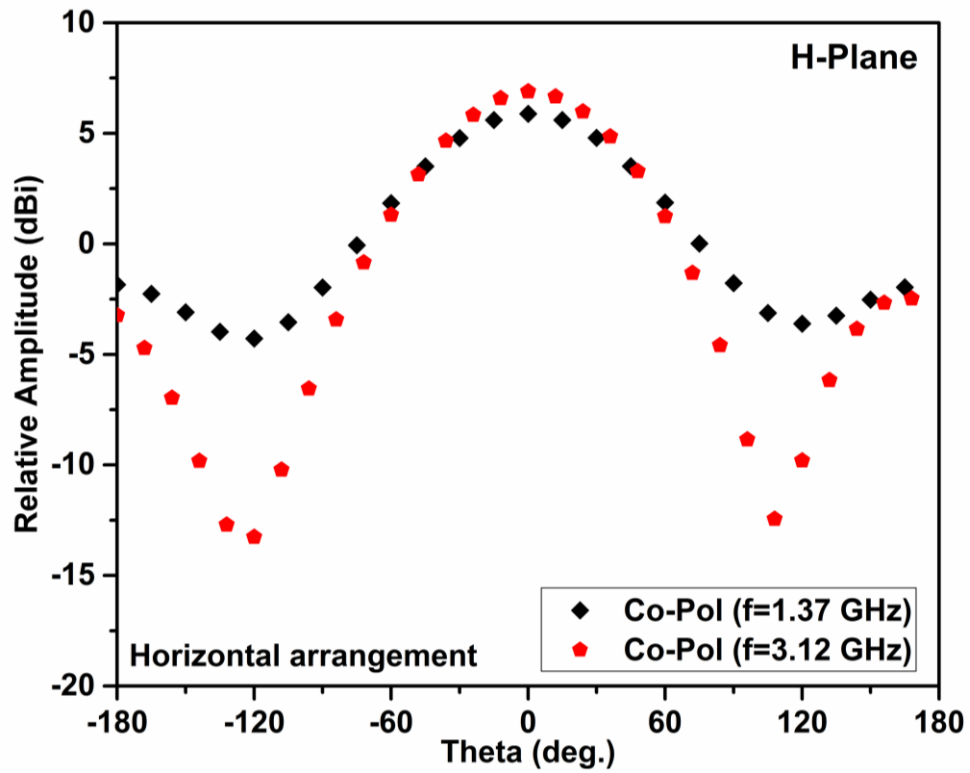


Figure 2.7 (b) H-plane Co-polarization of horizontal arrangement

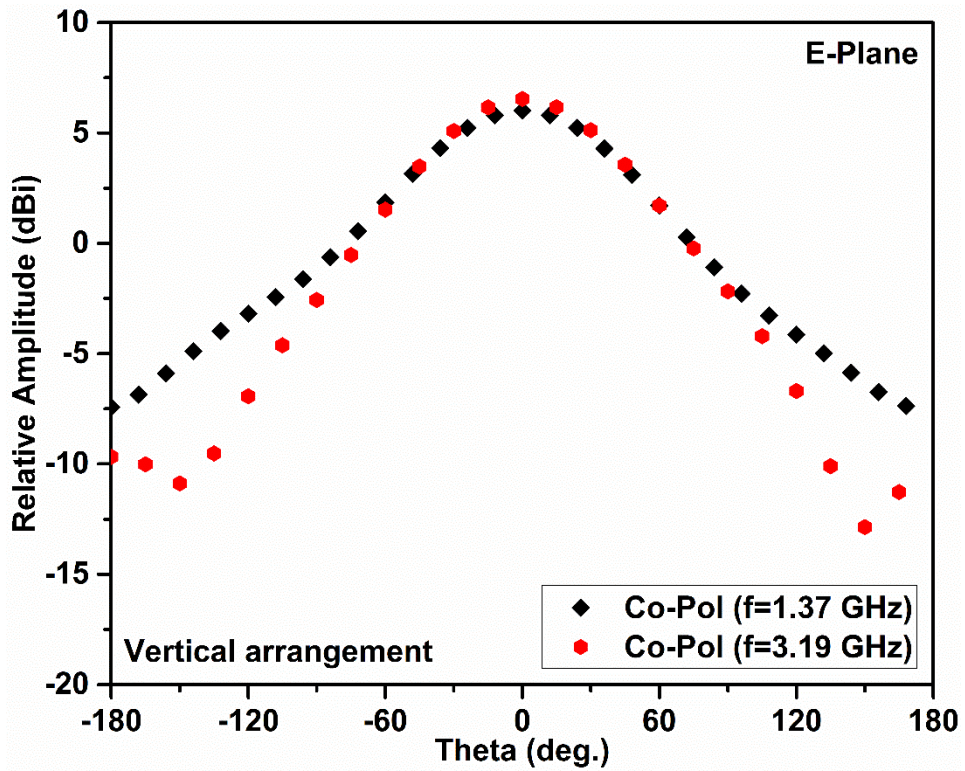


Figure 2.7 (c) E-plane Co-polarization of vertical arrangement

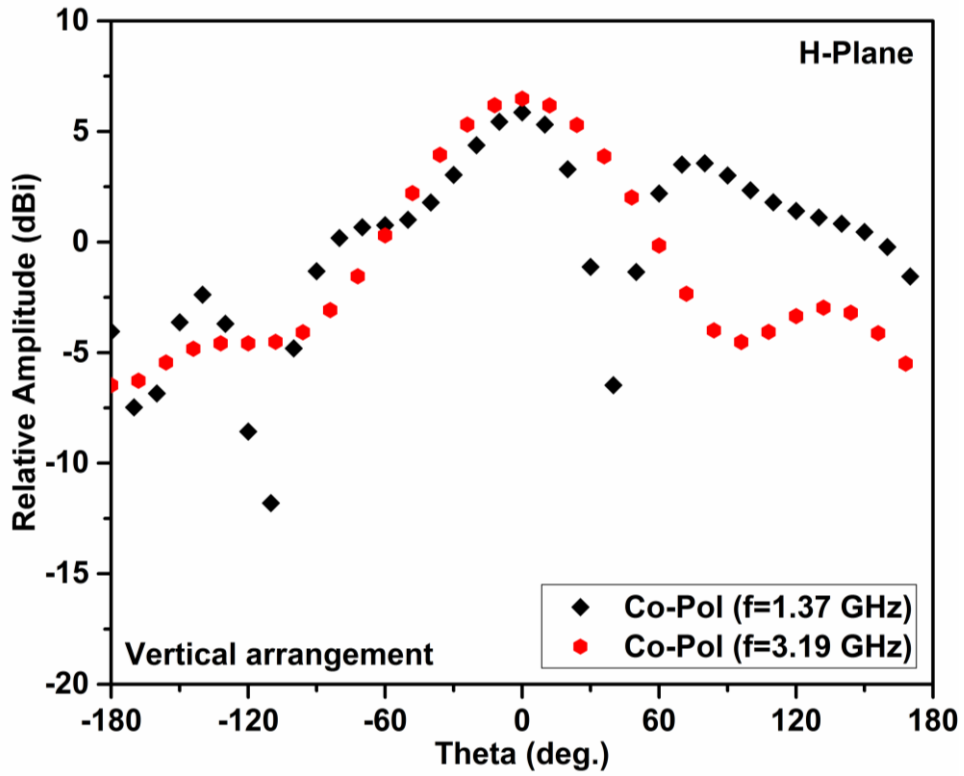


Figure 2.7 (d) H-plane Co-polarization of vertical arrangement

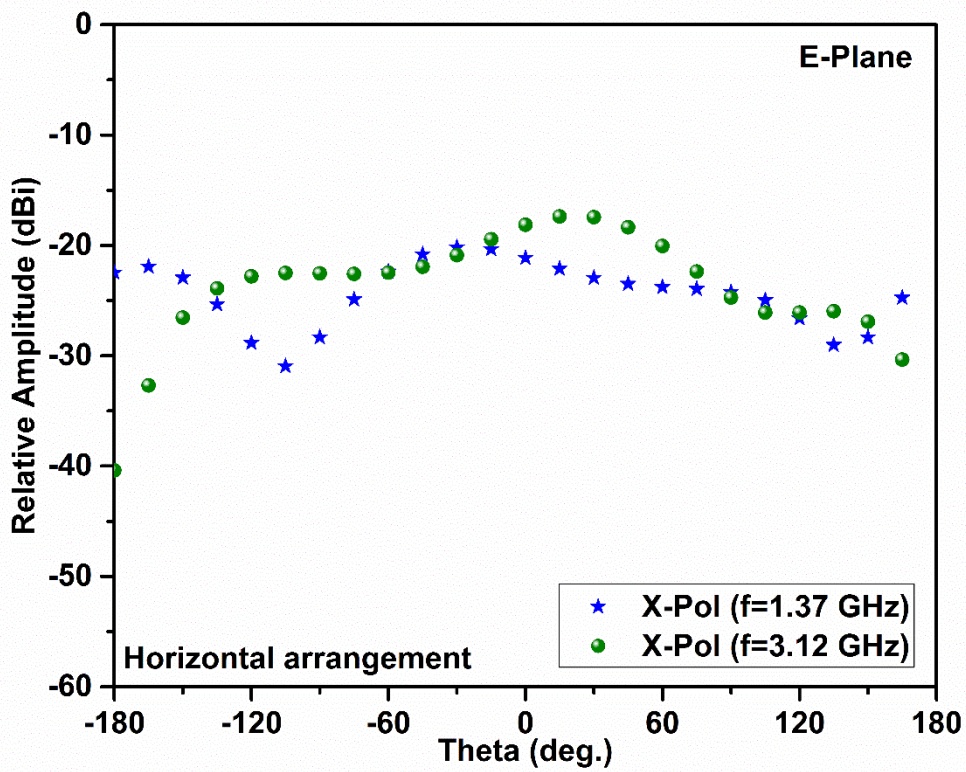


Figure 2.8 (a) E-plane cross-polarization of horizontal arrangement

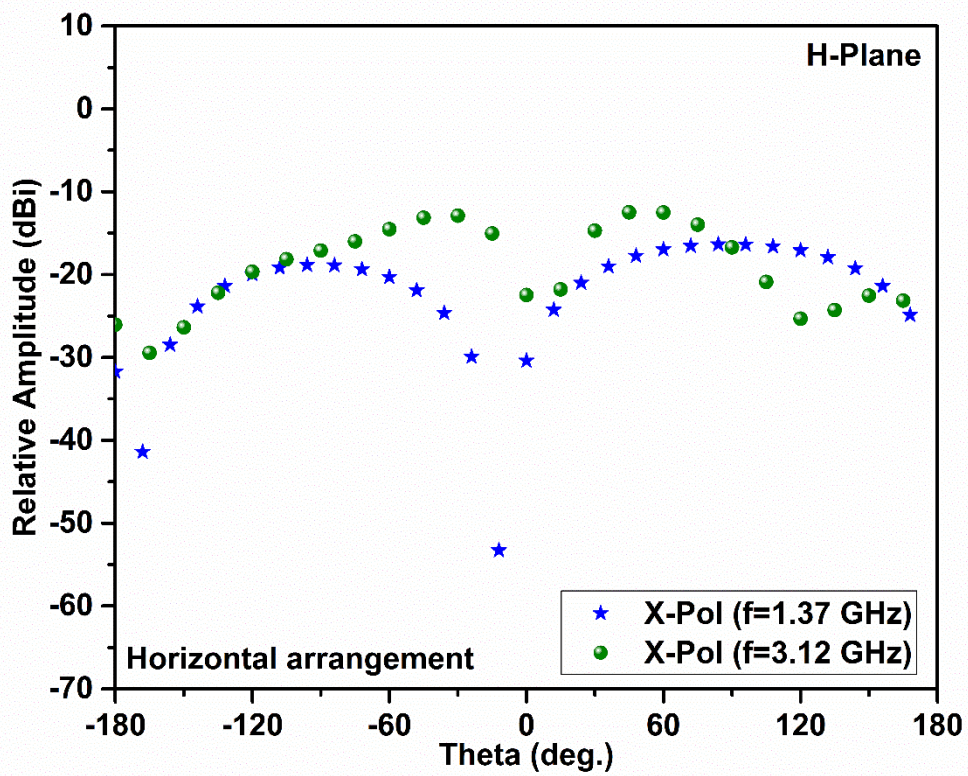


Figure 2.8 (b) H-plane cross-polarization of horizontal arrangement

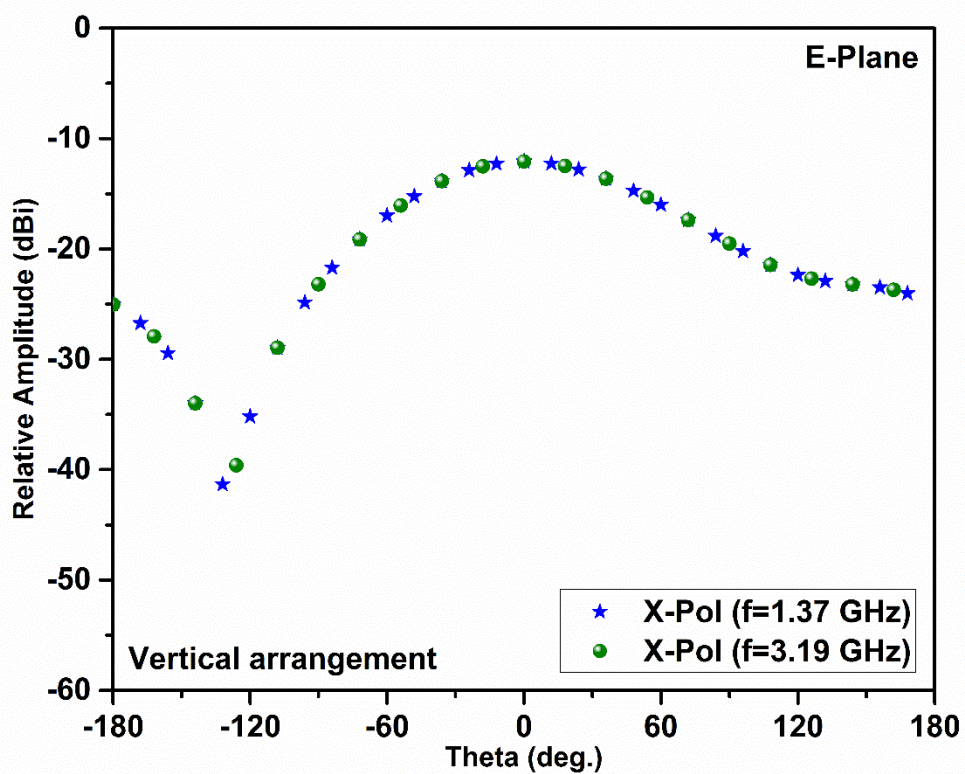


Figure 2.8 (c) E-plane cross-polarization of vertical arrangement

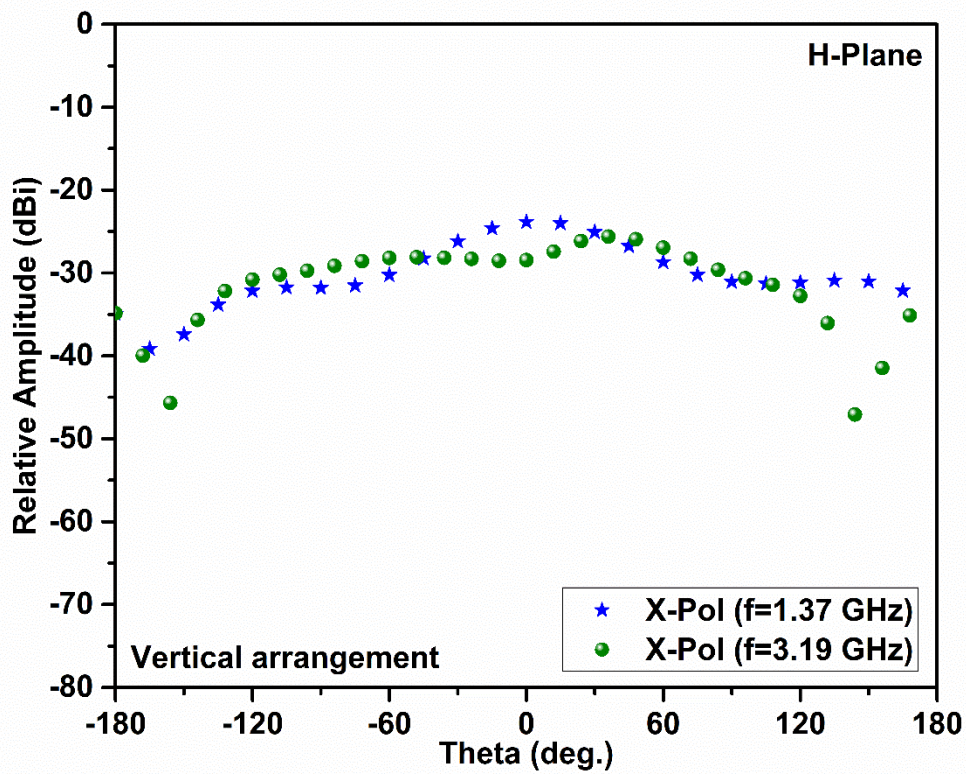


Figure 2.8 (d) H-plane cross-polarization of vertical arrangement

Table 2.2 Parameters values for Y-shape patch configurations

Parameters		Horizontal arrangement		Vertical arrangement	
		L-Band	S-Band	L-Band	S-Band
Resonant Frequency (GHz)	Simulated	1.37	3.12	1.37	3.19
	Measured	1.48	2.41	1.71	2.88
Return Loss (dB)	Simulated	-22.03	-23.00	-31.70	-35.45
	Measured	-21.35	-27.36	-25.22	-31.06
Co-Polar (dBi)	E-Plane	5.87	6.87	6.00	6.54
	H-Plane	5.87	6.88	5.86	6.48
Cross-Polar (dBi)	E-Plane	-21.13	-18.13	-12.08	-12.08
	H-Plane	-30.40	-22.48	-23.85	-28.44

Table 2.2 described that the “resonating frequency” for both the antennas is almost with the frequency ratio of 1:2. The “scattering parameters” are better than -20 dB in all the cases and the maximum value of -35.45 dB (S22) is achieved in S-band corresponds to the resonating frequency of 3.19 GHz in the vertical arrangement. A reasonable change in the “scattering parameters” was observed when the configuration of Y-shape was changed from horizontal to vertical. This may be due to comparative distance among two feed locations, which reduced the coupling between both of them and thus improved the overall performance. Although bandwidth is not much in all cases, due to which the application area for the designed antennas are limited to particular areas only, where multiple antennae are capable to resonate at the same frequency. Maximum isolation of about -25 dB is achieved in L-band, and -40 dB for S-band (corresponds to horizontal arrangement). The gain (co-polar) is better than 5 dBi in all cases and an extreme gain of 6.88 dBi (S-band) is accomplished for horizontal arrangement again due to comparative distance among two feed locations. The maximum cross-polarization of -30.44 dBi (L-band) is achieved again for horizontal arrangement.

### 2.3 Swastika Shaped Patch Antenna

Here a “Swastika” shaped MPA is presented using aperture sharing. The “Swastika” shaped patch is designed by using equivalent square-shaped MPA for calculation purpose. Here the “Swastika” shaped of the patch is achieved by using different rectangular strips (joined together). The unallocated space in the top-right angle of the said designed “Swastika” shaped MPA was covered with another MPA of seven (7)-shape having equally shaped rectangular strips on both sides. The antenna functioning is fully reliant on its dimension parameters which auxiliary hinge on the resonating frequency as well as other constraints. To attain the expected outcomes the dimensions parameters were optimized after giving some tuning, such as length reduction was performed for small strips of the “Swastika” shaped patch and for the placement of dot-shaped parasitic elements around the gap. Another L-shaped parasitic element was also placed in the lower-left side of the antenna to attain better performance of the overall structure. Some variation in the length of this parasitic patch was performed for the analysis of the effect on resonating antennas. The Swastika shaped patch antenna was recovered from a simple square-shaped MPA, while two rectangular patches were engaged at the top-right corner & joined together (forming a “7-

## **Non-Conventional Shaped Patch Antennas**

shaped” structure) acting as another MPA. The said “7-shaped” antenna was aimed/fabricated for space employment or to attain the multi-functionality of the antenna.

The above described “Swastika” shaped MPA was designed & fabricated for L-band (i.e. for 1-2 GHz) and exterior antenna comprising “seven (7)” shape was aimed & fabricated for resonating frequency in S-band (2-4 GHz) on commercially available dielectric substrate FR-4. Firstly “Swastika” shaped patch and “7-shaped” MPA were studied simultaneously, later on, the influence of above mentioned parasitic patch (comprising L-shape) with the adjustable shape/length at the bottom-left angle of the substrate was witnessed. The basic configuration for the overall MPA without and with “parasitic” element is shown below in fig. 2.9 (a) and (b).

The optimized length (L)/width (W) proportion for the said dielectric substrate (i.e. “1:1”) and that of external patch i.e. amid  $L_t$  and  $L_r$  was the same i.e. “1:1”. The length of parasitic patches (i.e.  $L_l$  and  $L_b$ ) is equal to that of  $L_t$  and  $L_r$ . The adjustable dimension of the coupling patch ( $L_v$ ) was used for the optimization purpose and to attain required results; also to observe the effect of the said “parasitic” element. The effect of this adjustment of this length was detected on several parameters of both the antennas/structures. The width or gap (denoted by ‘a’) of all the radiating sections are of 10 mm and the optimized diameter of the “circular patches” is 3 mm for all.

The numeric values of the designed prototype are given in table 2.3. After variation in  $L_v$ , three different prototype of antenna system are fabricated named as: (i) without the parasitic patch, (ii) with a parasitic patch of length 113.84 mm and (iii) with a parasitic patch of length 117.84 mm as shown in 2.10 (a), (b) and (c) respectively. The length of the parasitic patch was optimized by simulating and designed for the best case. The feed point location was calculated (fig. 1.1.) and optimized for the designed cases. The as-obtained results are discussed in the next section.

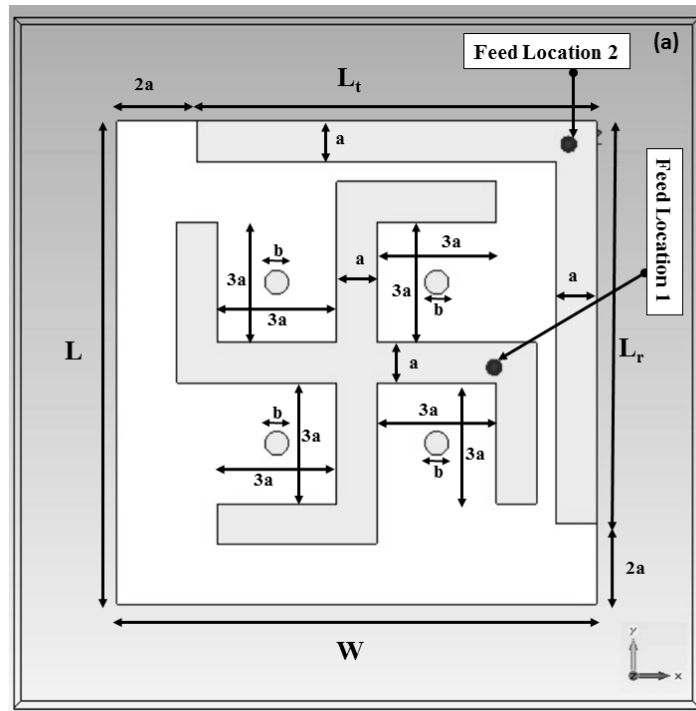


Figure 2.9 (a) Basic configuration of Swastika shape-based MPA without parasitic

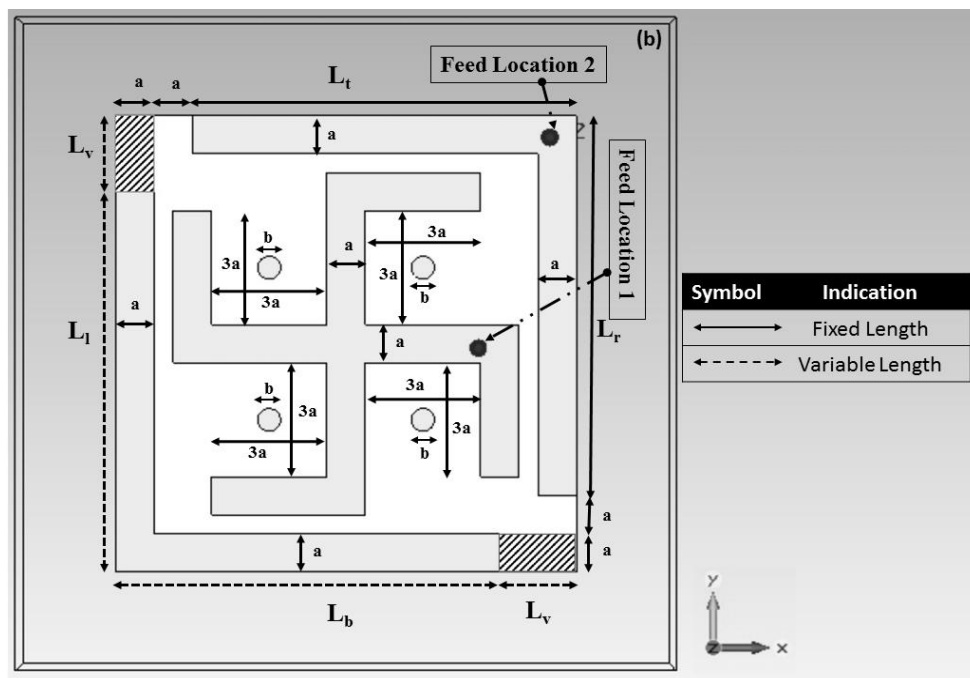


Figure 2.9 (b) Swastika shape-based MPA with parasitic element

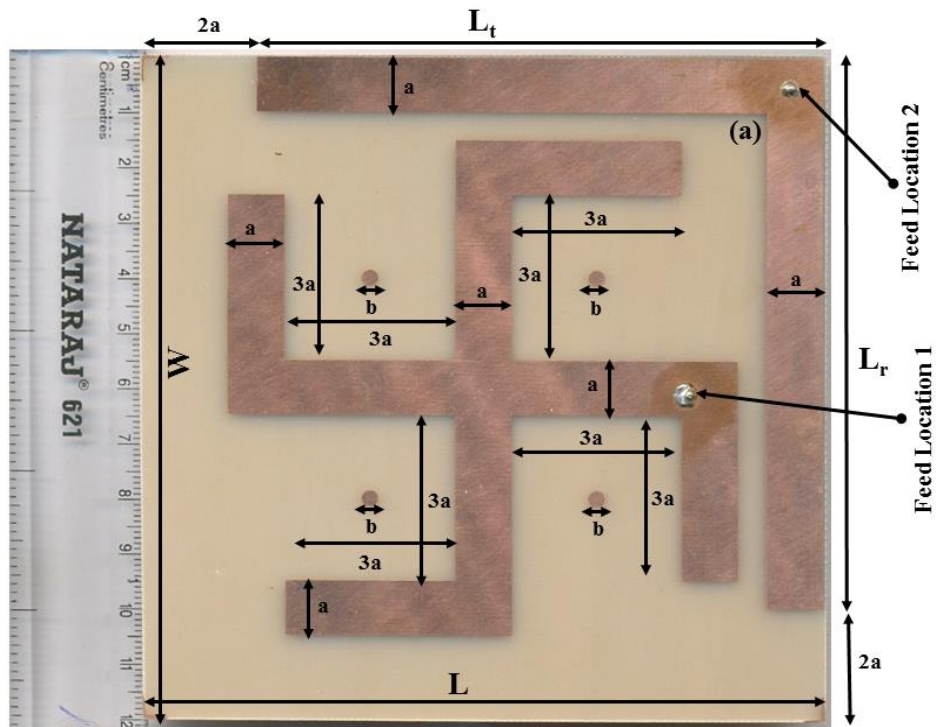


Figure 2.10 (a) Layout of fabricated Swastika shape-based MPA without parasitic

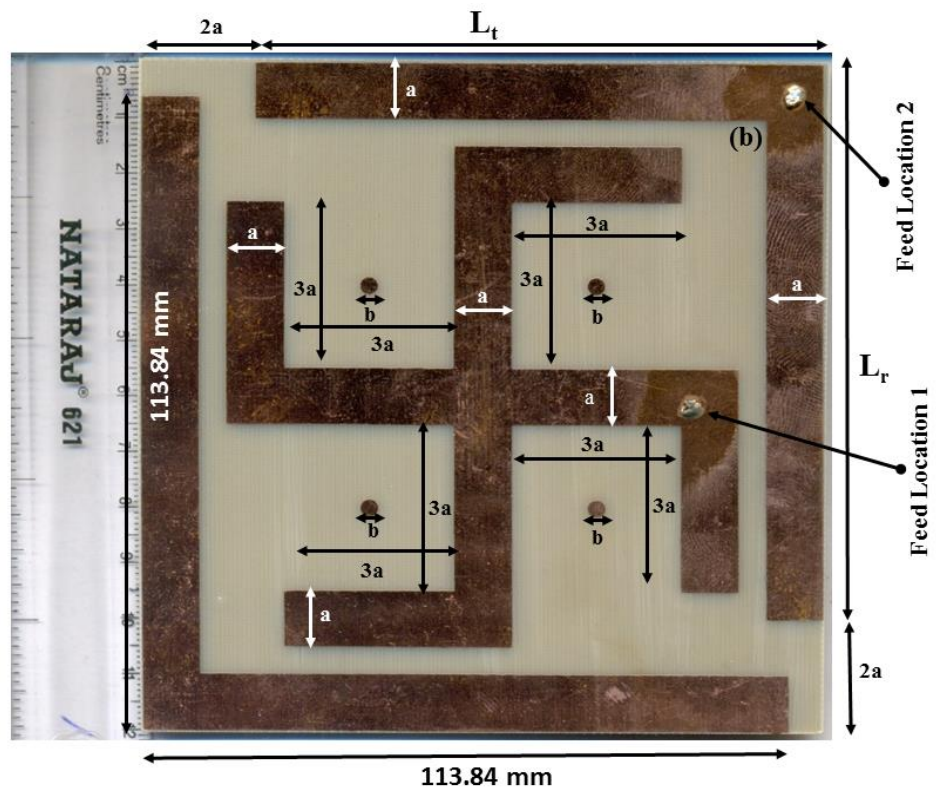


Figure 2.10 (b) Layout of fabricated MPA with a parasitic element ( $L_b + L_v = 113.84$  mm)

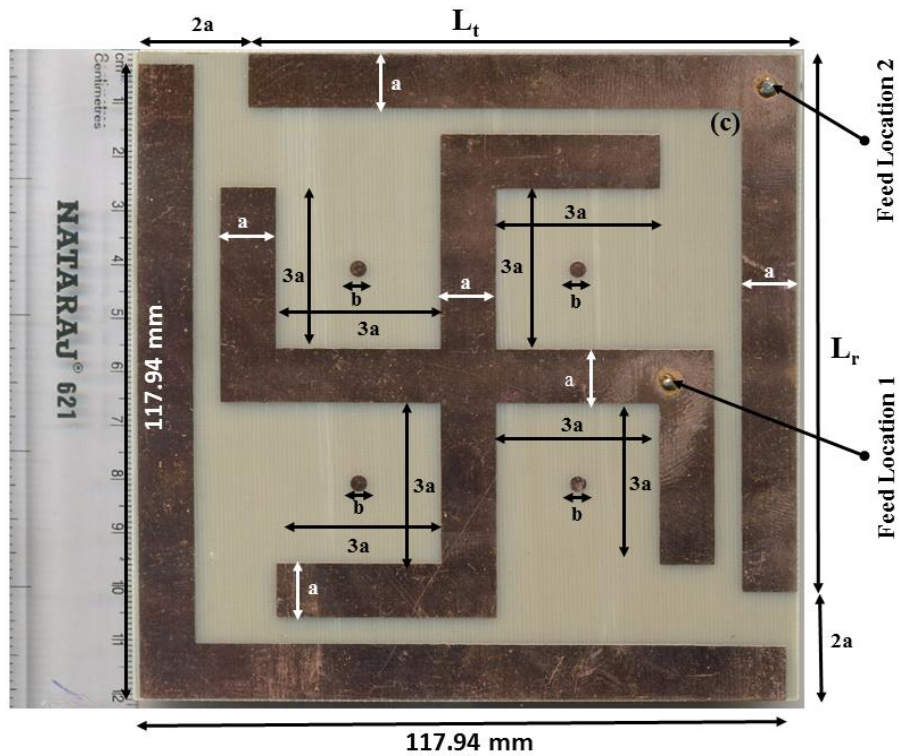


Figure 2.10 (c) Layout of fabricated MPA with a parasitic element ( $L_b + L_v = 117.94$  mm)

Table 2.3 Description and numeric design values of the MPA

Sr. No.	Variable	Description	Design Values (in mm)
1.	<b>L</b>	Length of the aperture	120
2.	<b>W</b>	Width of the aperture	120
3.	<b>L<sub>t</sub></b>	Topside length of the 7-shaped microstrip patch	100
4.	<b>L<sub>r</sub></b>	Right side length of the 7-shaped Microstrip Patch	100
5.	<b>L<sub>b</sub></b>	Bottom side length of the parasitic patch	100
6.	<b>L<sub>1</sub></b>	Left side length of the parasitic patch	100
7.	<b>L<sub>v</sub></b>	Variable-length parameter of the parasitic patch	13.84 & 17.94
8.	<b>a</b>	Width or gap	10
9.	<b>b</b>	Diameter of the circle	3

### 2.3.1 Results and Discussion

The antenna system was analysed for different design parameters. Three different configurations of antennas were analysed for both L and S-band named as: without the parasitic patch & with parasitic patch having two optimized length values. Scattering parameters were acquired from simulated and measured data. Co/Cross-polar results were obtained using “CST microwave studio”. Scattering results are shown for various configurations in fig. 2.11 (a) to (f), along with the isolation as shown in 2.12 (a) to (c). The Co/Cross-polar results for all configurations comprising E/H-planes are shown in fig. 2.13 (a) to 2.13 (f) & 2.14 (a) to 2.14 (f). The comparative study of different configurations are briefly described in Table 2.4 (a) and (b).

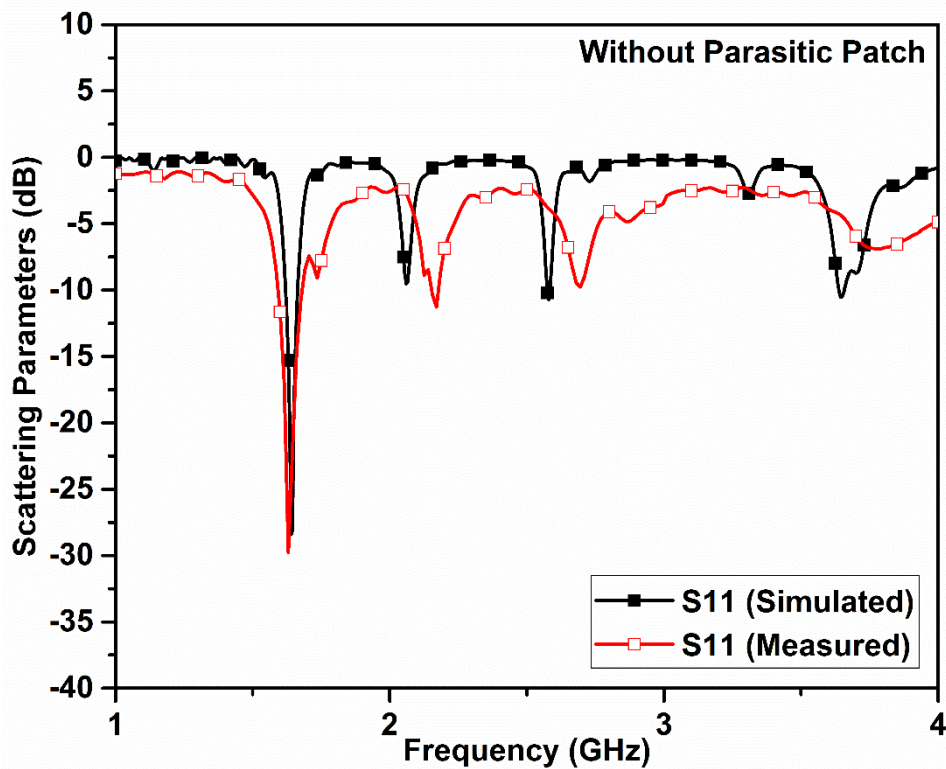


Figure 2.11 (a) Scattering parameters (S11) of MPA (without parasitic element)

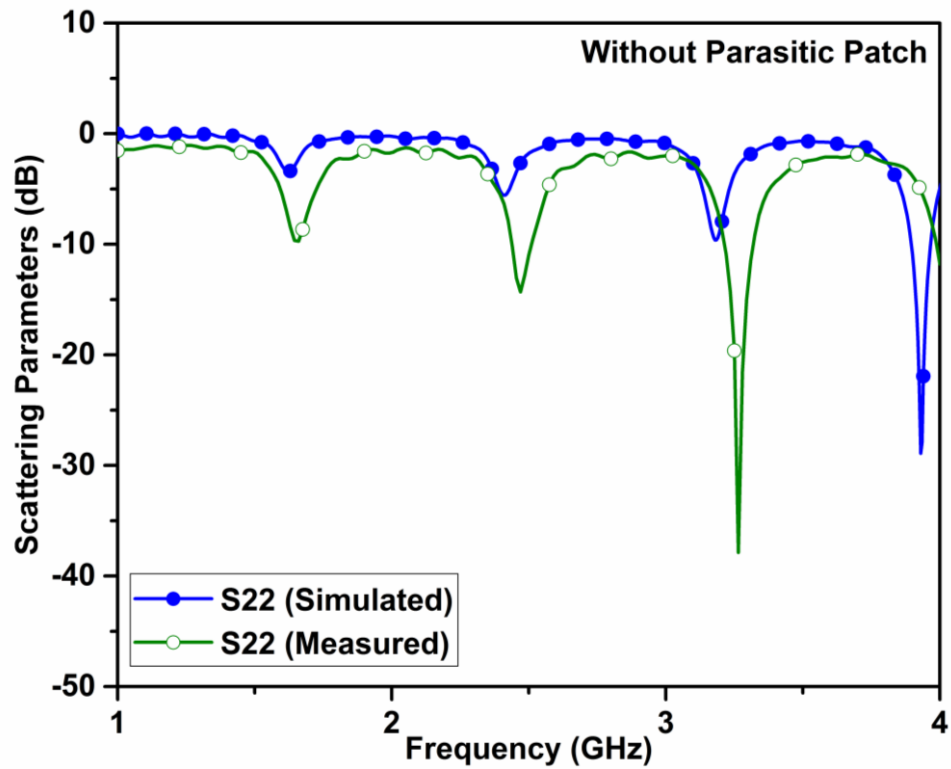


Figure 2.11 (b) Scattering parameters (S22) of MPA (without parasitic element)

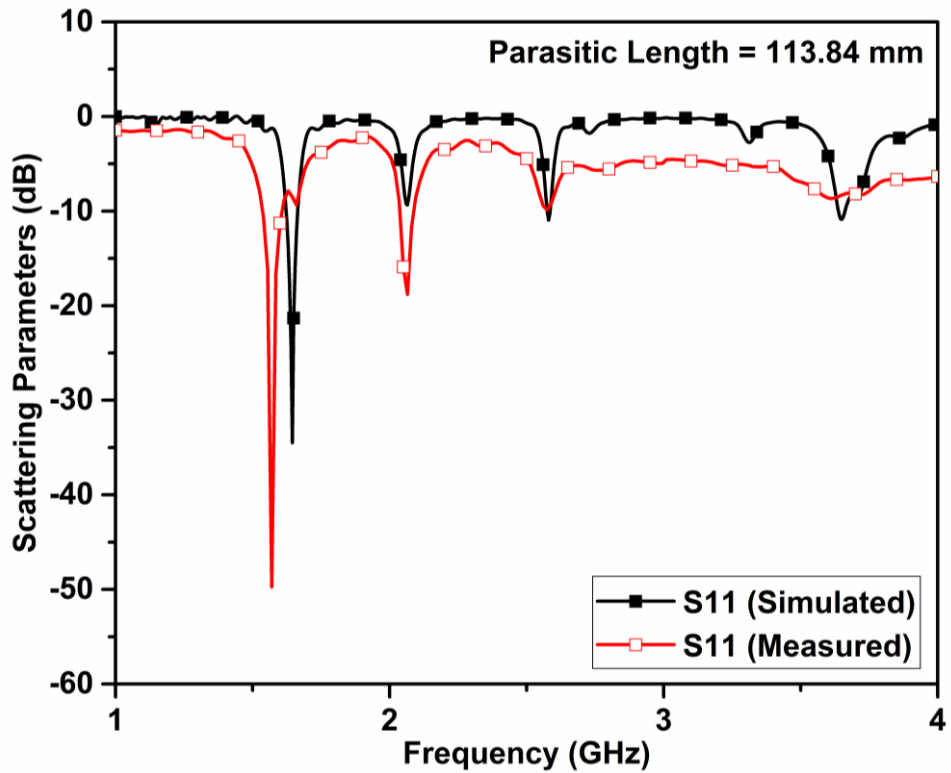


Figure 2.11 (c) Scattering parameters of MPA (S11) (parasitic length =113.84 mm)

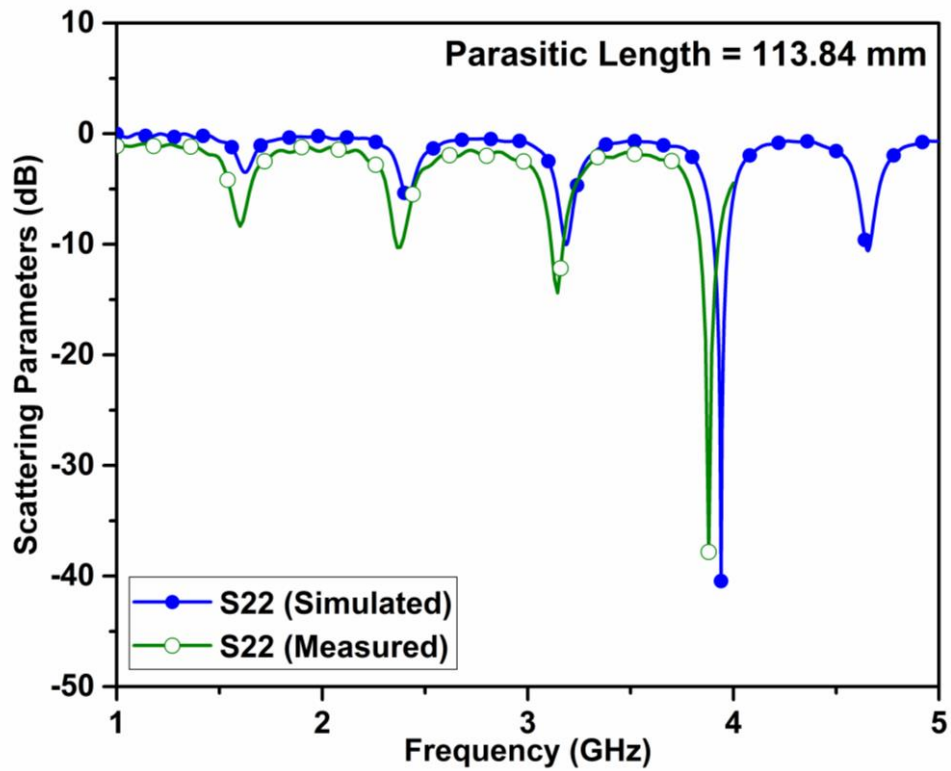


Figure 2.11 (d) Scattering parameters of MPA (S22) (parasitic length =113.84 mm)

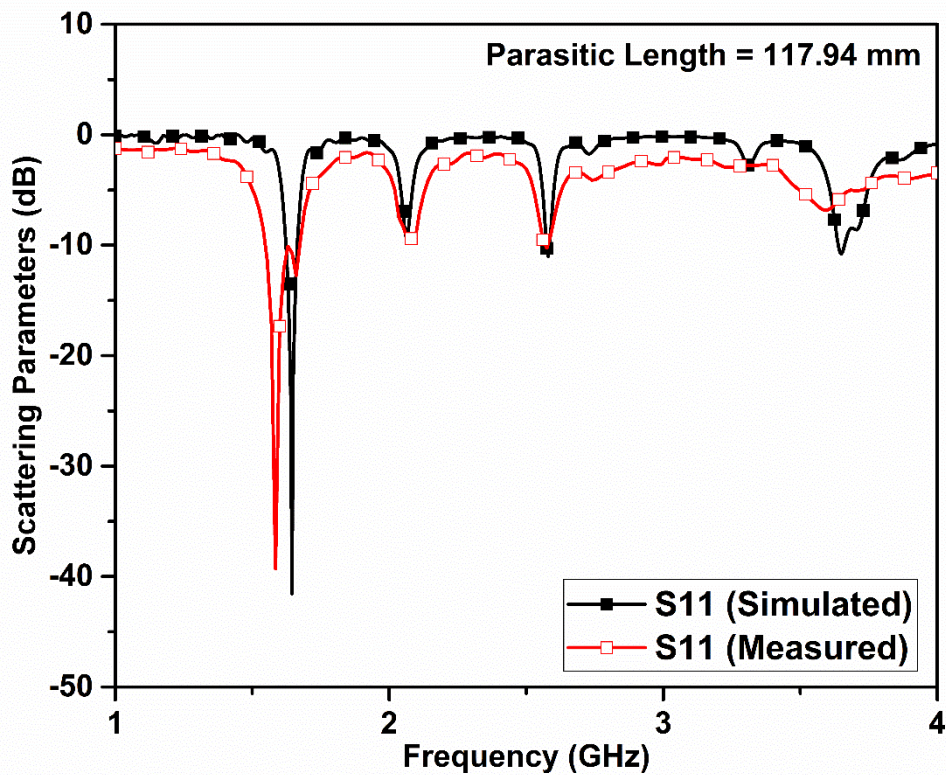


Figure 2.11 (e) Scattering parameters (S11) of MPA (parasitic length =117.94 mm)

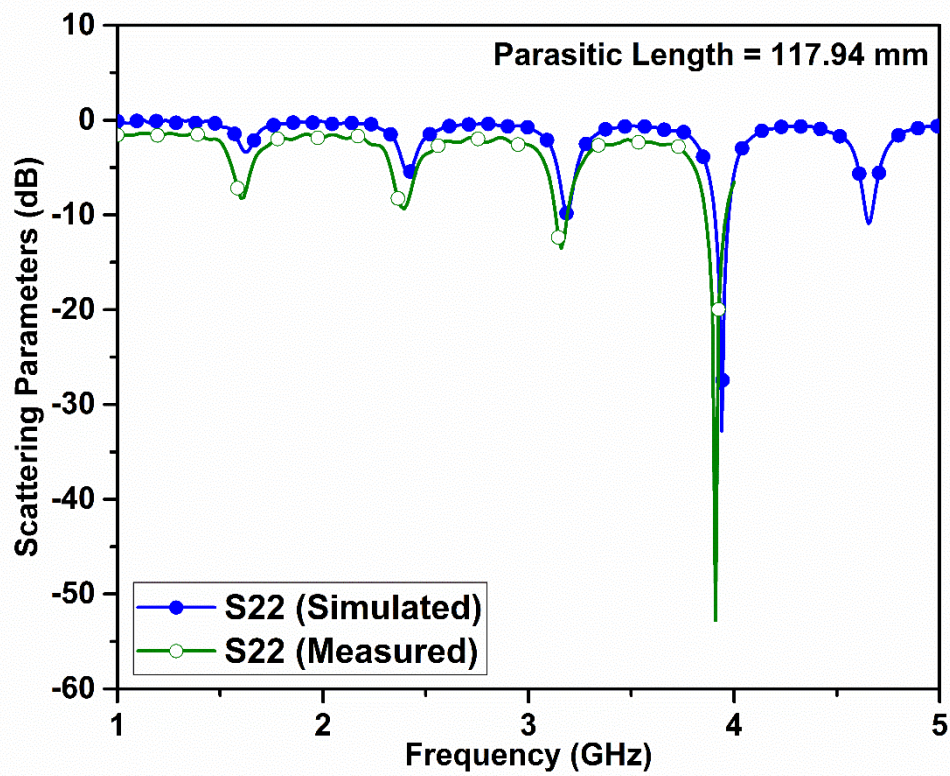


Figure 2.11 (f) Scattering parameters (S22) of MPA (parasitic length =117.94 mm)

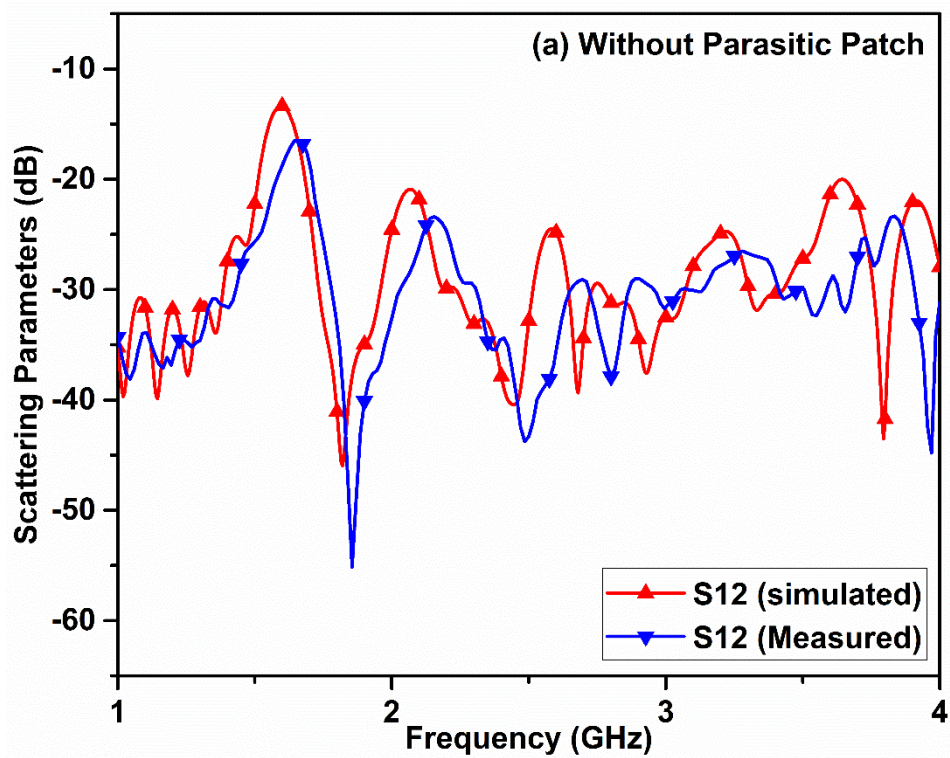


Figure 2.12 (a) Isolation between two MPA (without parasitic element)

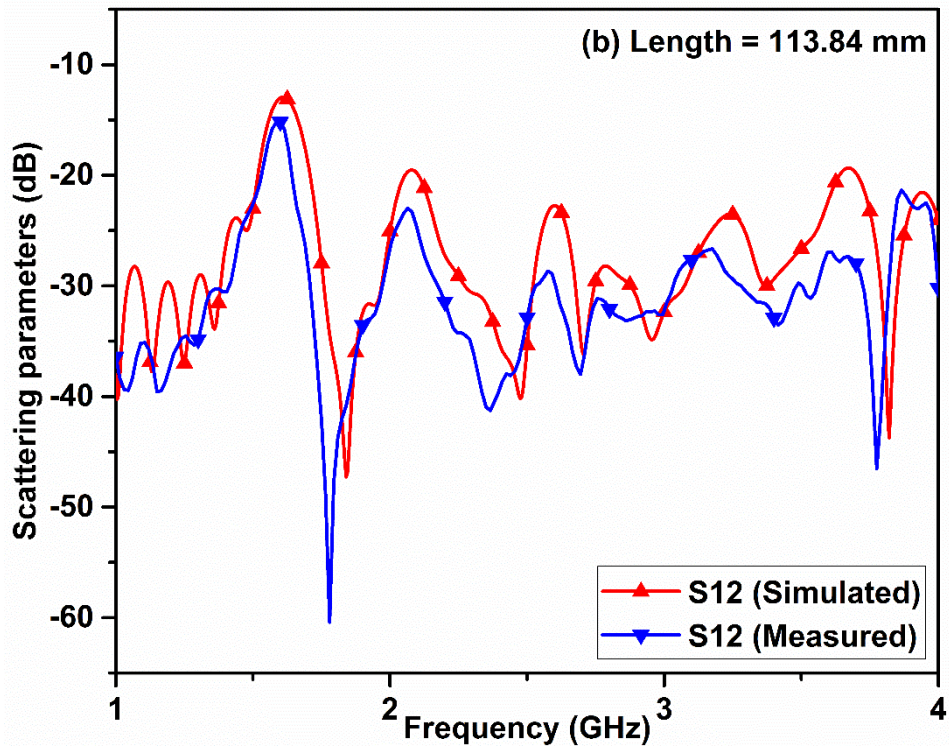


Figure 2.12 (b) Isolation between two MPA (parasitic length =113.84 mm)

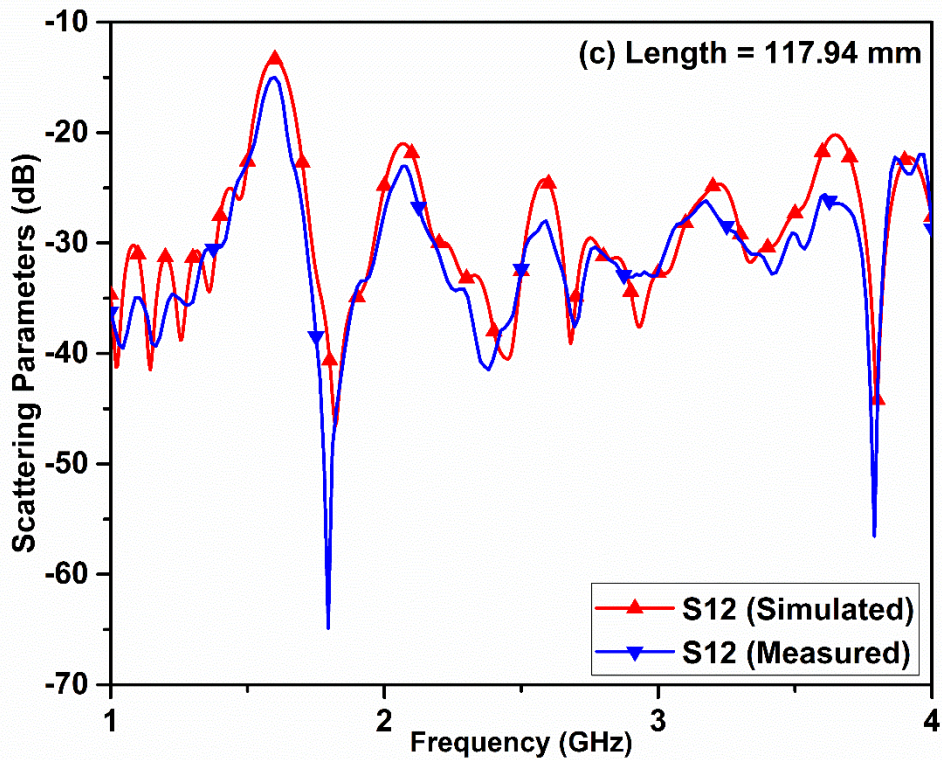


Figure 2.12 (c) Isolation between two MPA (parasitic length =117.94 mm)

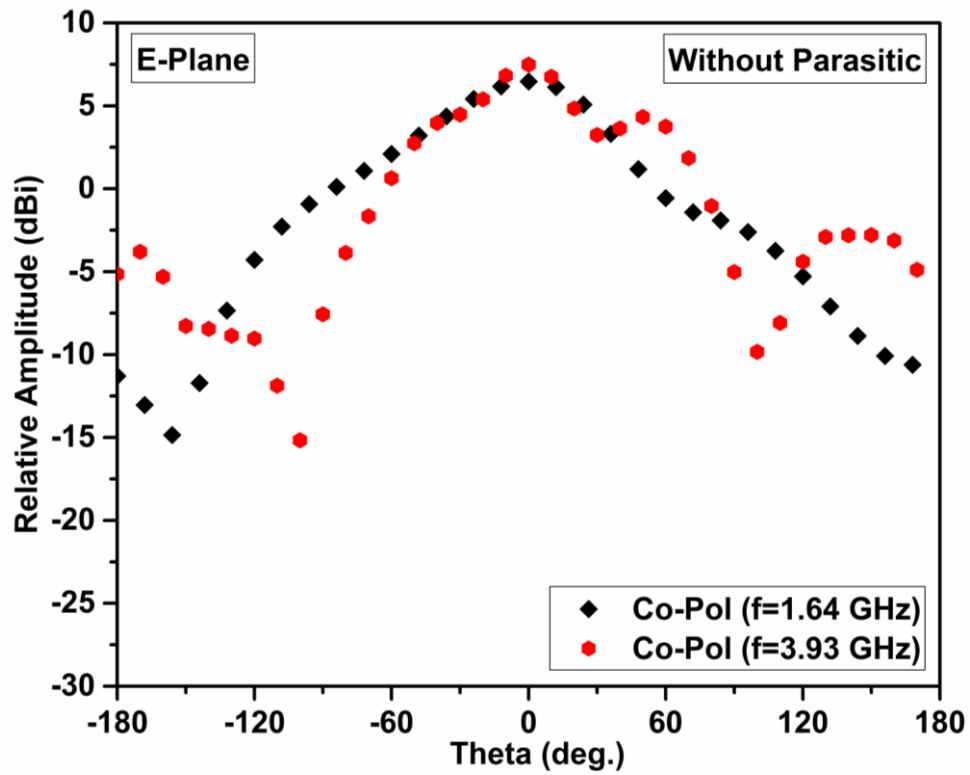


Figure 2.13 (a) Co-polar data of E-plane (without parasitic element)

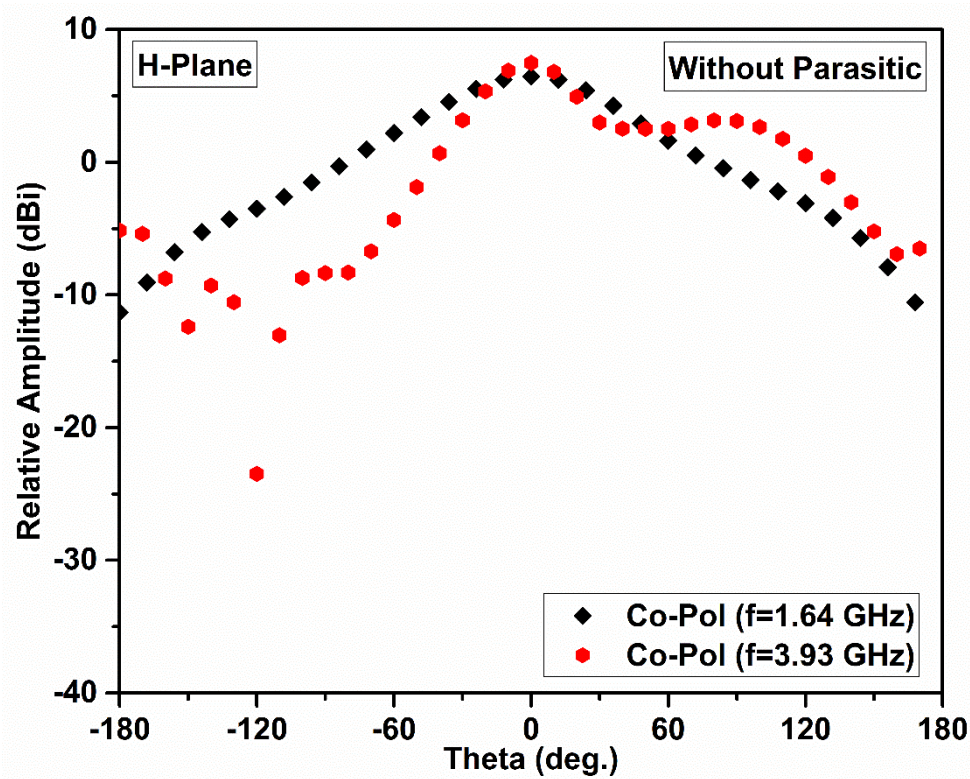


Figure 2.13 (b) Co-polar data of H-plane (without parasitic element)

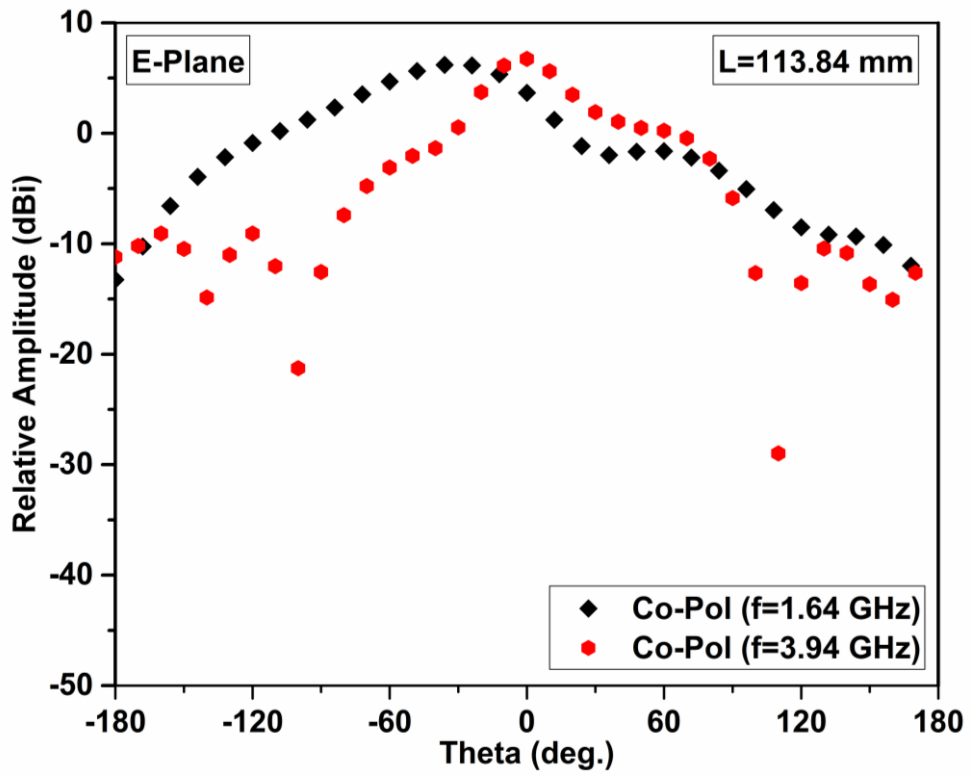


Figure 2.13 (c) Co-polar data of E-plane (parasitic length =113.84 mm)

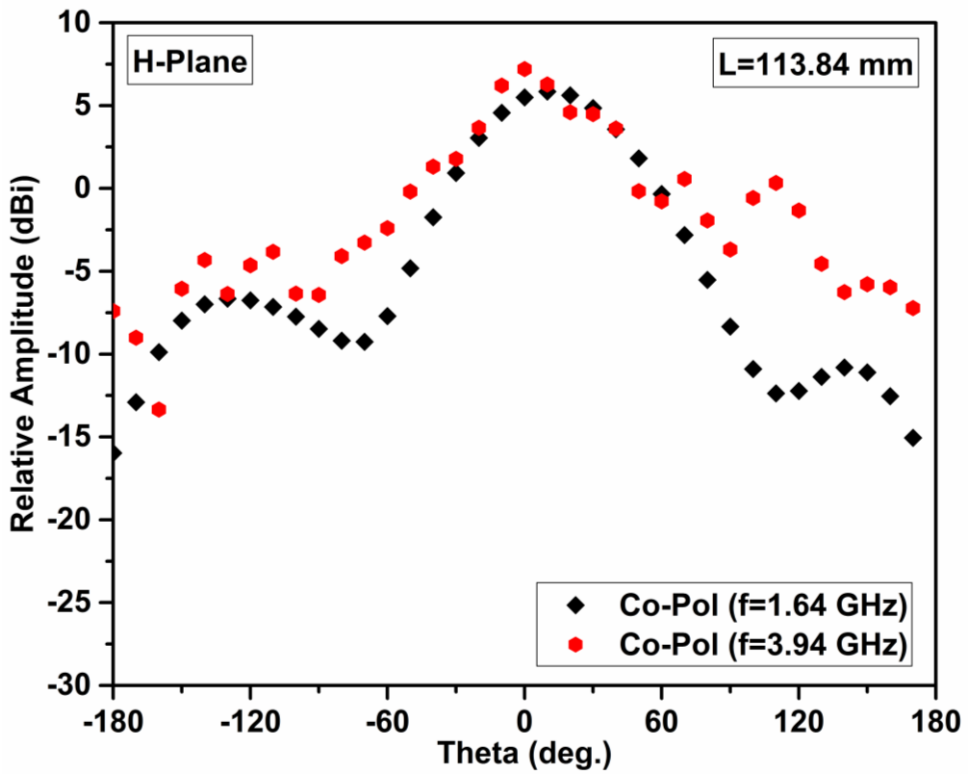


Figure 2.13 (d) Co-polar data of H-plane (parasitic length =113.84 mm)

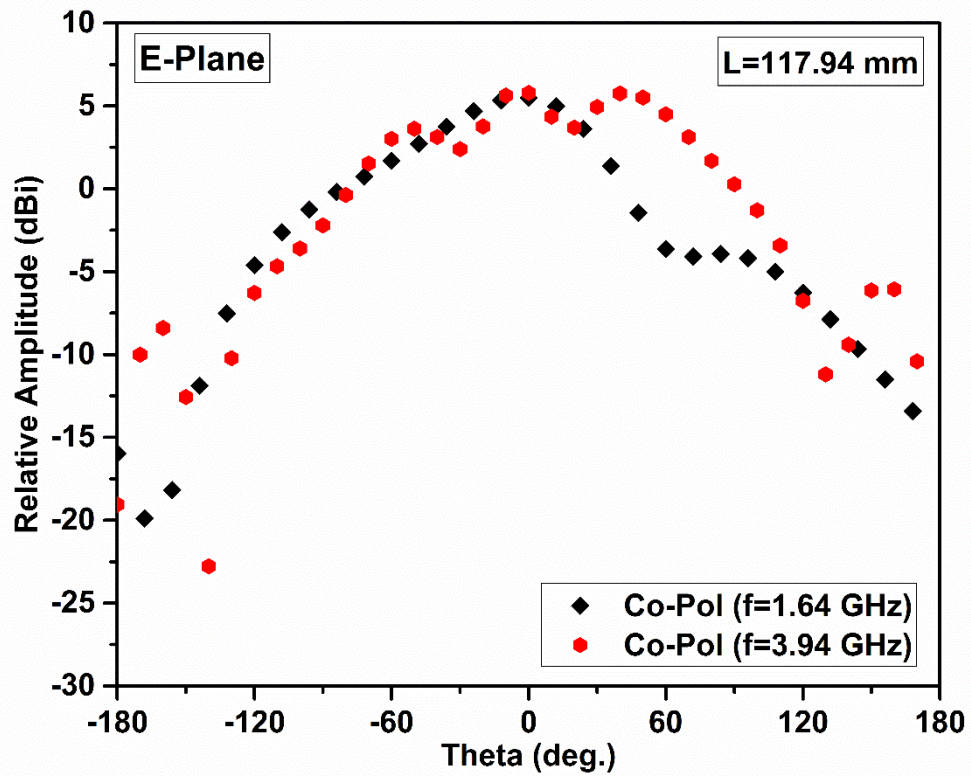


Figure 2.13 (e) Co-polar data of E-plane (parasitic length =117.94 mm)

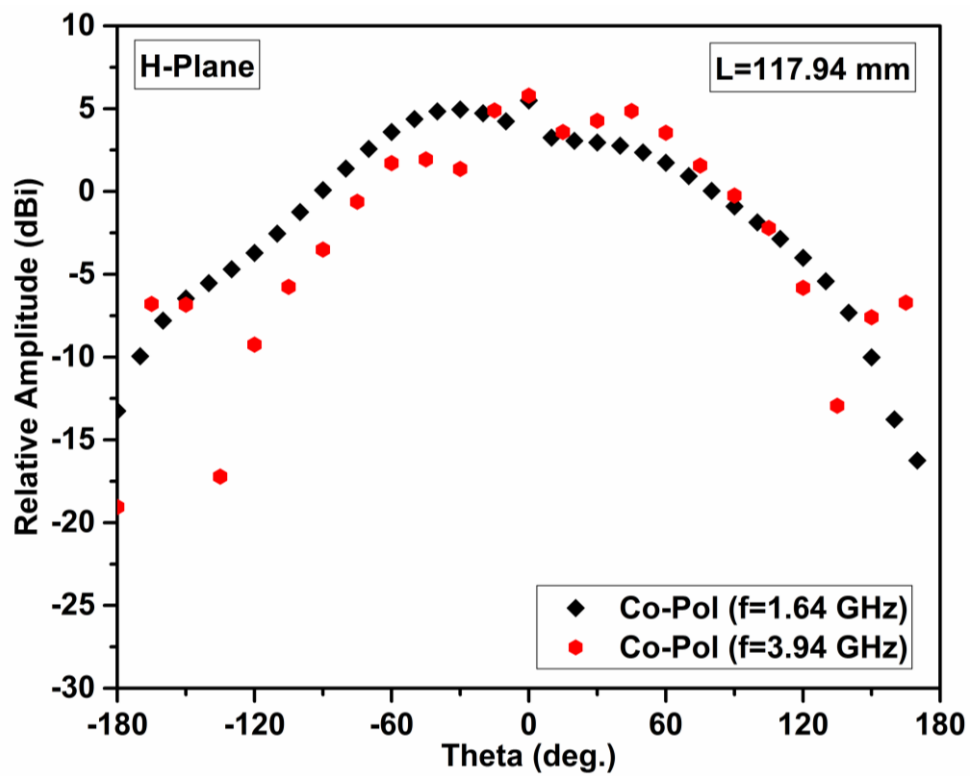


Figure 2.13 (f) Co-polar data of H-plane (parasitic length =117.94 mm)

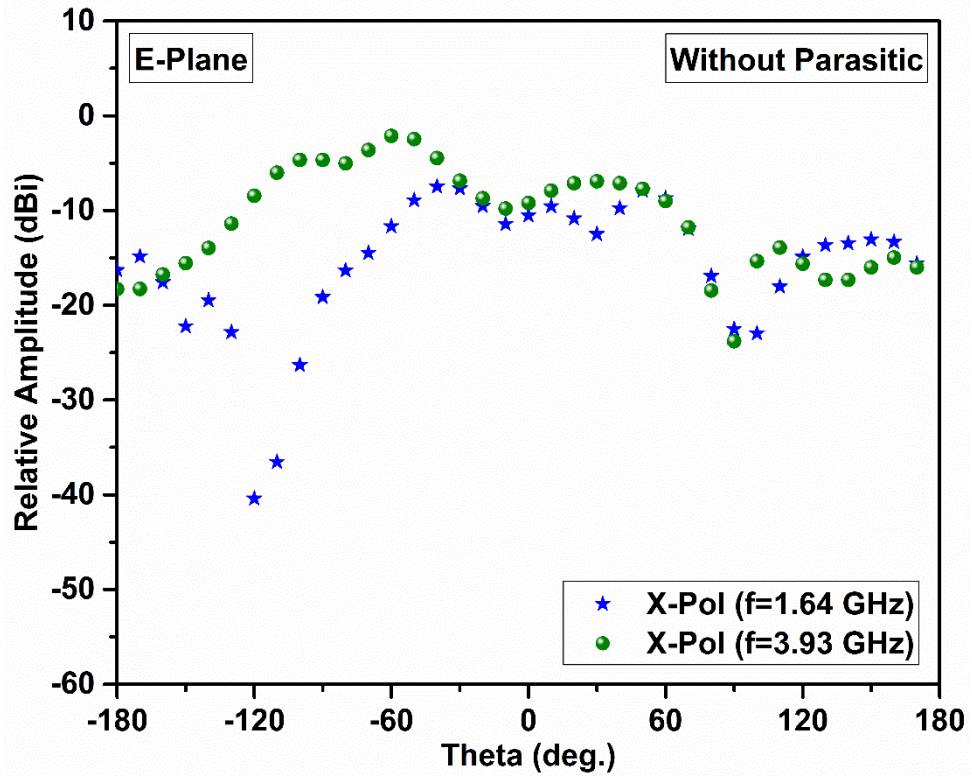


Figure 2.14 (a) Cross-polar data of E-plane (without parasitic element)

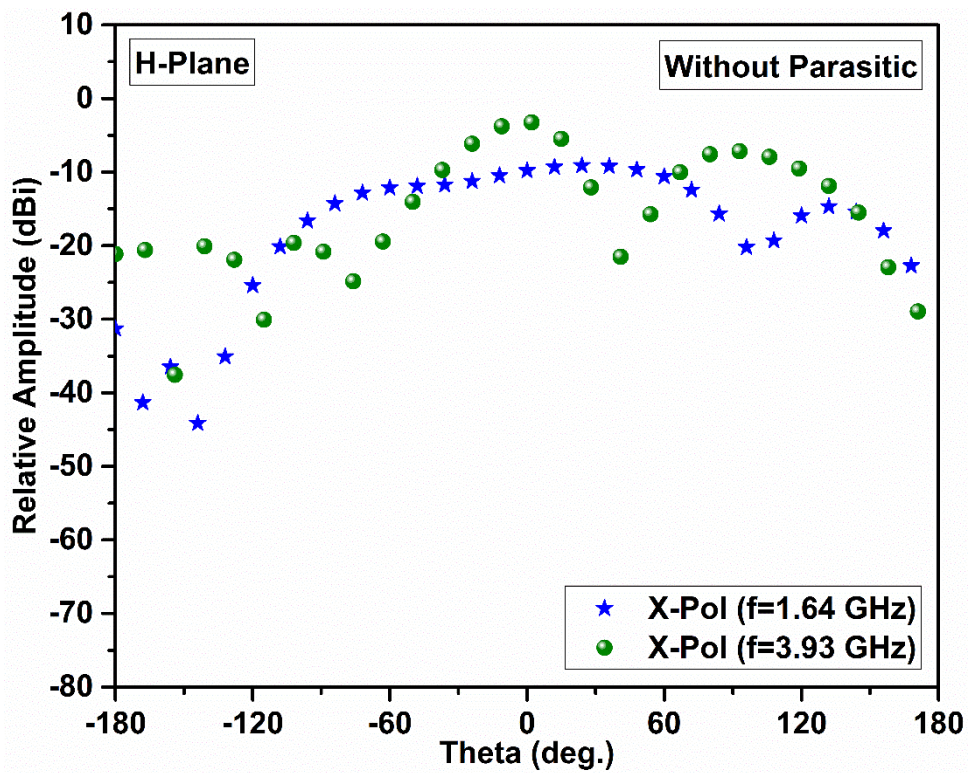


Figure 2.14 (b) Cross-polar data of H-plane (without parasitic element)

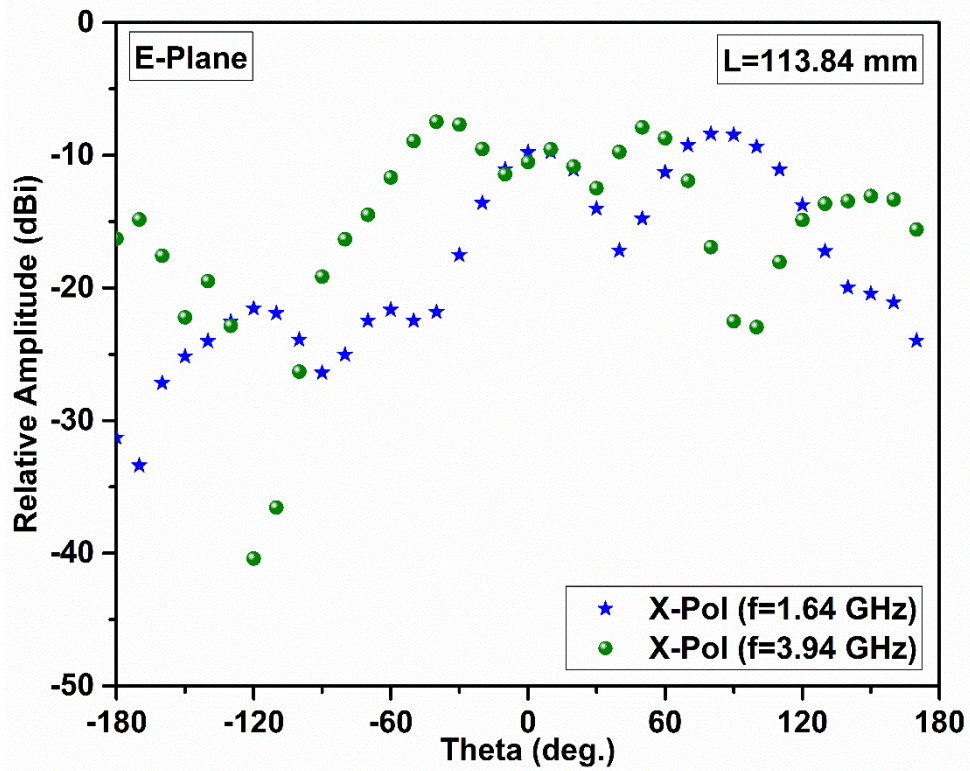


Figure 2.14 (c) Cross-polar data of E-plane (parasitic length =113.84 mm)

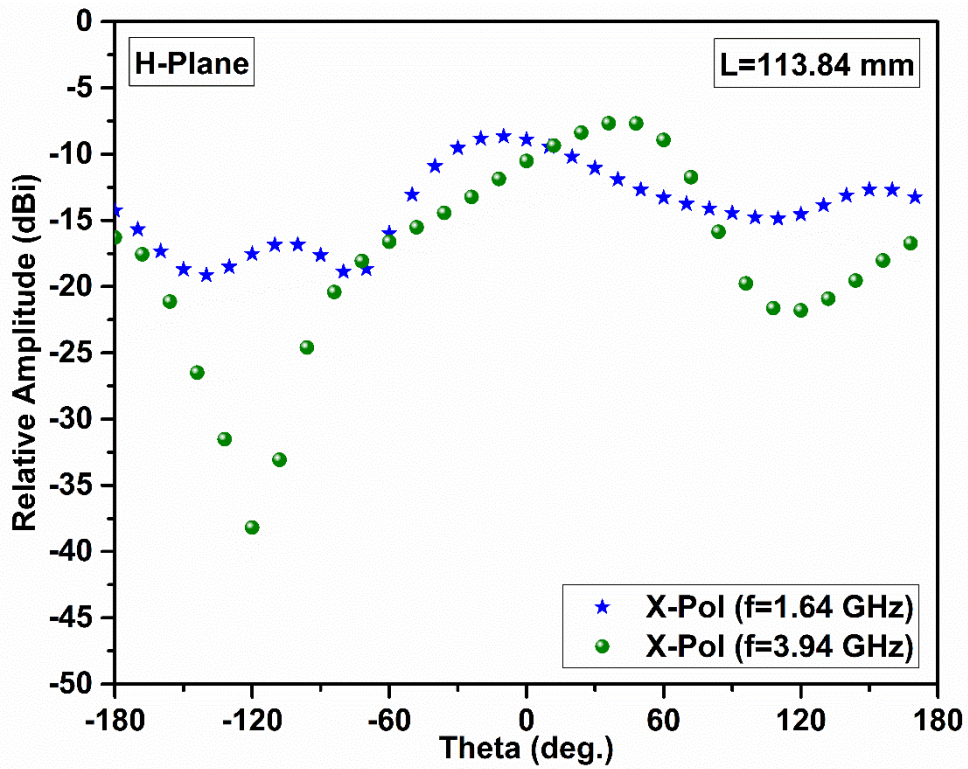


Figure 2.14 (d) Cross-polar data of H-plane (parasitic length =113.84 mm)

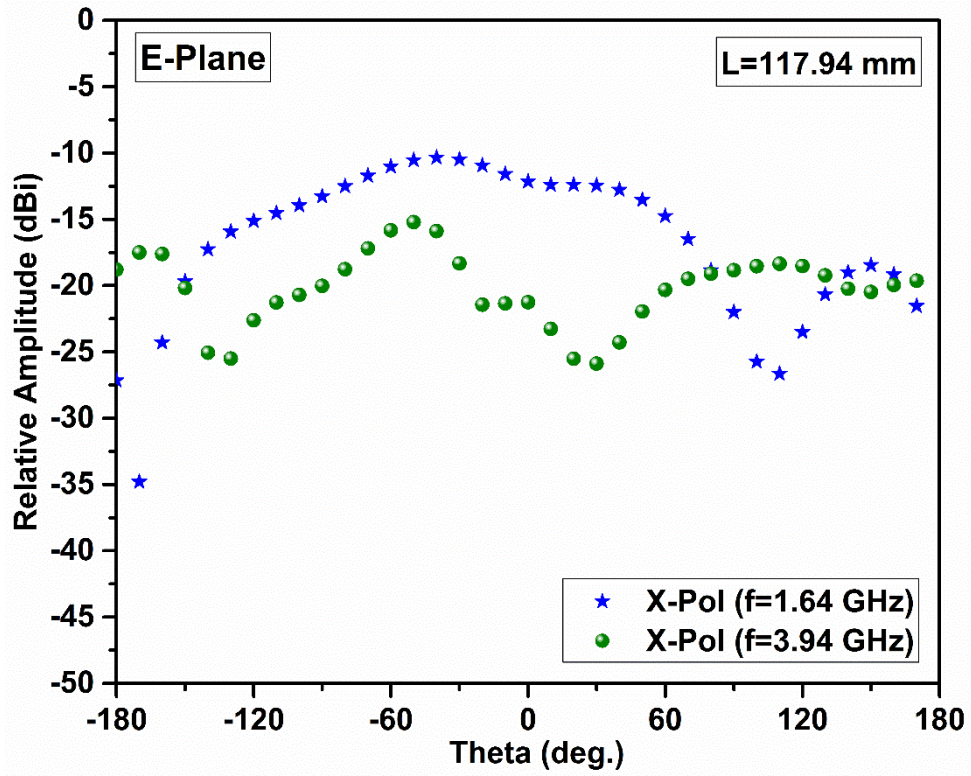


Figure 2.14 (e) Cross-polar data of E-plane (parasitic length = 117.94 mm)

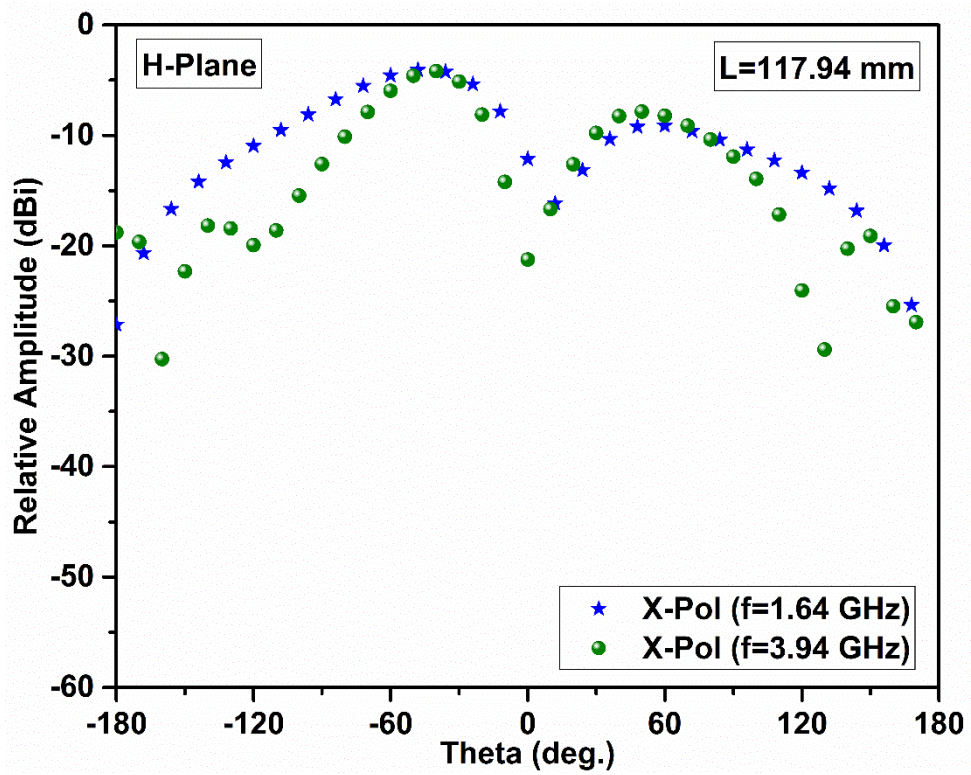


Figure 2.14 (f) Cross-polar data of H-plane (parasitic length = 117.94 mm)

**Table 2.4 (a)** Various parameters obtained from Swastika shaped MPA

Swastika-shaped patch antenna				
Parameters vs. Configuration		Without Coupling	With Coupling	
			Length = 113.84 mm	Length = 117.94 mm
Resonant Frequency (GHz)	Simulated	1.64	1.64	1.64
	Measured	1.63	1.57	1.58
Return Loss (dB)	Simulated	-28.41	-34.48	-41.55
	Measured	-29.75	-49.73	-39.30
Bandwidth (%)	Simulated	2.66	2.56	2.51
	Measured	5.4	4.19	8.07
Co-Polar (dBi)	E-Plane	6.46	3.67	5.49
	H-Plane	6.46	5.49	5.49
Cross-Polar (dBi)	E-Plane	-10.52	-9.78	-12.15
	H-Plane	-9.78	-8.89	-12.15

**Table 2.4 (b)** Various parameters obtained from Seven (7) shaped MPA

Seven (7)-shaped patch antenna				
Parameters vs. Configuration		Without Coupling	With Coupling	
			Length = 113.84 mm	Length = 117.94 mm
Resonant Frequency (GHz)	Simulated	3.93	3.94	3.94
	Measured	3.26	3.88	3.91
Return loss (dB)	Simulated	-28.90	-40.45	-32.79
	Measured	-37.87	-37.82	-52.78
Bandwidth (%)	Simulated	1.78	1.74	1.72
	Measured	3.30	2.68	2.58
Co-Polar (dBi)	E-Plane	7.48	6.47	5.78
	H-Plane	7.48	7.2	5.78
Cross-Polar (dBi)	E-Plane	-9.19	-10.52	-21.25
	H-Plane	-3.16	-10.52	-21.25

The comparative study shows that the resonating frequencies are almost the same in all configurations i.e. for antenna without and with parasitic elements. However, significant changes were observed in scattering parameters for both the antennas corresponds to both bands. The S11 values changed from -28.41 dB to -41.55 dB for simulated data and from -29.75 dB to -49.73 dB for measured data corresponds to L-band (i.e. for the “Swastika” shaped patch) due to the presence of the parasitic element. Similarly, the S22 values changed from -28.90 dB to -40.45 dB for simulated data and from -37.87 dB to -52.78 dB for measured data corresponds to S-band (i.e. for 7-shaped patch). The maximum bandwidth of 8.07% was obtained in measured data corresponds to “Swastika” shaped patch antenna (L-band), due to presence of parasitic element of length 117.94 mm. Where the “parasitic” element affected the overall impedance due to the change in capacitance closed to Swastika shaped patch along with isolation value of better than -15dB. Cross-polarization was improved among all the antennas due to parasitic elements, but overall gain performance was not good when compared with antenna in the absence of parasitic element. Which may be due to the presence of both the resonating elements in proximity of each other.

### **2.4 Parasitic Patch Antenna**

Here, In this design “multifunctionality” of the system is done using an aperture sharing technique. A hollow “square” shape (after rotation) is used as a base element for patch antenna. The said structure was transformed into four parts after removing two “rectangular” notches (horizontally and vertically). The said resulted configuration was comprising two probe fed radiating elements/patches along with two parasitic elements/patches. “Probe feeding” using a vertical port thru the dielectric substrate was accomplished. The complete assembly was designed and fabricated using a square-shaped substrate (having adjusted measurements). Some reduction in coupling was observed due to the existence of “parasitic” elements/patches. The length/width of the above-mentioned radiating sections was close to half of the wavelength, though, approximately optimization was accomplished in the structures of the said antenna. The proposed prototype of the antenna was designed to work in L/S bands concurrently.

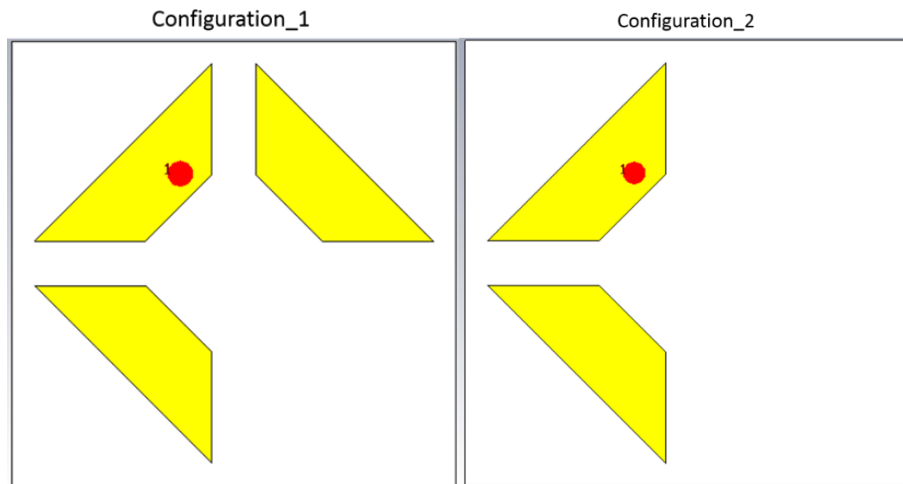


**Figure 2.15 (a)** Configuration 1 & 2 of the designed structure

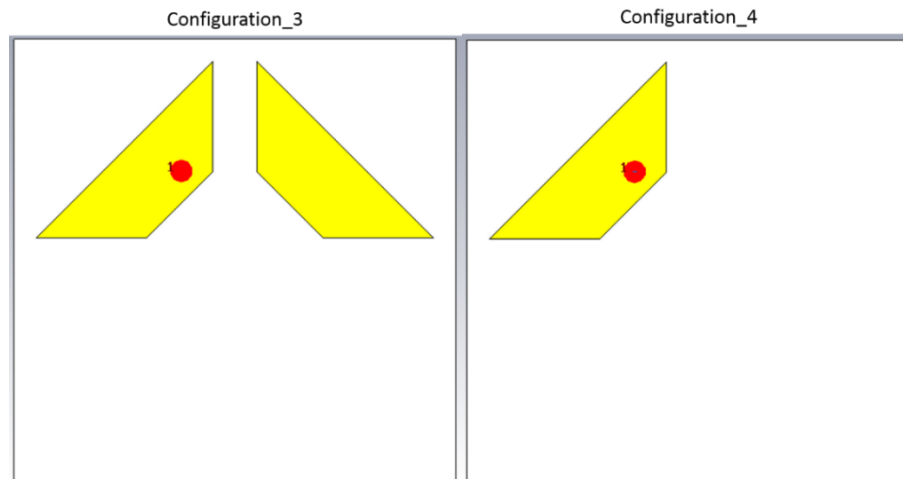


**Figure 2.15 (b)** Configuration 3 & 4 of the designed structure

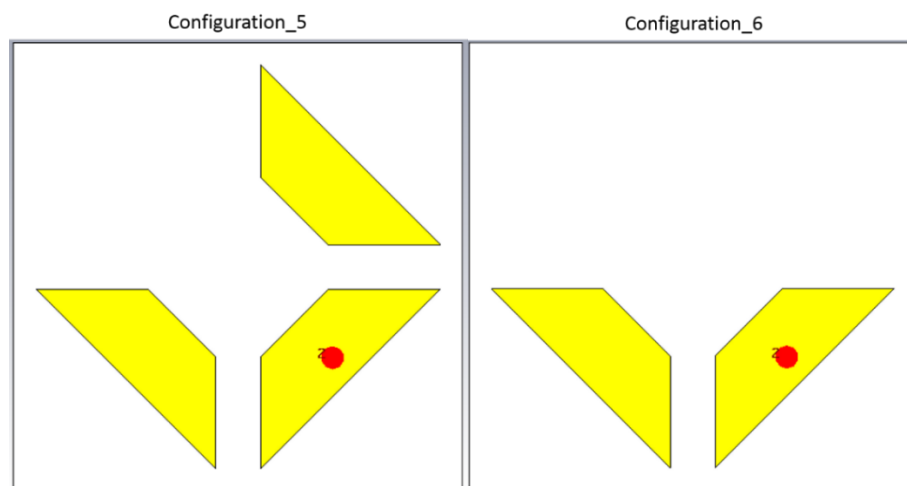


**Figure 2.15 (c)** Configuration 5 & 6 of the designed structure

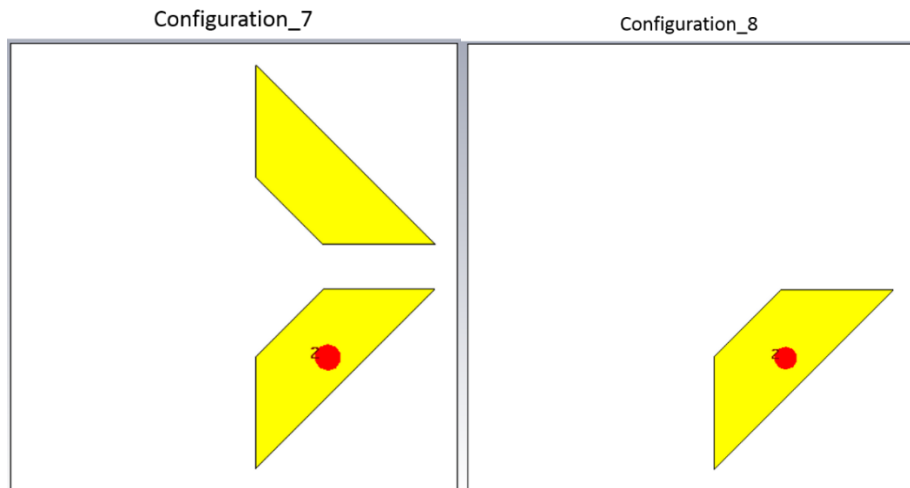


**Figure 2.15 (d)** Configuration 7 & 8 of the designed structure

As the basic design was started from a square shape, so the antenna performance of both the antennas was observed separately. Firstly, we observed each antenna performance in the presence as well as the absence of parasitic elements. Then the performance of both the antennas was observed in the absence of parasitic elements, to observe the effect on antenna performance.

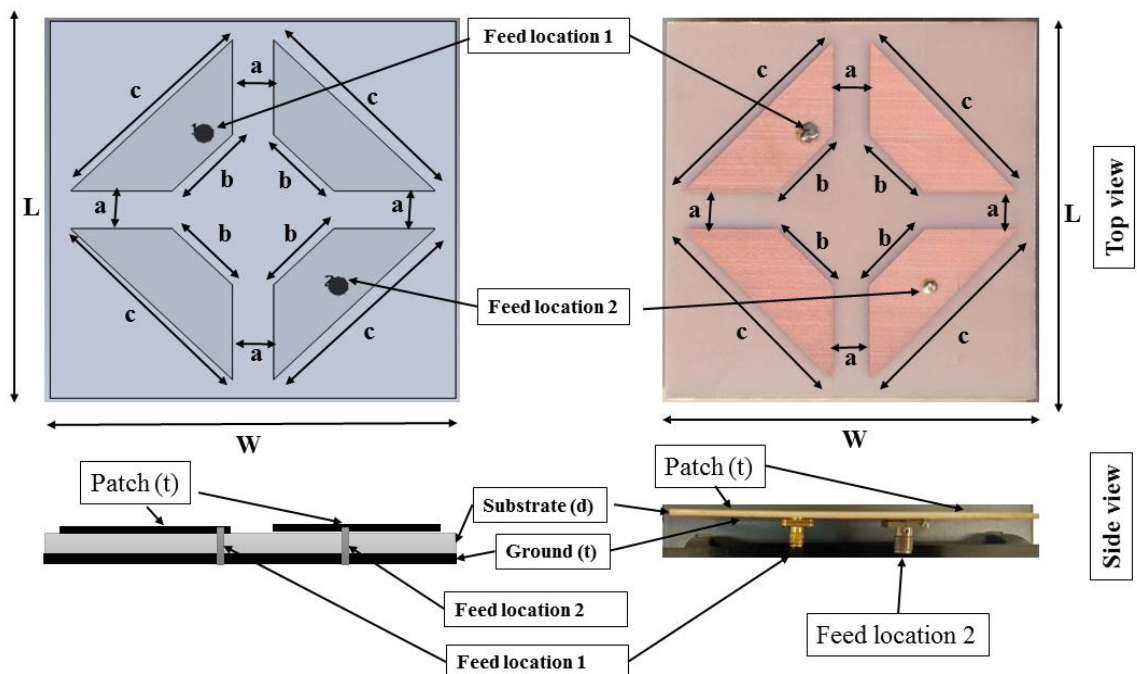


**Figure 2.16** Basic configuration of the proposed parasitic patch antenna

Finally, for comparative study overall performance was carried out in the presence of both the parasitic elements. A reasonable change was observed in the performance of both the antenna when compared with antenna performance separately. The basic steps for measurement are shown in fig. 2.15 (a to d). The basic configuration of the final proposed antenna is shown in fig. 2.16 along with basic parameters (table 2.5). The “L” and “W” are the length/width of the substrate, “d” and “t” are the thinness of substrate & patch respectively. The feed location was calculated using the basic equation and are shown in table 1.1.

**Table 2.5** Description and numeric design values of the MPA

Sr. No.	Variable	Design Values (in mm)
1.	a	10 mm
2.	b	5.6 times of a
3.	c	2.1 times of a
4.	d	1.6 mm
5.	t	0.06 mm
6.	L	9.9 times of a
7.	W	9.9 times of a

### 2.4.1 Results and Discussion

The MPA structure was designed by using commercially available “FR-4 (dielectric substrate)”. The upper-left MPA was designed to resonate in L-band and MPA placed on the lower-right side was designed to resonate in S-band. The basic parameters as obtained from different configurations of fig. 2.15 (a to d) are exposed in fig. 2.17 (a to h) and 2.18 (a to h) corresponds to scattering as well as far-field parameters respectively. The as-obtained

measured/simulated scattering (S11 & S22) parameters for the finally designed antenna are shown below in fig. 2.19 (a & b). The measured data/results were comparatively similar to the simulated results/data. Isolation better than 18 dB was achieved (fig. 2.20) due to the existence of two “parasitic” elements. The Co/Cross-Polarization of both the antennas in E/H-planes (separately) and are shown in below-mentioned fig. 2.21 (a) to (d). Table 2.6 giving a brief description of the comparative analysis for all obtained data.

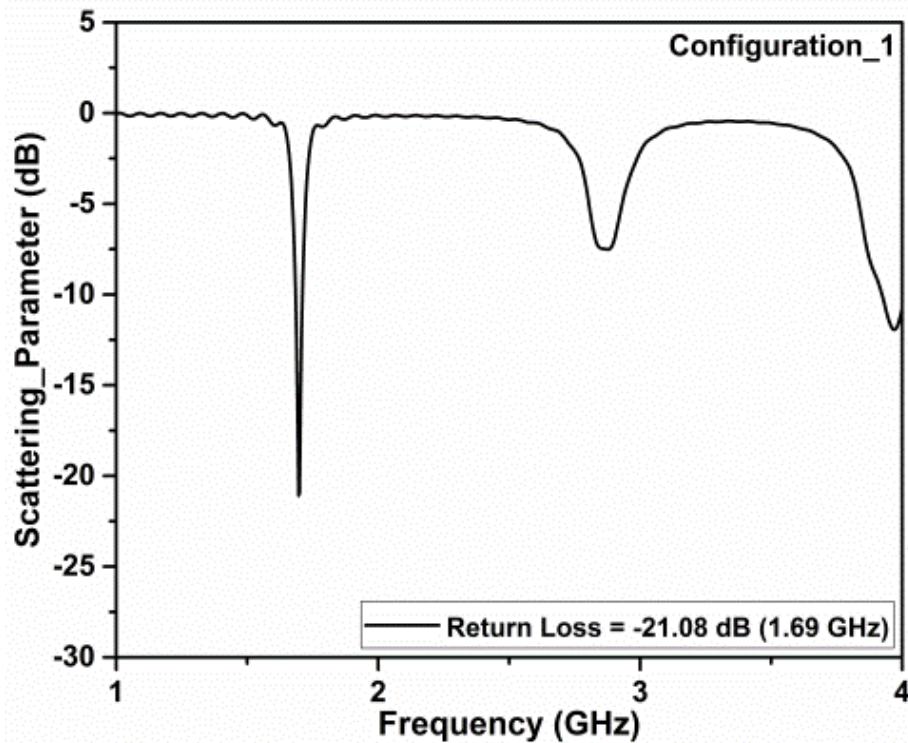


Figure 2.17 (a) Scattering parameters for configuration\_1

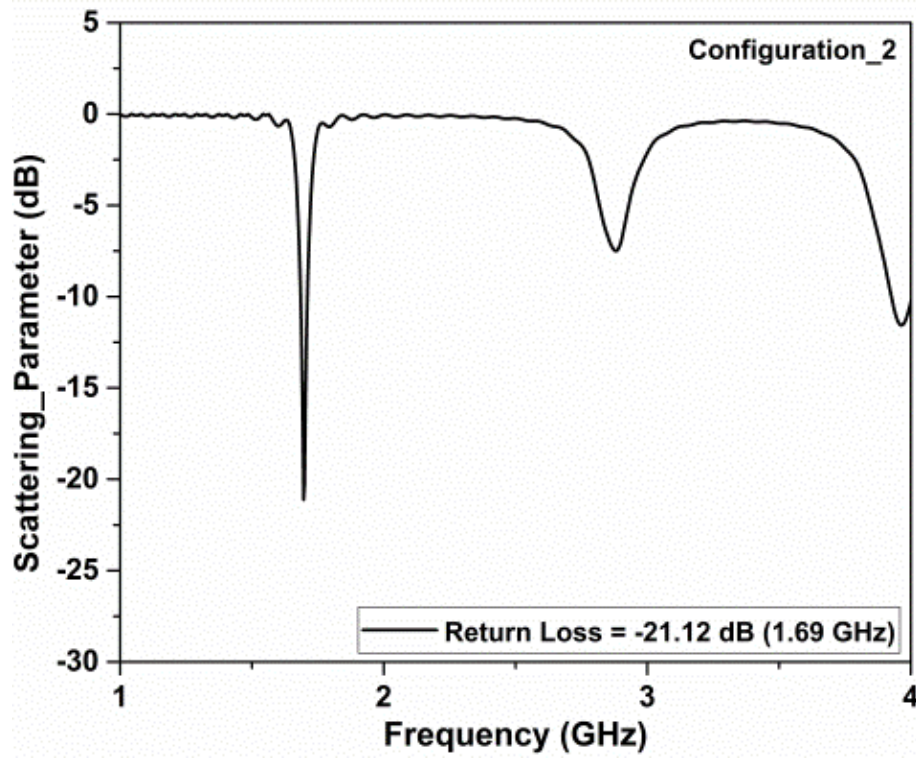


Figure 2.17 (b) Scattering parameters for configuration\_2

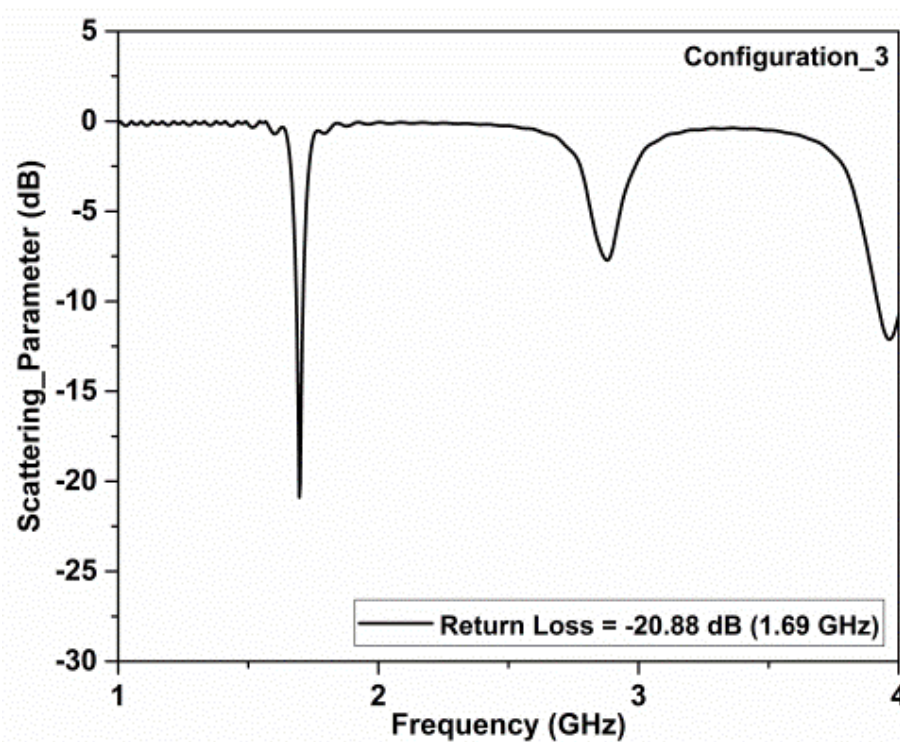


Figure 2.17 (c) Scattering parameters for configuration\_3

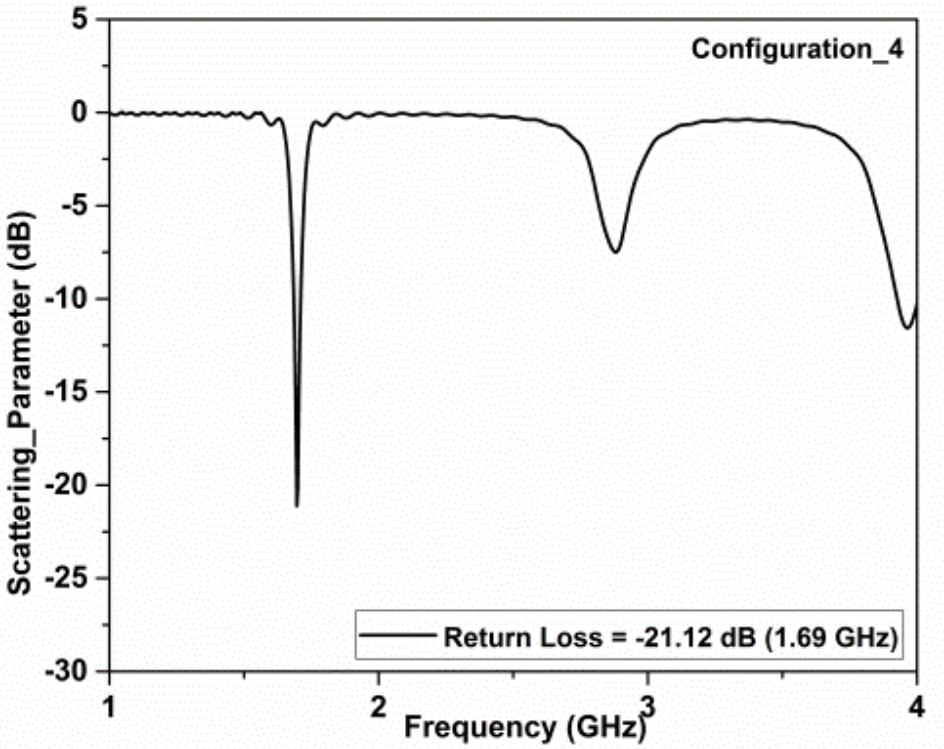


Figure 2.17 (d) Scattering parameters for configuration\_4

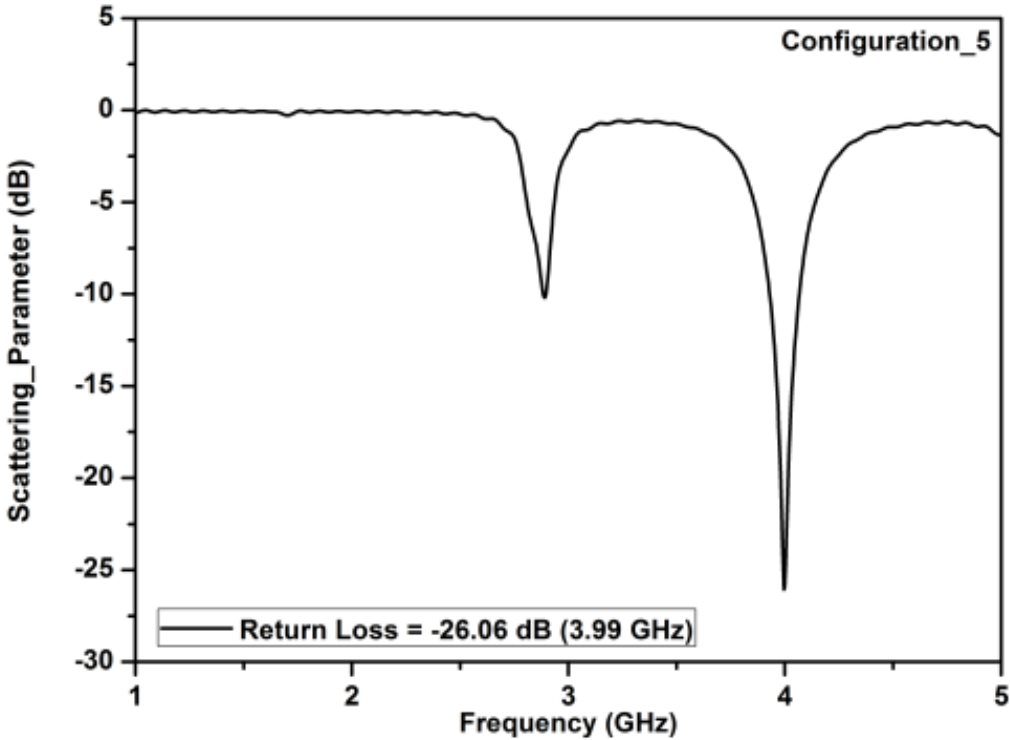


Figure 2.17 (e) Scattering parameters for configuration\_5

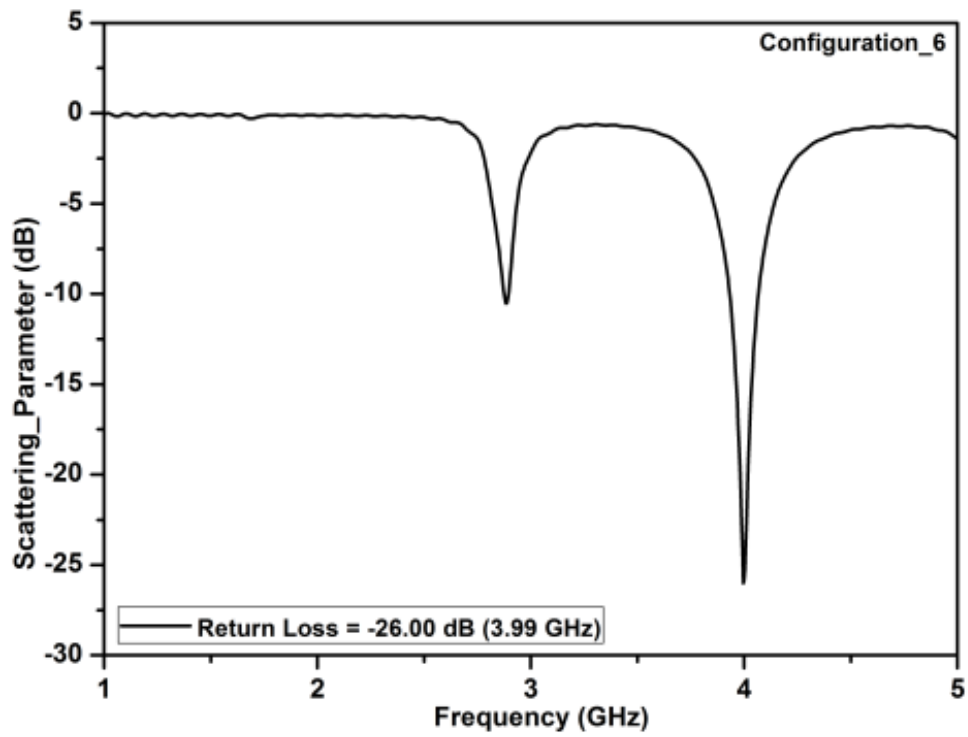


Figure 2.17 (f) Scattering parameters for configuration\_6

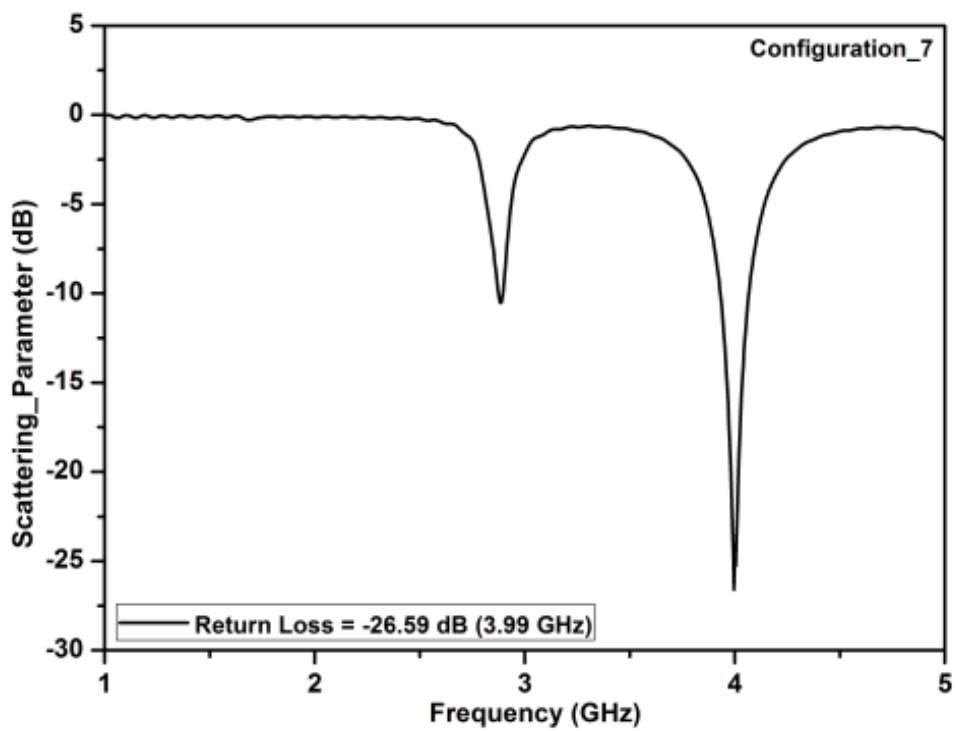


Figure 2.17 (g) Scattering parameters for configuration\_7

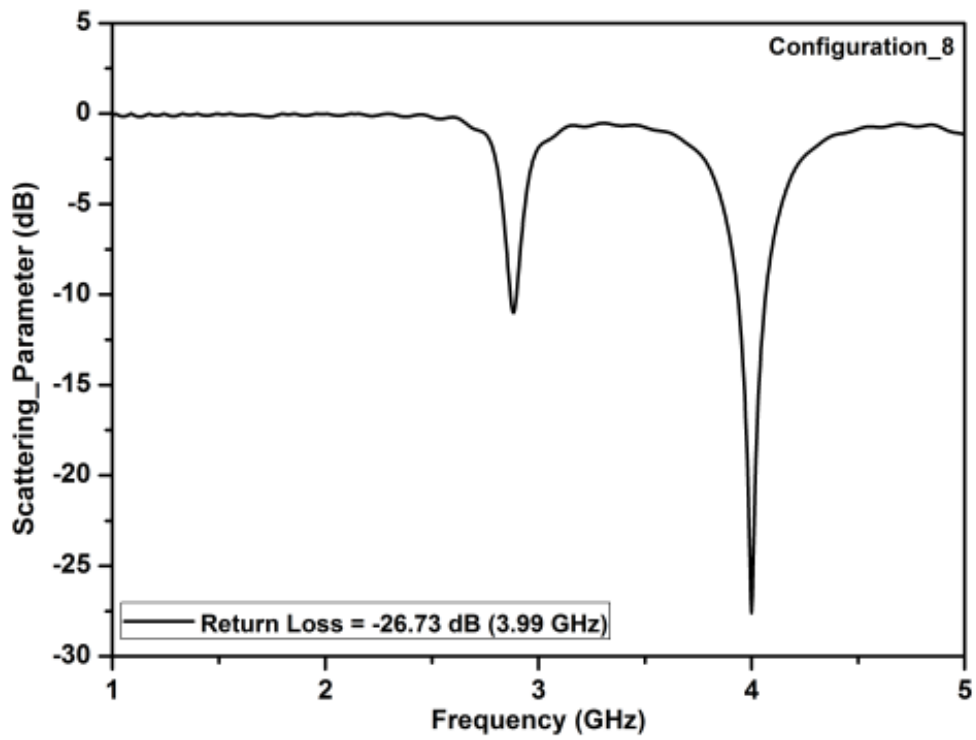


Figure 2.17 (h) Scattering parameters for configuration\_8

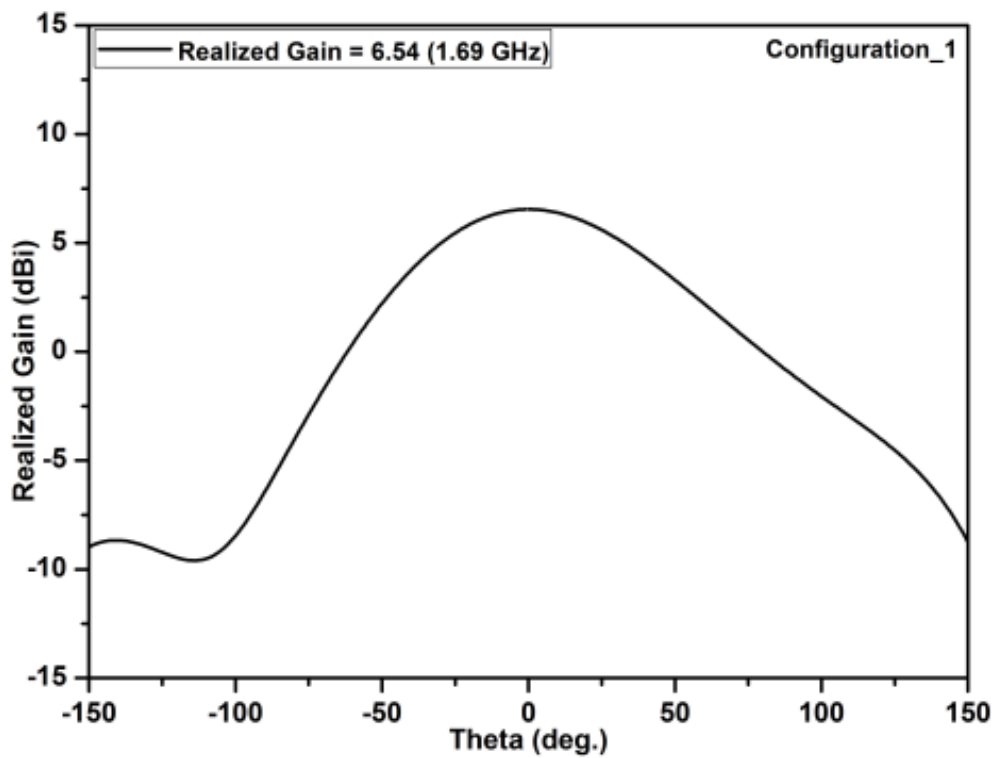


Figure 2.18 (a) Realized gain for configuration\_1

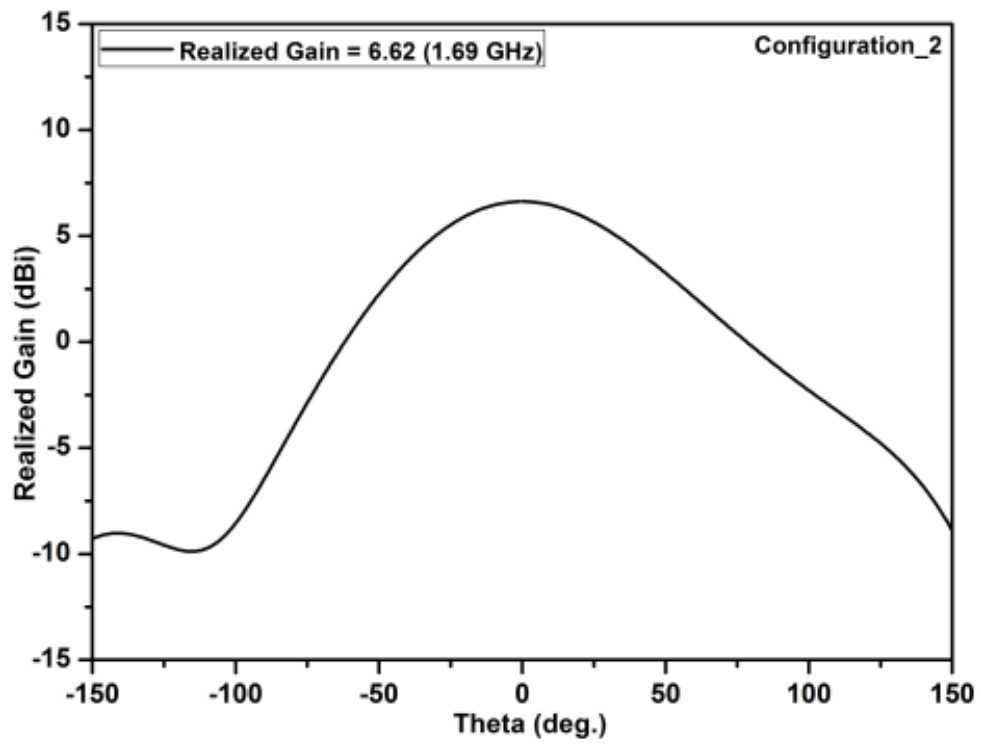


Figure 2.18 (b) Realized gain for configuration\_2

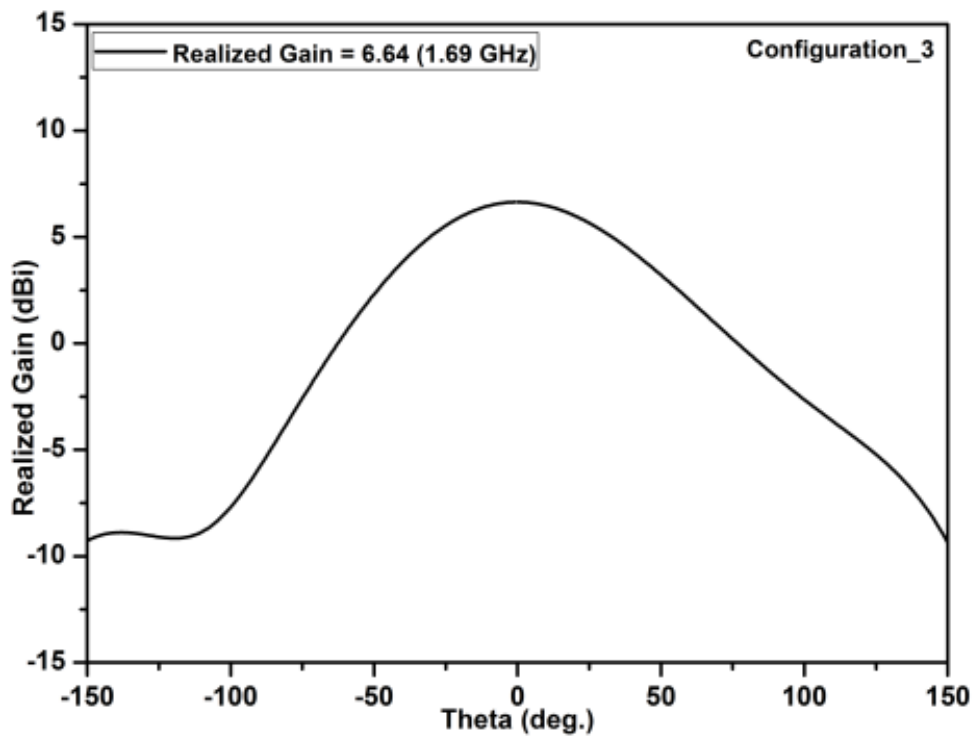


Figure 2.18 (c) Realized gain for configuration\_3

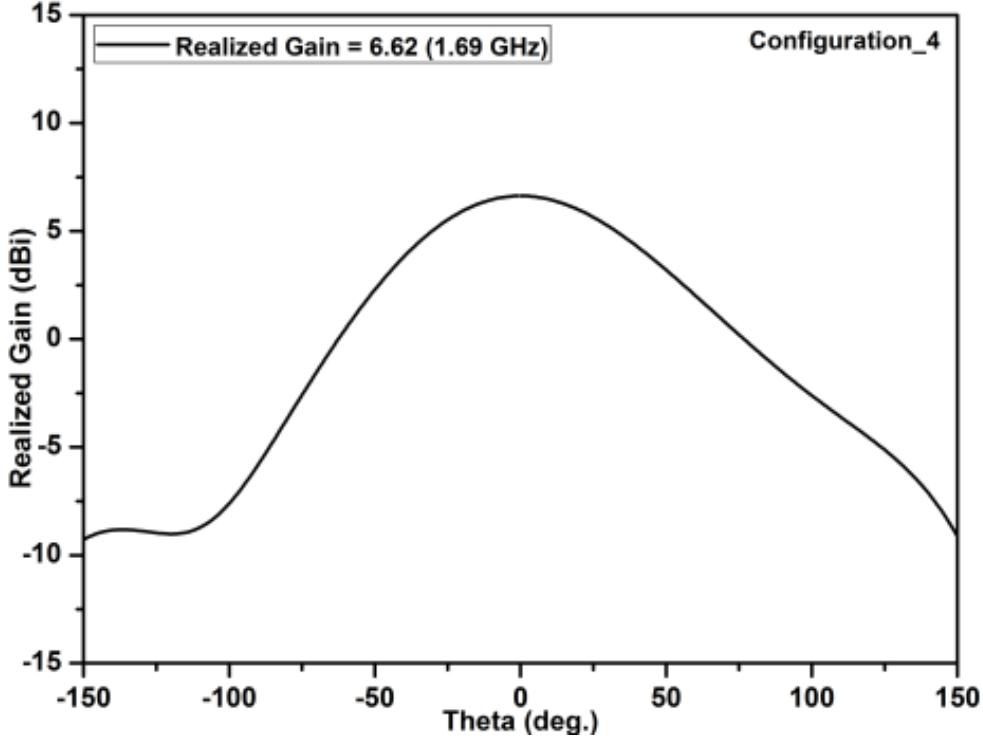


Figure 2.18 (d) Realized gain for configuration\_4

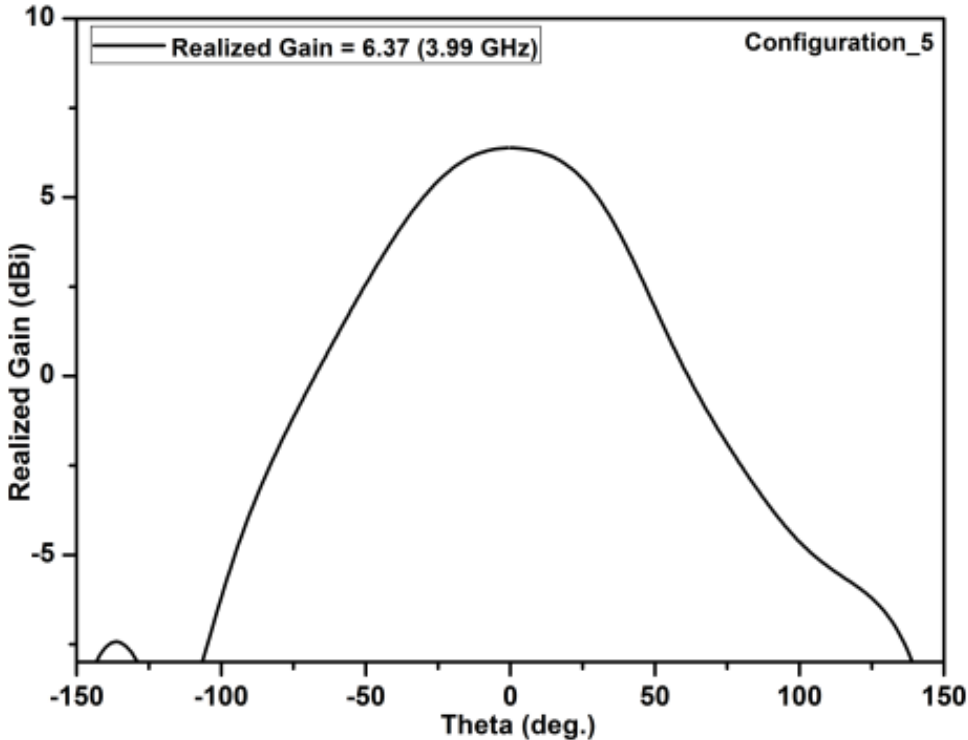


Figure 2.18 (e) Realized gain for configuration\_5

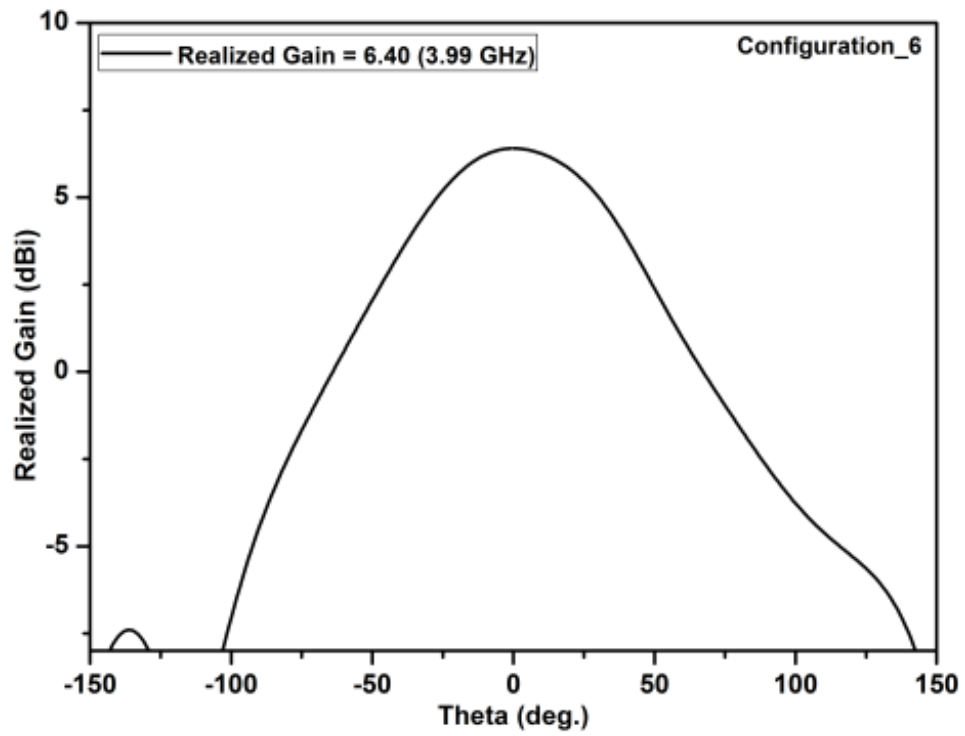


Figure 2.18 (f) Realized gain for configuration\_6

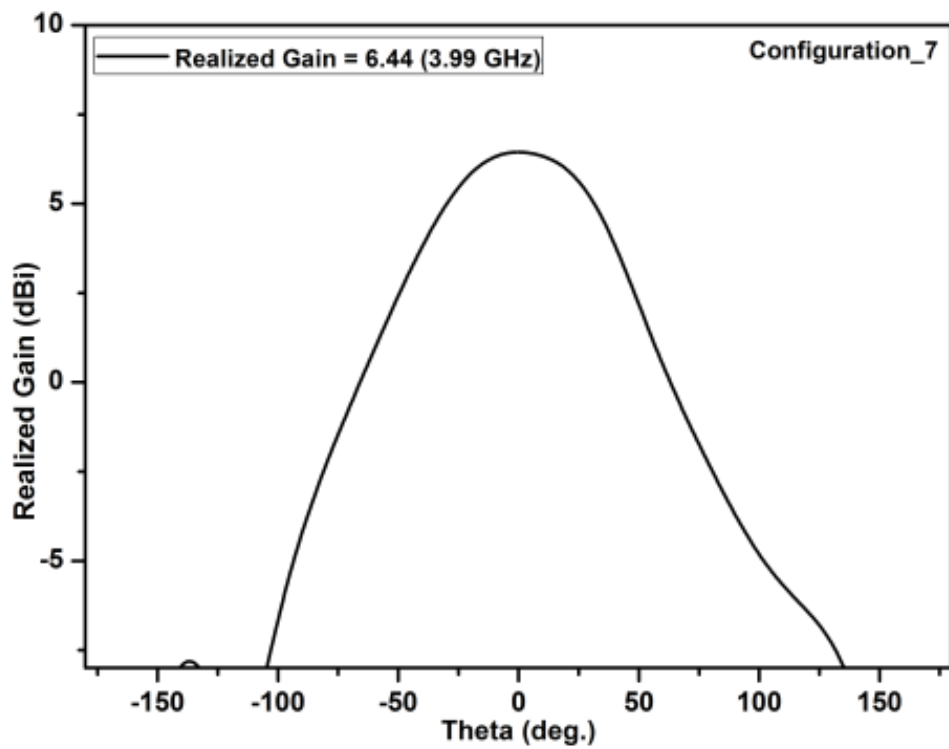


Figure 2.18 (g) Realized gain for configuration\_7

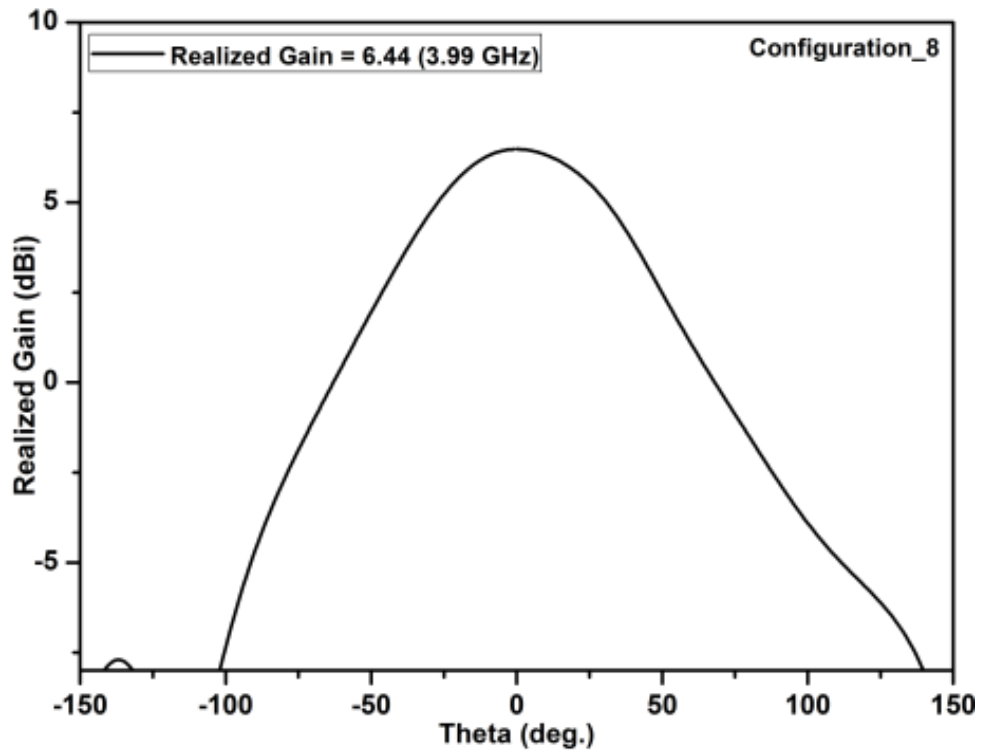


Figure 2.18 (h) Realized gain for configuration\_8

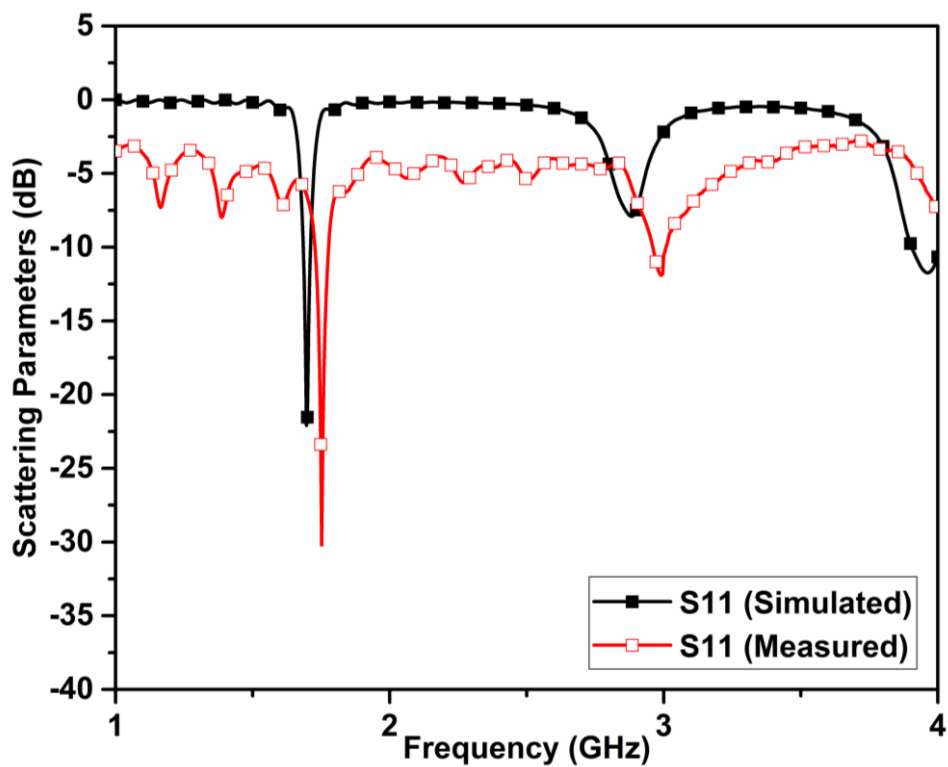


Figure 2.19 (a) Scattering parameters (S11) of MPA

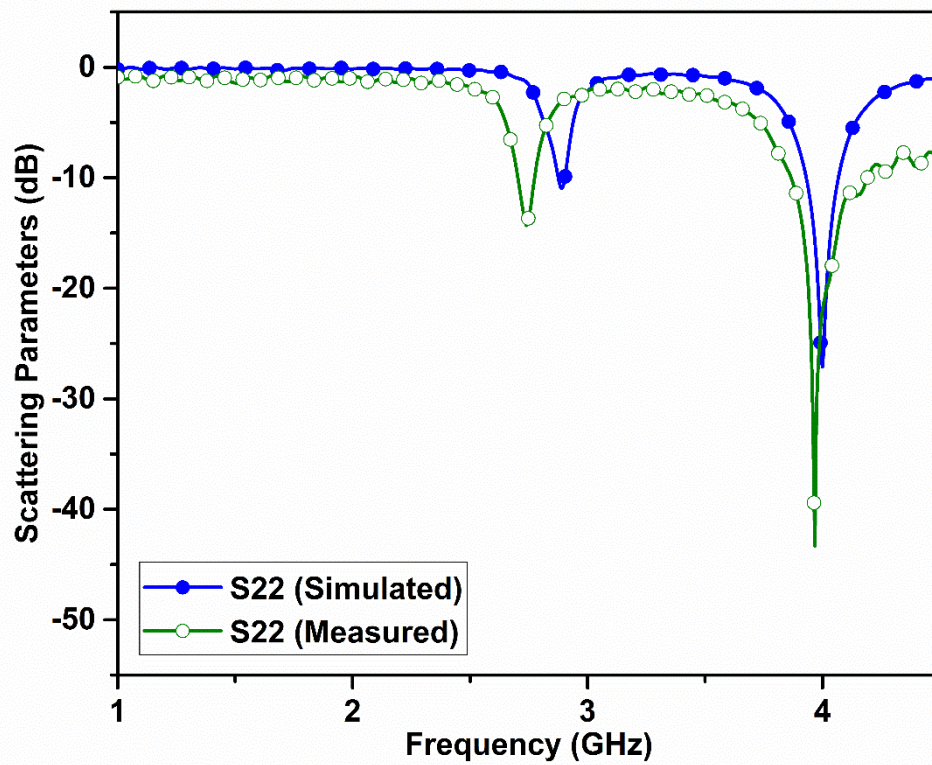


Figure 2.19 (b) Scattering parameters (S22) of MPA

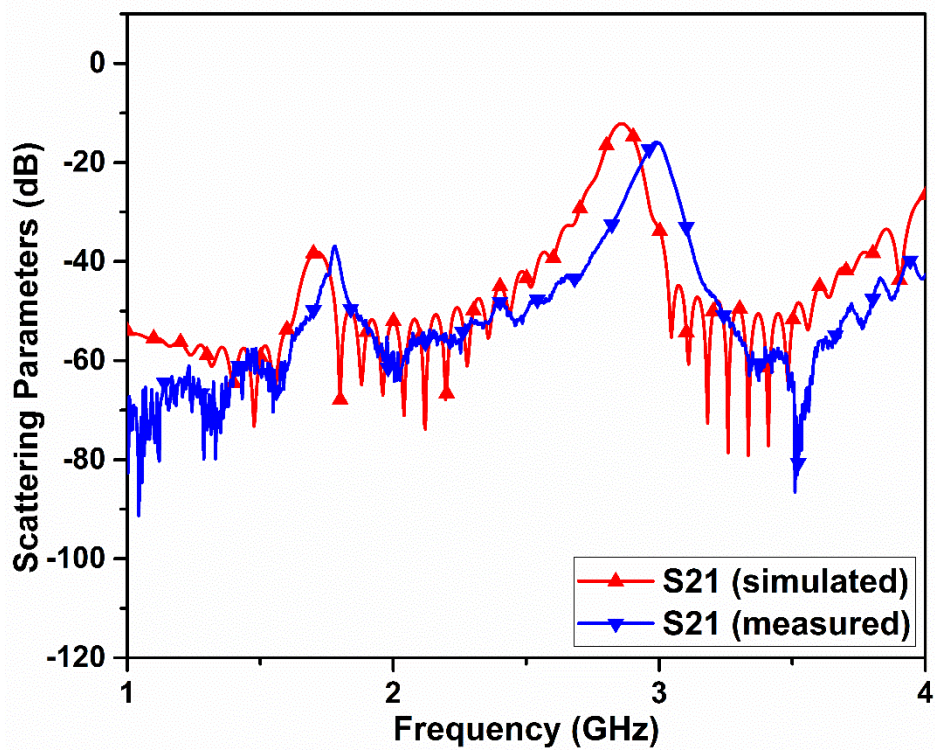


Figure 2.20 Isolation between two MPA

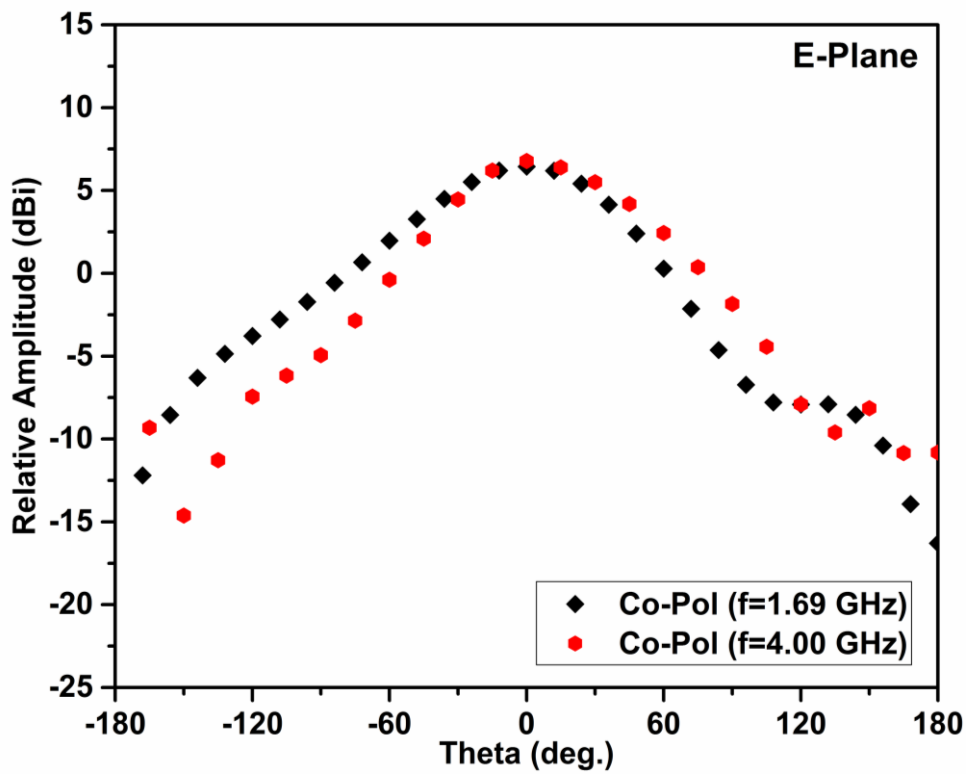


Figure 2.21 (a) Co/Cross polar plot for E-Plane

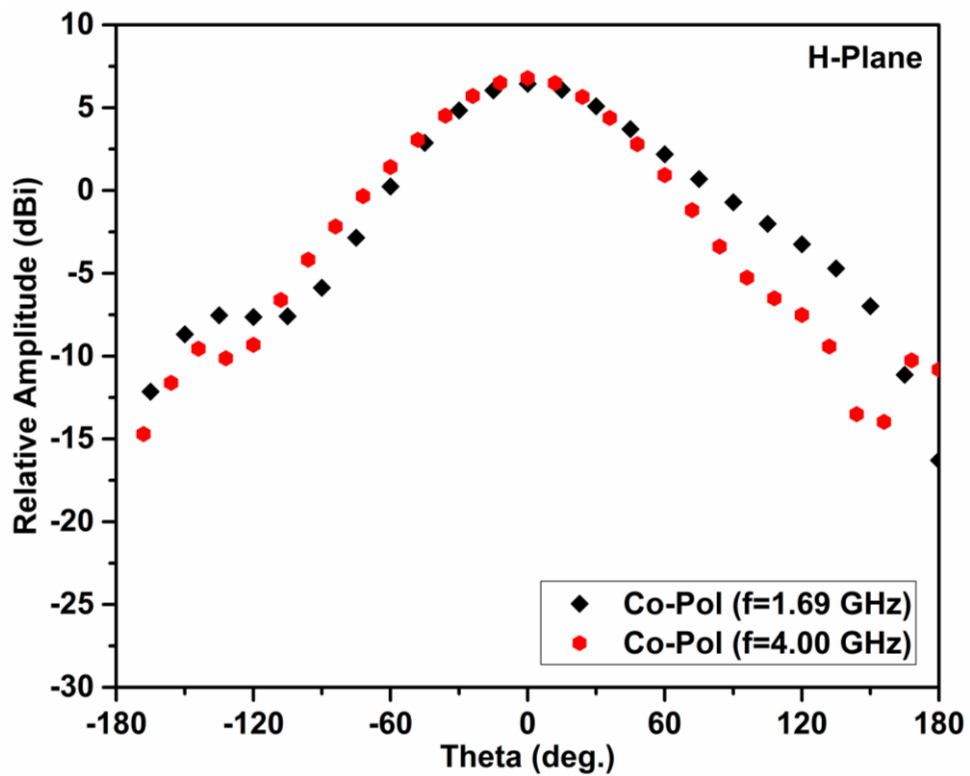


Figure 2.21 (b) Co polar plot for H-Plane

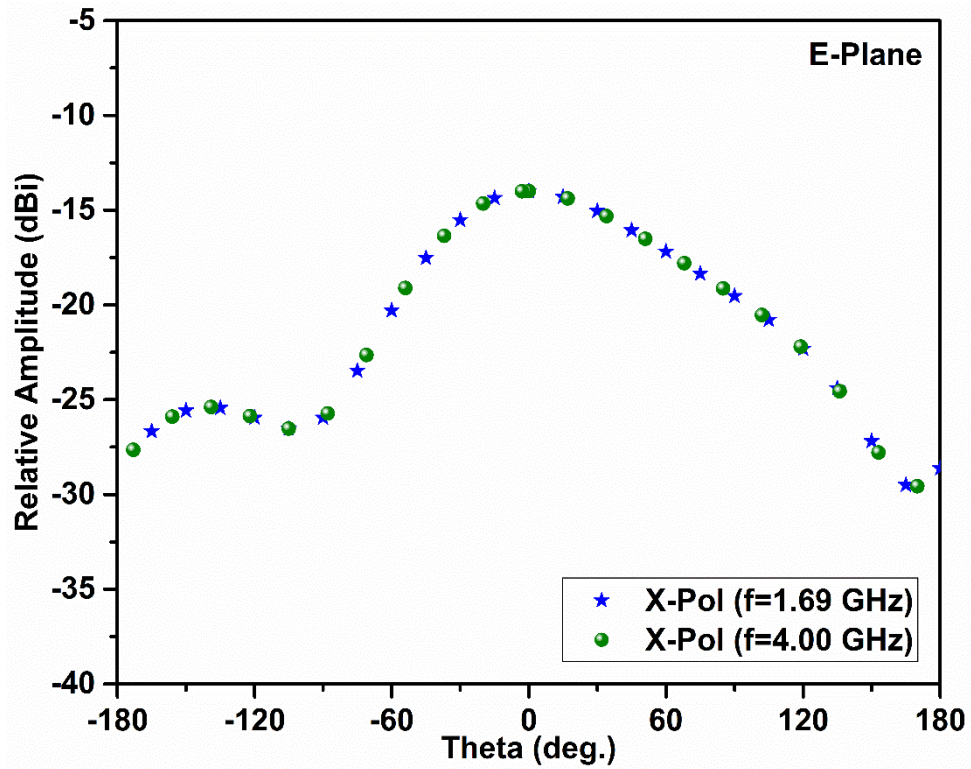


Figure 2.21 (c) Cross polar plot for E-Plane

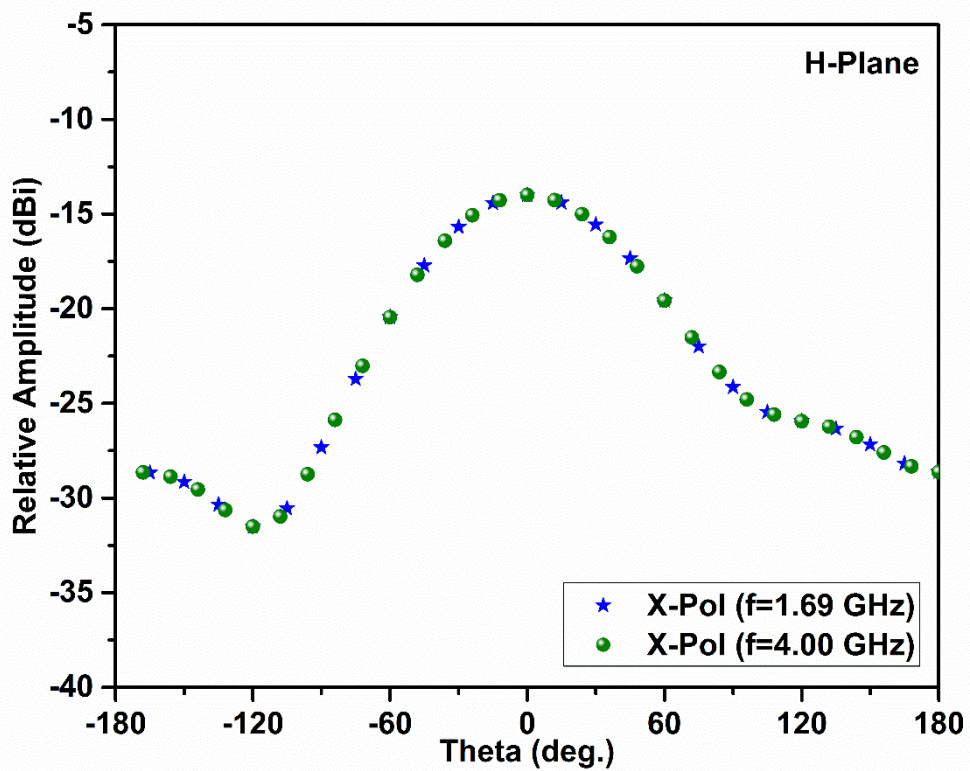


Figure 2.21 (d) Cross polar plot for H-Plane

**Table 2.6** Parameter as obtained from parasitic patch-based MPA

Parameters		Parameter Values	
		L-Band	S-Band
Resonant Frequency (GHz)	Simulated	1.69	4.00
	Measured	1.75	3.96
Return loss (dB)	Simulated	-22.10	-27.12
	Measured	-30.20	-43.32
Bandwidth (%)	Simulated	1.65	3.50
	Measured	3.19	8.16
Co-Polar (dBi)	E-Plane	6.44	6.78
	H-Plane	6.44	6.78
Cross-Polar (dBi)	E-Plane	-14.00	-14.00
	H-Plane	-14.00	-14.00

Here, the designed antennas are separated by a distance via two parasitic elements. The scattering parameters are comparatively the same in simulated as well as measured data and having the ratio of almost 1:2. The S11 better than -30.20 dB and S22 better than -43.32 was obtained for measured data. Due to the presence of “parasitic element” the isolation better than -40dB was achieved for L-band and almost better than -20 dB for S-band. The parasitic elements here enhanced the comparative gain of both the antennas, where the maximum gain of 6.44 dBi and 6.78 dBi is achieved for L-band and S-band along with cross-polarization of -14dB for both. The overall change was observed due to the change in normalized impedance near/close to the radiating zoned because of the presence of parasitic elements. Where the change in overall capacitance closed to the radiating zone resulted in better impedance matching & also resulted in enhancement of antenna performance.

## 2.5 Conclusion

Different configurations for Y-shape based patch antennas along with the influence of the parasitic patch on the resonating frequency and the isolation among two MPA was successfully investigated. Two different configurations named as horizontally, as well as vertically placed Y-shapes, were represented in this chapter. The effect of placement of Y-shape on resonating frequency was successfully observed.

In another configuration, the MPA based on “Swastika” shape (resonating in “L-Band”) and another patch antenna of 7-shape (resonating in “S-Band”) was denoted and analysed fruitfully. Further, the influence of coupling of another non-resonating section (or “parasitic element”) of L-shape was likewise investigated. It was witnessed that the coupling can shake the antenna act in a twin way. The overall antenna performance is influenced by upon proportions of the afresh positioned radiating section/element/patch. Some modification on the performance of the swastika-shaped patch was observed due to the existence of the said “parasitic” element, due to the placement of the said parasitic element near the swastika-shaped patch.

Another configuration represented in this chapter was based on “parasitic patch antenna” comprising a “2x2” matrix-like structures with 4-elements placed beside each other on the same surface. The said 4 elements were not connected to each other, and two of them were acting as resonating elements while others were acting as parasitic elements. Due to the existence of the said “parasitic elements” some reduction in coupling was observed along with the enhancement of other parameters. Three different configurations were designed and represented successfully for L and S-band using aperture sharing. The “parasitic element” basically affect the overall impedance of the nearby surface, thus affecting the overall performance of the resonating elements in that particular area. The variation of better experimental results than simulated are mostly attributed to the simulation parameters on the space constraint of the simulator.



**CHAPTER 3**  
**CONVENTIONAL SHAPED PATCH ANTENNAS**



### 3.1 Introduction

For multifunctionality and multiband operation, arrays of patch antenna are mostly used [1] to overcome the problem of space constraint. Instead of using antenna array for multi-band operation, one can choose either notch loaded patch antennas [2] or shared aperture patch antennas [3-7] for the utilization of available space. Notch loaded patch antennas can be castoff for a solitary band or multi-band task. A number of authors already reported notch loaded MPA consisting of different shapes and size, such as E-shape [8, 9], H-shaped [10], etc. Few of them also reported shorted MPA for multi-band wireless communication systems [11]. The shared aperture method is also the best systems because multi-antennas uses the same aperture for communication without band interferences. Shared aperture method works for multiband operation as reported for L/C [6, 7], L/X [8] and for L/S [9] band, etc. In aperture sharing, the number of the patches are placed on the same aperture, which can resonate simultaneously or separately (based on time/frequency multiplexing), it supports multiple frequency bands for different applications resulting in the reduction of size, weight, and cost [11]. The realization of aperture sharing results in the minimization of the volume & weight for the antenna system. The base of shared aperture antenna design is the availability of unallocated space for both bands of operation which in turn is the direct consequence of the frequency ratio of both bands. Lower the frequency ratio, higher is the ease to design the antennas, as for lower ratios the variations in dimensions for both bands is high. The common designs are based on the frequency ratio of lower than 1:4, while for adjacent bands, the design ratio is quite higher and the design of such antennas are challenging. These two methods are independent of each other. So, shorted MPA and aperture sharing based MPA would give multi-band frequency of operation and it will be beneficial if we combine both of these methods. Which is discussed in this chapter.

Basically, here we applied both of these techniques simultaneously. Two structures with a square shape as a base are presented here. In the first structure, a circular notch is created within a square MPA, and utilization of this notched area is done by placing another MPA of 7-shape. Thus whole design (comprised of two MPA's) resulted in same substrate resonating in L/S- bands. In the second structure, the shorted square shape was transformed into plus shape, after creating notches at four corners, rest remains the same. Resulted in MPA resonating again in the same band with a decrease in 10 dB bandwidth. Both of these structures are described here separately. However, due to notch creation, the overall

impedance of the structure was changed, which further affects the coupling among both of them. So the feed location was optimized to achieve better performance along with less coupling while having matched input impedance & the normalized feed location values are shown in table 1.1.

### **3.2 Notch loaded square-shaped MPA**

A square-shaped patch was designed using commercially available substrate “FR-4” having a dielectric constant of “4.3” with optimized dimensions. A circular notch is created at the center of this patch. This notched area was used to create another patch antenna of “7-shape” for the utilization of the notched area, designed to resonate in L-band. Outer notch loaded square patch resonates in S-band simultaneously. The basic geometry for the simulated along with fabricated patch antennas (fig. 3.1) along with dimension parameters (table 3.1) is shown below. The patch antenna was designed using with copper as the conducting material for the radiating patch as well as for the ground surface. Other parameters are discussed briefly in the next section.

**Table 3.1.** Basic parameters of the patch antenna

<b>Sr. No.</b>	<b>Parameter</b>	<b>value (in mm)</b>
1.	L	90
2.	W	90
3.	r	25
4.	a	10
5.	t	0.06
6.	d	1.60

### 3.2.1 Results and Discussion

The designed antennas were analysed using different parameters, such as scattering parameters, Cross/Co- polarization. The scattering parameters based upon simulated as well as measured data are shown in fig. 3.2 and 3.3 for L/S band respectively. Measured results show a reasonable shift in frequency of resonance for both the antennas. Fig. 3.4 shows that the isolation value is better than 25 dB. Fig. 3.5 (a & b) and 3.6 (a & b) giving Co/Cross-polarization for E/H-planes separately. Results are briefly described in Table 3.2

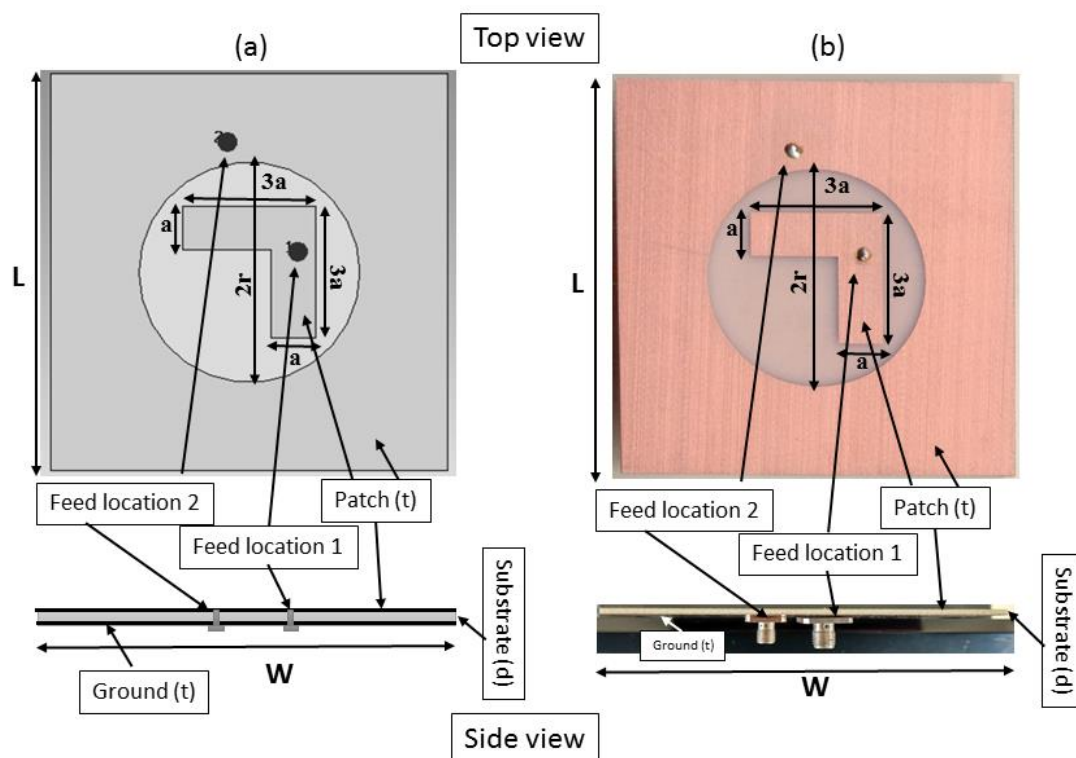


**Figure 3.1** Basic geometry of notch loaded patch antenna (a) simulated (b) fabricated

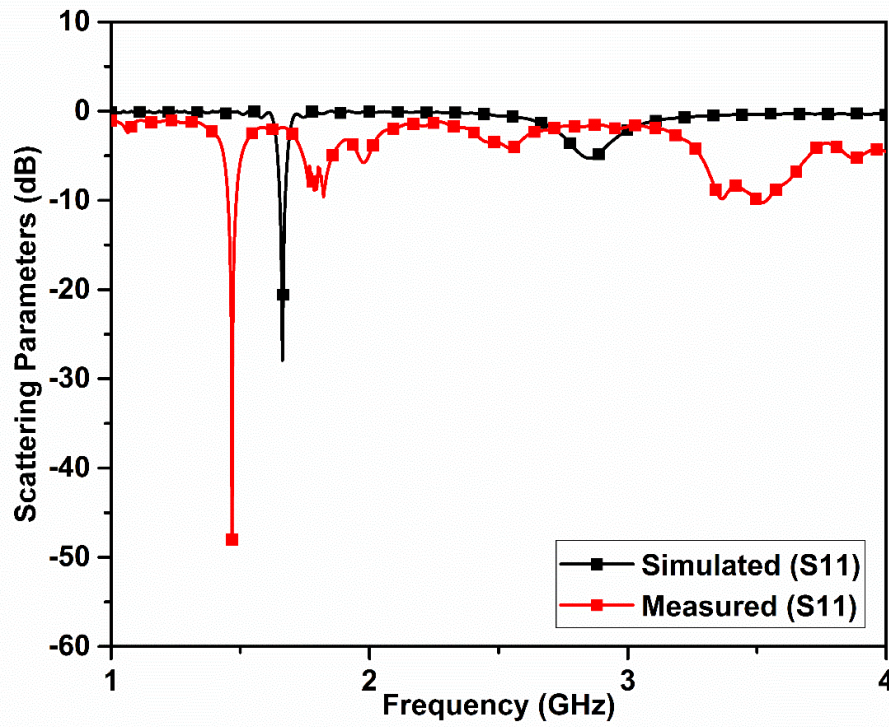


Figure 3.2 S11 parameters of notch loaded patch antenna in L-band

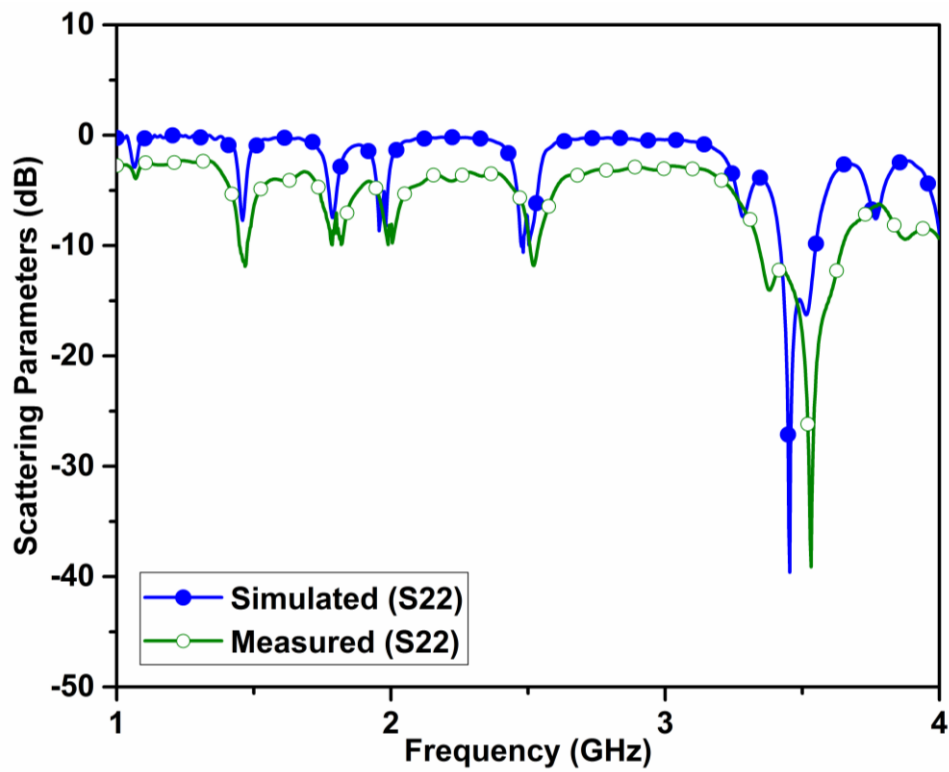


Figure 3.3 S22 parameters of notch loaded patch antenna in S-band

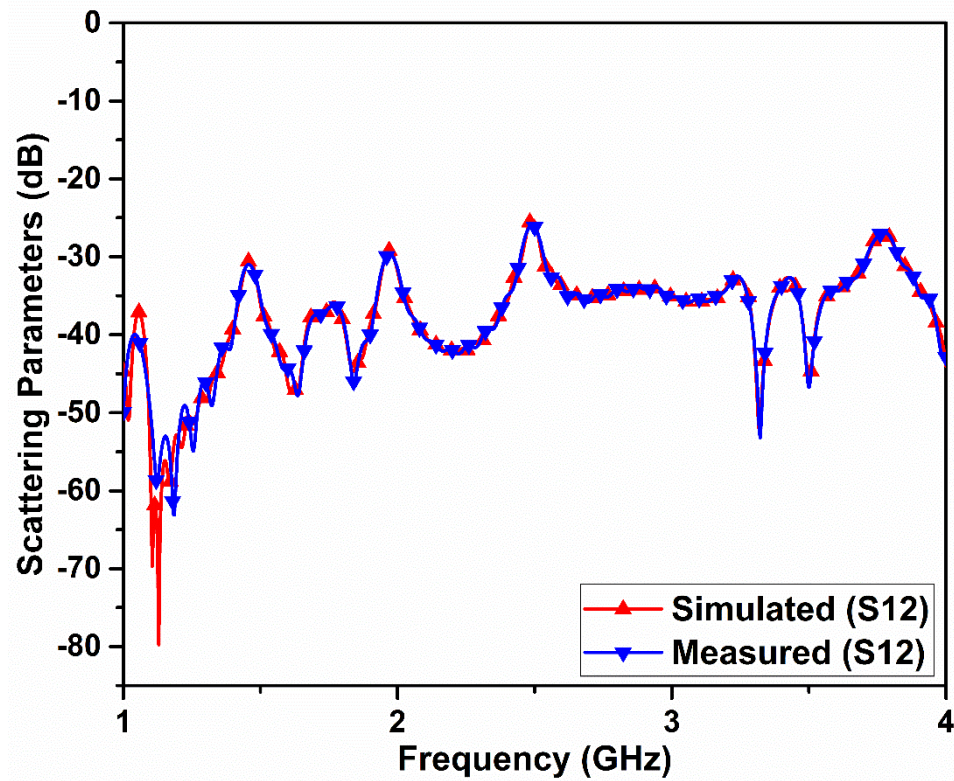
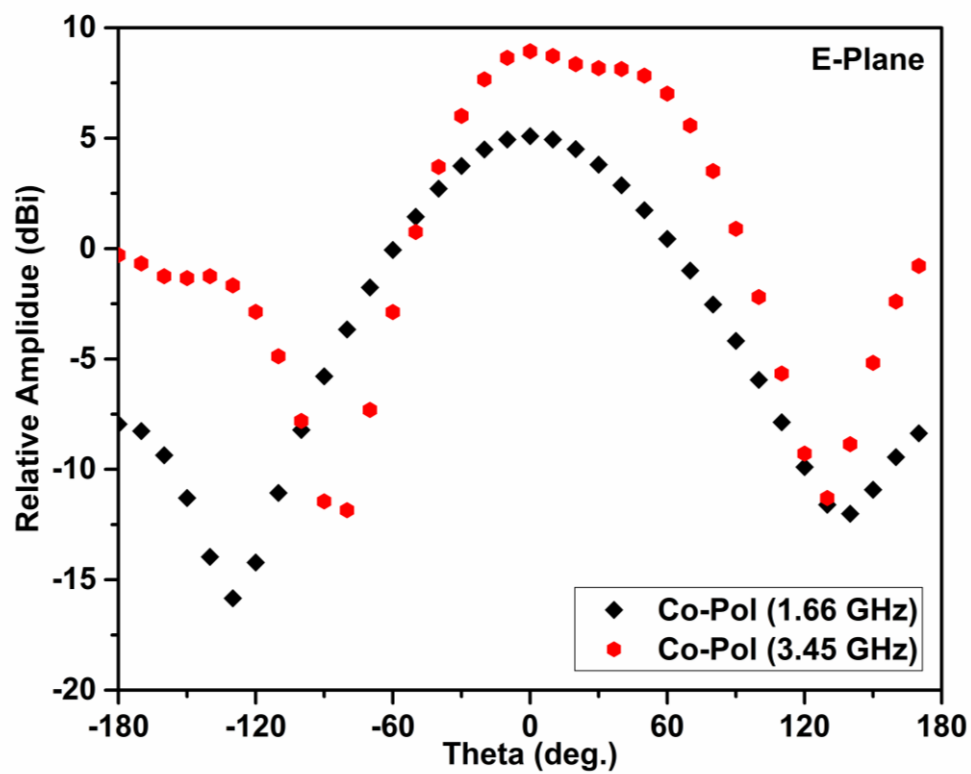
Figure 3.4 Isolation between patch antennas ( $S_{12}$ )

Figure 3.5 (a) Co-polarization for E-plane

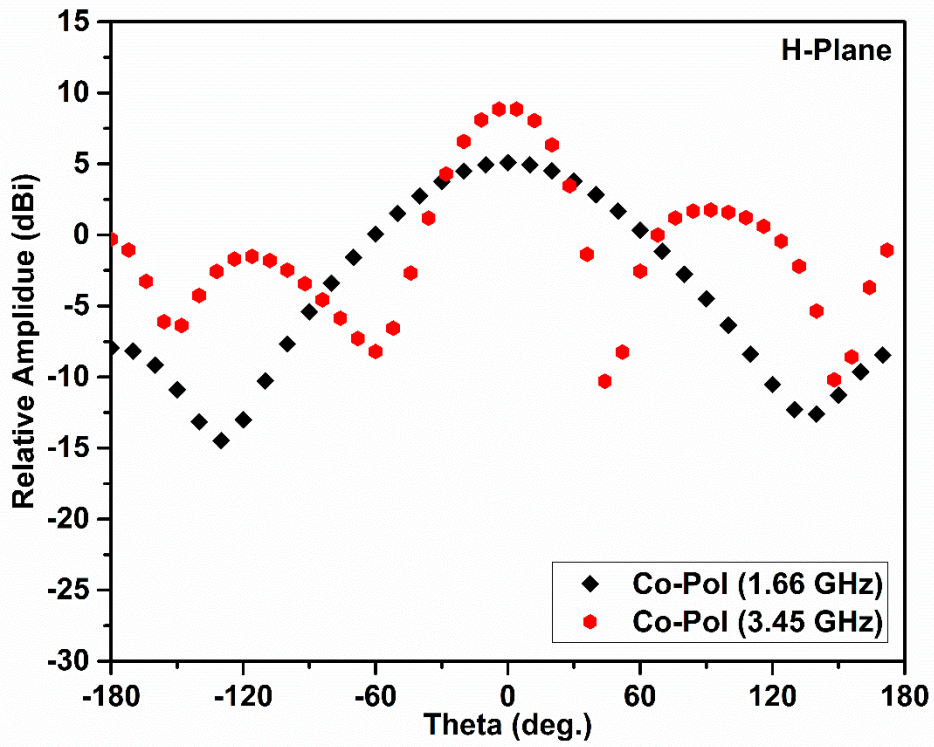


Figure 3.5 (b) Co-polarization for H-plane

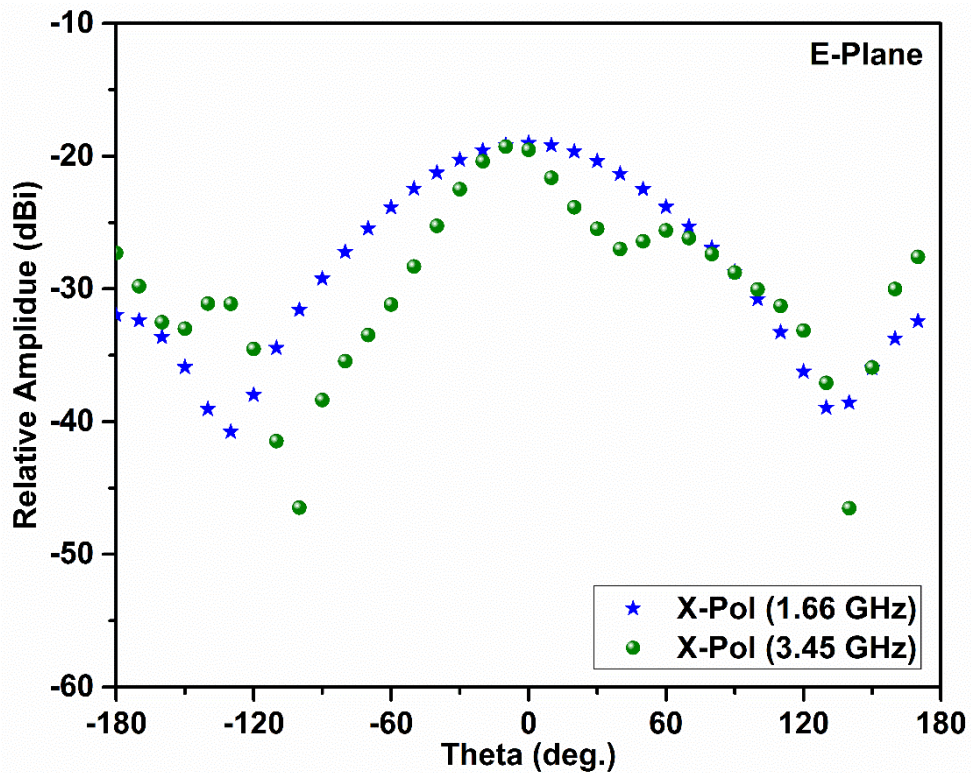


Figure 3.6 (a) Cross-polarization for E-plane

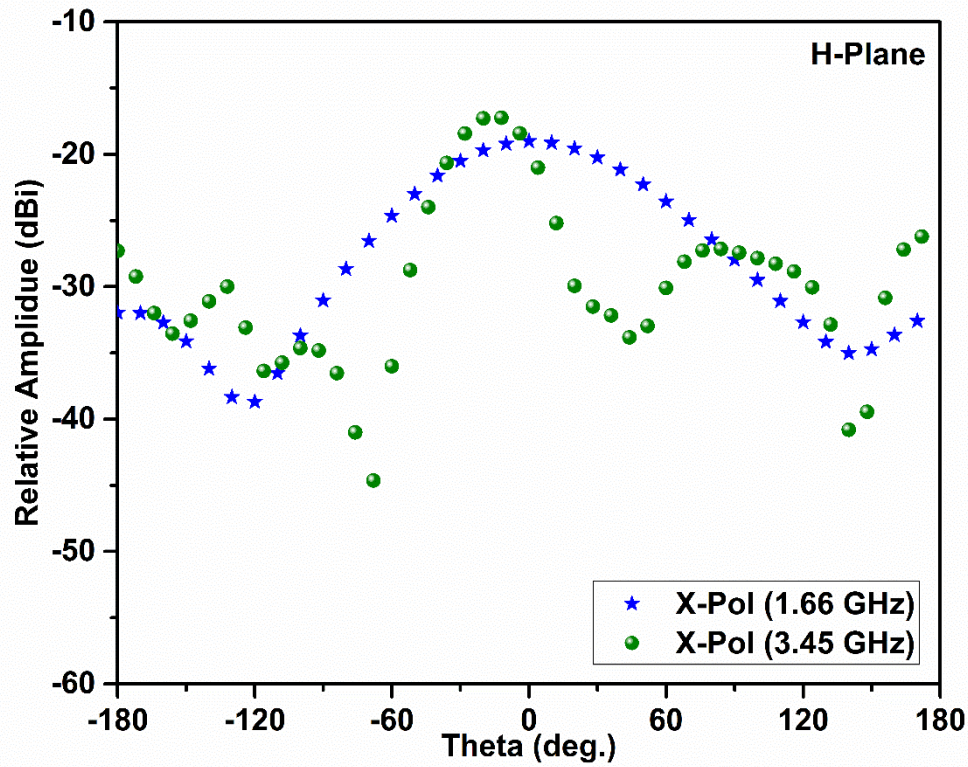


Figure 3.6 (b) Cross-polarization for H-plane

Table 3.2 Basic parameters obtained from MPA

Parameters		Parameter Values	
		L-Band	S-Band
Resonant Frequency (GHz)	Simulated	1.66	3.45
	Measured	1.46	3.53
Return loss (dB)	Simulated	-27.92	-39.60
	Measured	-48.04	-39.11
Bandwidth (%)	Simulated	1.44	4.02
	Measured	2.46	8.89
Co-Polar (dBi)	E-Plane	5.09	8.94
	H-Plane	5.09	8.94
Cross-Polar (dBi)	E-Plane	-19.02	-19.52
	H-Plane	-19.02	-19.52

The ratio of resonating frequency for both the antennas is close to 1:2 and almost the same for both simulated and measured data. The scattering parameters are better than -20 dB for both the antennas & S11 better than -39 dB and S22 better than -48 dB was achieved. Isolation was better than -30 dB and -25 dB for L & S-band. Overall gain was also better than 5 dBi for both the antennas and a maximum gain of almost 9 dBi was achieved corresponds to S-band. Bandwidth was also approximately equal to 9% for S-band. However, due to the mutual coupling effect, the resonating parameters for inner antennas are restricted thus limited to low values. However, the cross-polarization was better than -19 dBi for both the antennas.

### **3.3 Plus shape-based shorted MPA**

The new design is the modification of the previous one and originally designed from a square-shaped patch. But here we have removed square shapes from all outer four corners, resulting in the change of overall impedance due to decrement in overall capacitance, which further lead to change in port location for outer patch too. This resulted in impedance change due to change of port location further resulted in reduction of mutual coupling among both the antennas. The resulted patch looks like a plus shape. “Copper” with a thickness (t) of 0.06 mm was used for ground surface/plane as well as for the patch and “FR-4” ( $\epsilon = 4.3$ ; d = 1.6 mm) as the dielectric material. The antenna was fabricated (fig. 3.7) on a general-purpose PCB (Printed Circuit Board). All the dimension are shown in terms of ‘a’, whose value is 10 mm. The proposed antenna was excited using “50  $\Omega$  co-axial feed”.

#### **3.3.1 Results and Discussion**

The designed antennas were analysed using different parameters, such as scattering parameters, Cross/Co- polarization. The scattering parameters were represented by simulated and simulated as well as measured results for L/S band respectively (fig. 3.8). Fig. 3.9 shows that the isolation value is better than 30 dB. Fig. 3.10 and 3.11 giving Cross/Co-polarization for E/H-planes separately. Results are briefly described in Table 3.3.

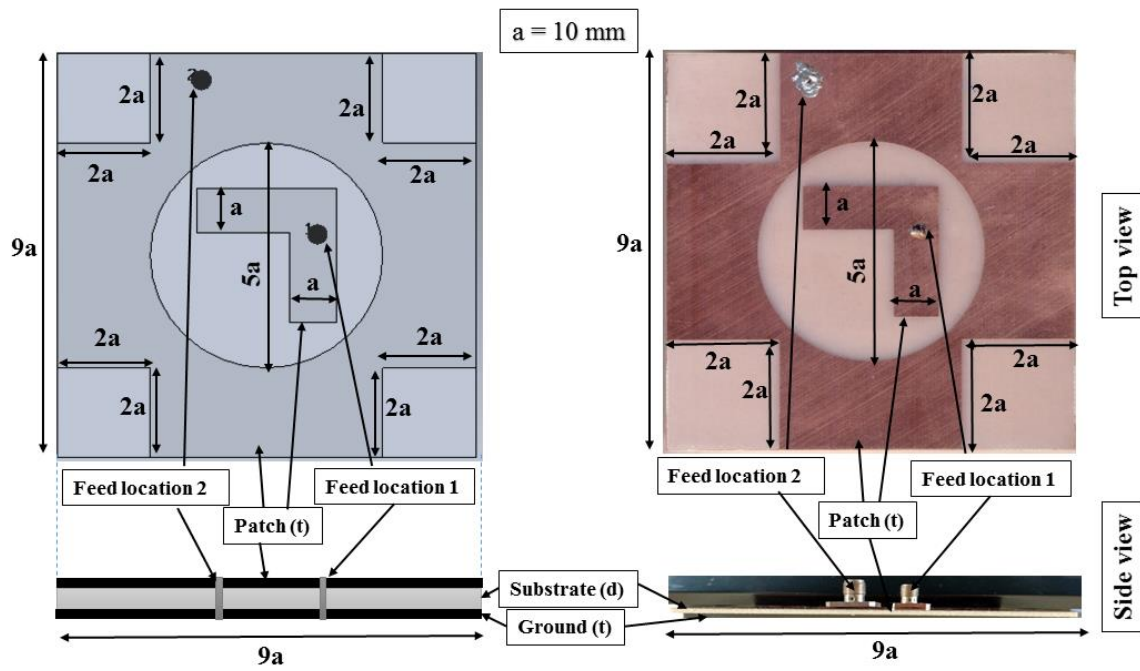


Figure 3.7 Basic geometry of shorted MPA

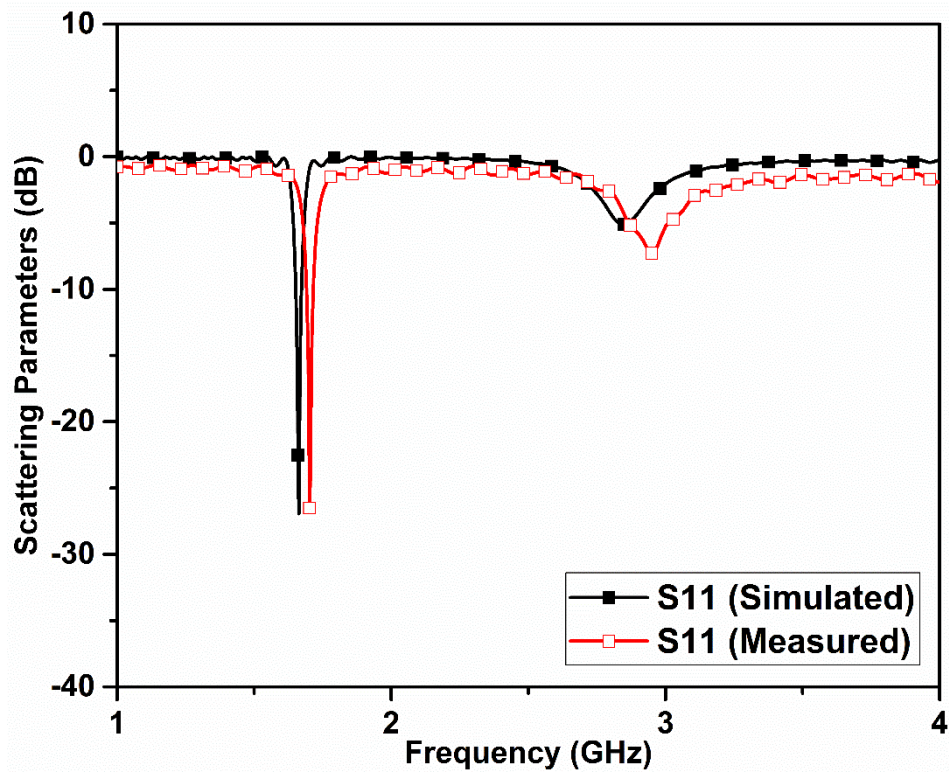


Figure 3.8 (a) Scattering parameters (S11) of shorted MPA

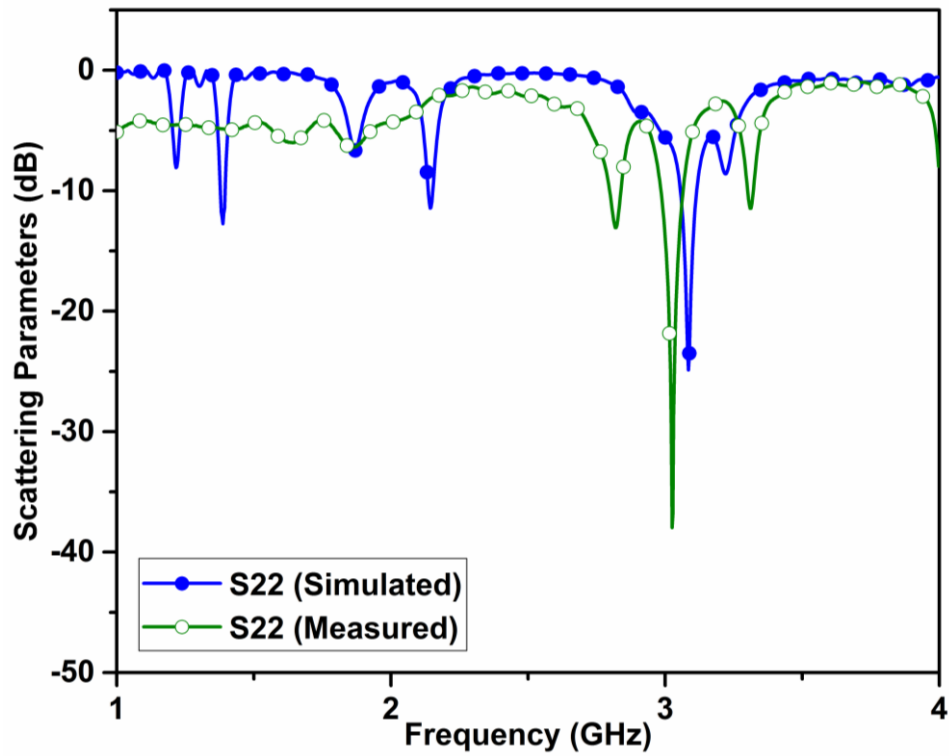


Figure 3.8 (b) Scattering parameters (S22) of shorted MPA

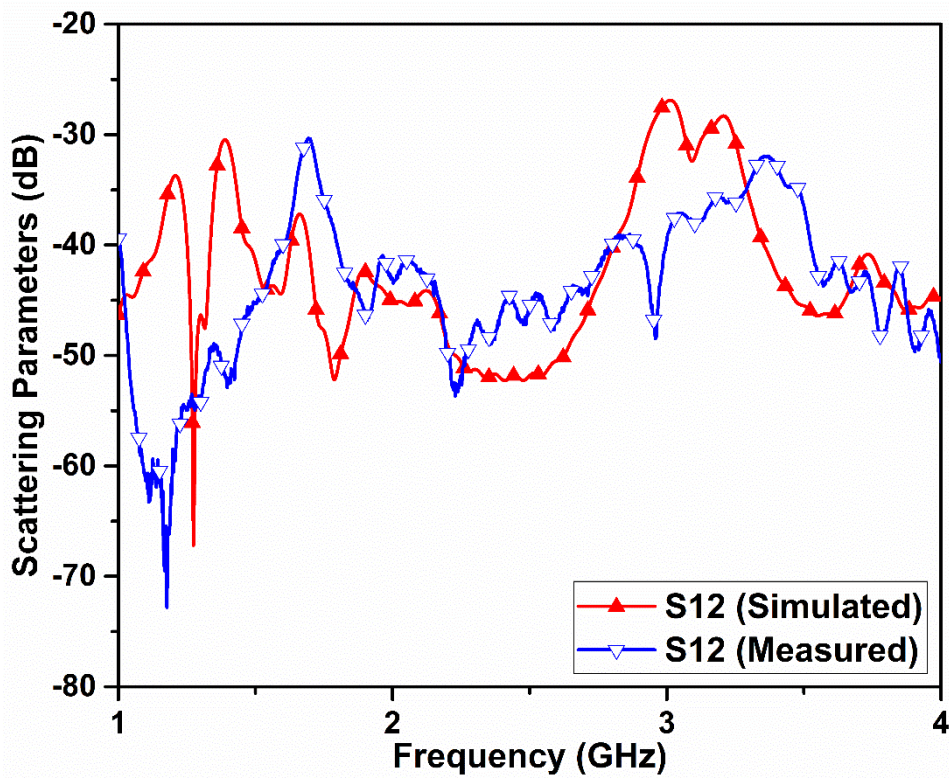


Figure 3.9 Isolation (S12) between shorted MPA

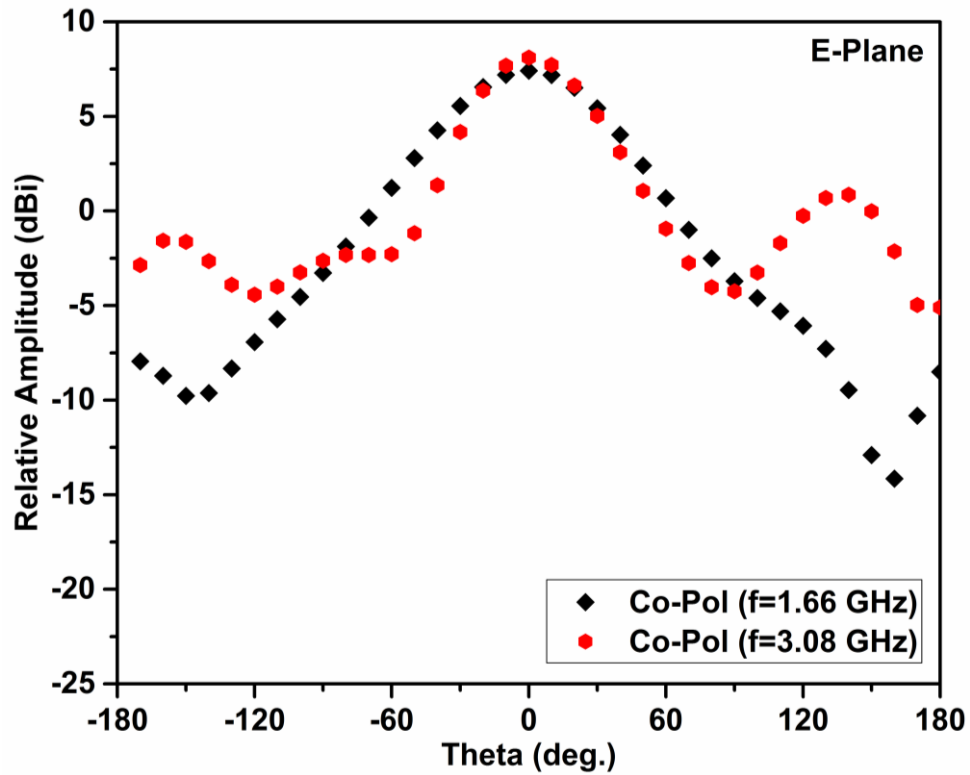


Figure 3.10 (a) Co-polarization of notch loaded MPA (E-plane)

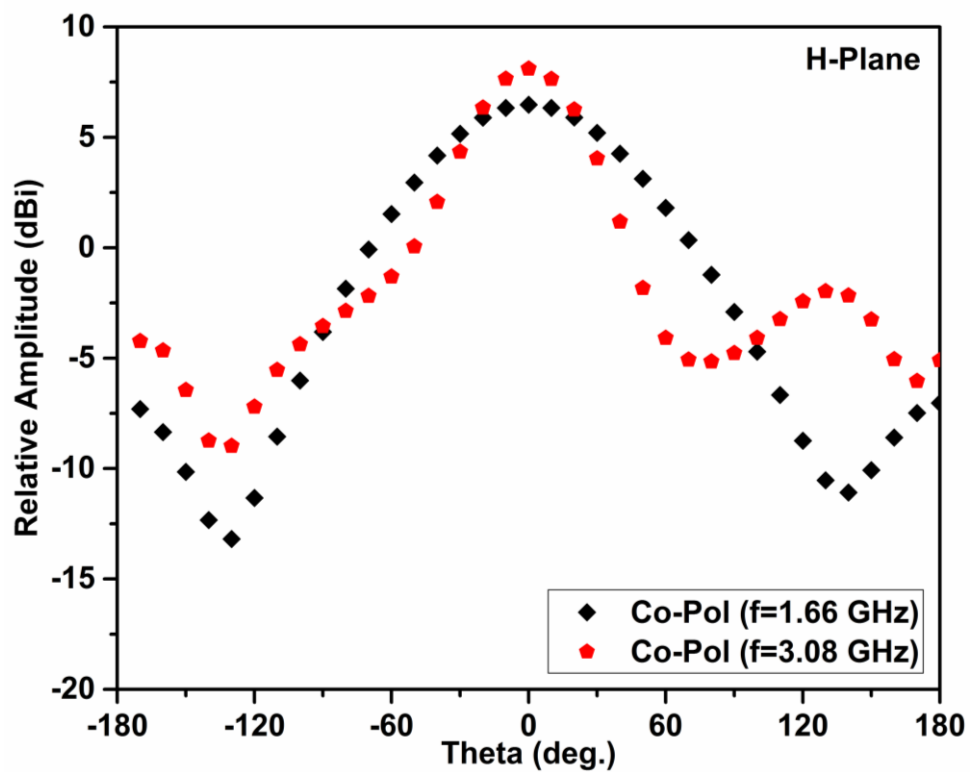


Figure 3.10 (b) Co-polarization of notch loaded MPA (H-plane)

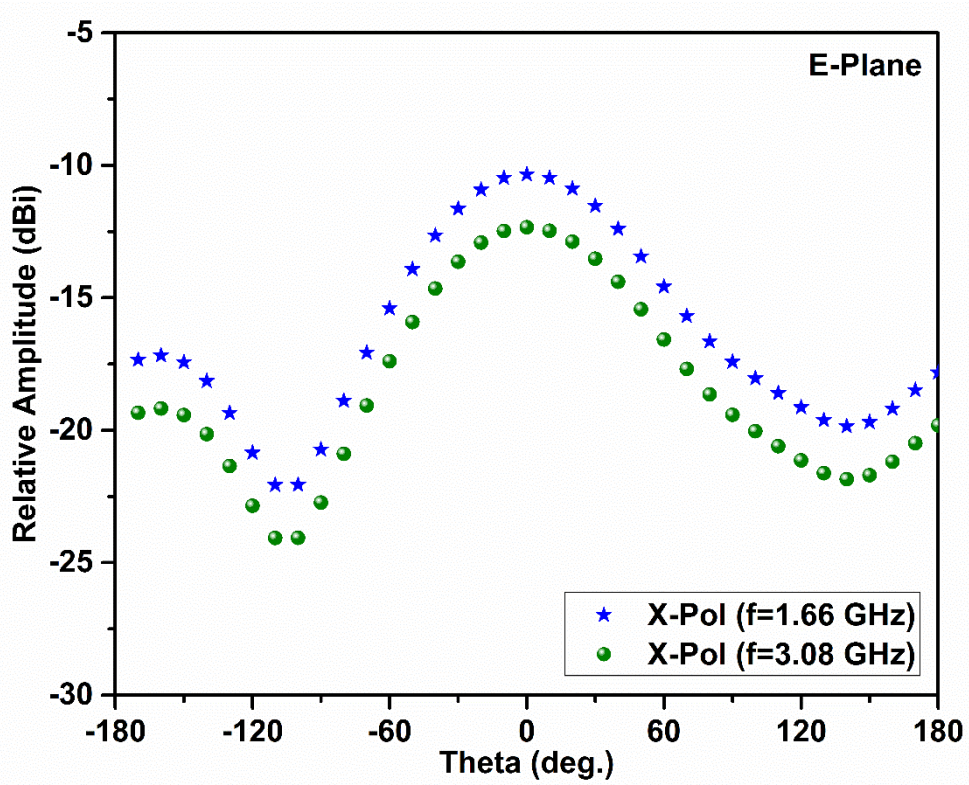


Figure 3.11 (a) Cross-polarization of notch loaded MPA (E-plane)

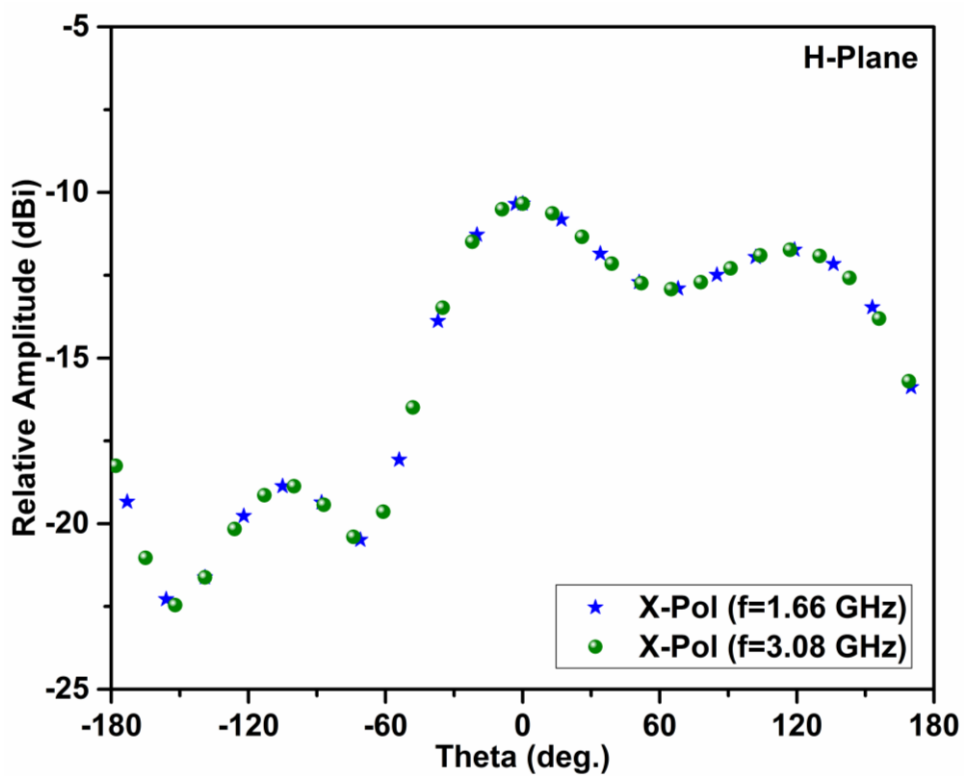


Figure 3.11 (b) Cross-polarization of notch loaded MPA (H-plane)

**Table 3.3** Basic parameters obtained from shorted MPA

Parameters		Parameter Values	
		L-Band	S-Band
Resonant Frequency (GHz)	Simulated	1.66	3.08
	Measured	1.70	3.02
Return loss (dB)	Simulated	-26.94	-24.88
	Measured	-26.50	-37.97
Bandwidth (%)	Simulated	1.44	1.944
	Measured	1.58	2.77
Co-Polar (dBi)	E-Plane	7.41	8.10
	H-Plane	6.48	8.10
Cross-Polar (dBi)	E-Plane	-10.34	-12.34
	H-Plane	-10.34	-10.34

Here, the ratio of resonating frequency for both the antennas is more than 1:2 but almost same for both simulated and measured data. Again, the scattering parameters are better than -20 dB for both the antennas where S11 better than -26.94 dB and S22 better than -37.97 dB was achieved. Isolation was better than -30 dB for L & S-band. Here also, the overall gain was better than 5 dBi for both the antennas and a maximum gain of almost 8.10 dBi was achieved corresponds to S-band. However reduction in bandwidth was reported when compared with previous structure and is approximately equal to 2.77 % for S-band, & the cross-polarization was better than -10 dBi for both the antennas.

### **3.4 Conclusion**

Two different configurations of shorted MPA are discussed here. Both the structures are almost alike to each other and resonating in L/S-Bands. It has been observed that when we place two patch antennas side-by-side, affecting the working of both the antenna depends upon internal patch width as well as the width of the notch. The overall antennas were designed with less cross-interference and reduced coupling. The designed antenna configuration shows reasonable validation between simulated and measured data for S-band. The antenna system is suitable for multifunctional systems like “Synthetic-Aperture Radar (SAR)” applications. Due to narrow bandwidth in L-Band, the antenna can be used in application areas where multiple devices operate at the same frequency such as “GPS” systems. Some improvement in isolation, as well as cross-polarization, was also observed due to notch creation in the patch structure. This was because of the change in overall capacitance of the antenna around the corners of the substrate. The variation of better experimental results than simulated are mostly attributed to the simulation parameters on the space constraint of the simulator.

**CHAPTER 4**  
**Microstrip Antenna Array**



## 4.1 Introduction

In some cases, a single “Microstrip Patch Antenna (MPA)” is not appropriate for numerous application, where high gain, “beam scanning” or “bandwidth” enhancement are the requirements. Gain enhancement and beam steering capability can be achieved using arrays of the antenna. The antenna arrays may be linear, planar or conformal based on applications. Such as for radar communication schemes where the fine beam is preferred and henceforth planar array assembly are preferred.

The scheme of restricted arrays demands the engagement of the patches in a systematic arrangement/configuration so that the radiation in the preferred route can be accomplished while bearing in mind the edge influence. The fields due to different patches should get amalgamated in the segment towards the desired co-ordinates/directions and must cancel each other towards other co-ordinates/directions for better performance. In other words, the output of the individual patch is unified to acquire the fields radiated by the whole array arrangement. It is essential to footnote that radiation pattern of distinctive patch in the array is comparable when it functions in unconnected mode. Hereafter the whole resulting outline of the distinctive patch gets replicated by the array influence.

Some interaction between the elements was also observed due to the presence of both the element in close proximity. The element spacing along with the location among the array structures also affects the overall radiation pattern and other parameters. Thus the spacing among the radiating patches or components in the array is enforced, in relationships of wavelength for E/H-planes.

In Feb 2000, the “SIR C/X SAR” scheme fixed on the “American Space Shuttle Endeavor (ASSE)” accomplished the primarily high-resolution 3D imaging thru the globe, which engaged three dual-polarized sub-array operatives distinctly at “L/C & X-bands” [1, 2]. This resulted in huge and large arrangement weighing over 300 Kg or more. The method of “shared aperture” conformation basically reduce the overall volume along with weight of the antenna structure and comfort the distribution of collective subsystem rallies behind the array. The “shared aperture” based antennas are already present in literature such as perforated-patch [3, 4], ring/patch [5, 6] interlaced patch with dipole/slots [7-10]. The “shared aperture” method is nothing but applying numerous radiation utilities inside the same physical aperture, a concept referred to as “multifunctional array” [11]. Because it

reduces the overall cost and time, and number of elementary radiators can be integrated on same aperture. The individual radiators can be used for transmitting or receiving purpose simultaneously or separately.

In aperture sharing, radiators can be identical in shape and size or can be different. For multi-band operations, the size of radiators will always be different from each other. Again, critical issue while performing multi-band operation is the requirement of wide range of radiators. Which can't be solved using regular radiators and in some cases, single-element are incapable to meet the desired parameters, so to solve this problem here array formation was intended. As a solitary element exhibits a definite radiation pattern, then the array configuration will exhibit distinct radiation pattern. Especially when applied in antenna array and aperture sharing technique simultaneously. This can support numerous isolated frequency bands for communication, telemetry or radar, etc. [12, 13]. For independent dual-band or triple-band operations are obtained by designing and exciting the individual antenna elements for each band and placing the antenna elements in stacked configuration, thus increasing the overall size of antenna. In this chapter, an array antenna is designed for L and S-band using common aperture. One of the antennas shares the vacant space inside the other antenna on the same aperture. The designed antenna composed of  $2 \times 2$  array of planar annular rings with smaller and larger radius in shape of C. The array of larger rings array surrounds the array of smaller rings. The optimized design is prototyped and tested for L and S-band.

### **4.2 Antenna Design**

The basic configuration comprised four “circular” shapes forming an array of the larger shape. The same structure with reduced size was placed inside the large array (fig. 4.1). “Copper” (height 0.60 mm) is used as conducting medium and “FR-4” (dielectric constant 4.3 and height 1.6 mm) for a substrate. As we know that “shared aperture” based structures can be presented in any form [3-10]. Here we presented two array structures using planar configuration because the other arrangements cannot accommodate such design on a single footprint. Initially, each individual antenna was designed (simulated) and optimization was performed independently using “CST Microwave Studio” for L- & S-band. Optimization was achieved while discarding mutual coupling influence. Far ahead the antennas were incorporated into an aperture sharing based arrangement. After which each antenna was analysed to attain optimized feed locations for both of them (using “co-axial probe”) for

L/S-Band. Firstly, scattering parameters of both the antennas are verified at optimized locations (as described in table 1.1.)

**Table 4.1.** Basic parameters of the patch antenna

Sr. No.	Parameter	value (in mm)
1.	L	80
2.	R1	12
3.	R2	5
4.	r1	5
5.	r2	2
6.	a	18
7.	b	4
8.	c	5
9.	d	2

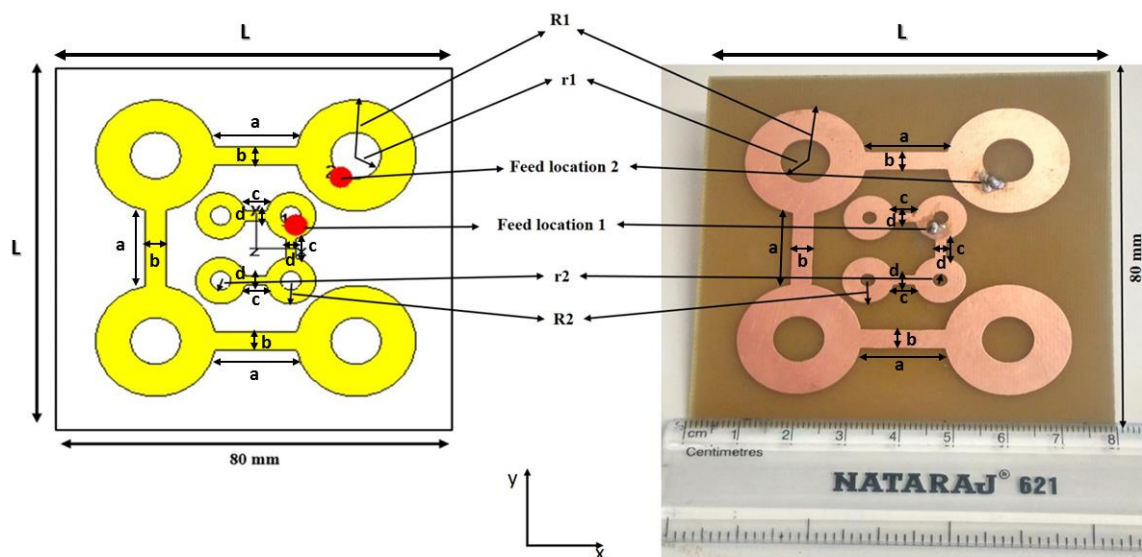


**Figure 4.1** Basic configuration of Microstrip antenna array

As the two bands are closely coupled the design represents noteworthy mutual coupling when incorporated into an array. Which needs to be controlled b/w radiating elements to avoid unnecessary inter-channel interference and it might not be used for parallel tuning of both the radiating elements. Considerable attention was given for the geometrical symmetry

maintenance and for better isolation of the feed lines, thus resulting in low cross-polarization. Antenna design and results are described in the next sections.

### 4.2.1 Results and Discussion

As discussed earlier, scattering parameters were obtained from simulated data after optimization of feed location, the finally obtained results are discussed here. The scattering parameters are exposed in fig. 4.2 (a) & (b) for both the antenna arrays (as S11 & S22). Here simulated as well as measured results are presented simultaneously.

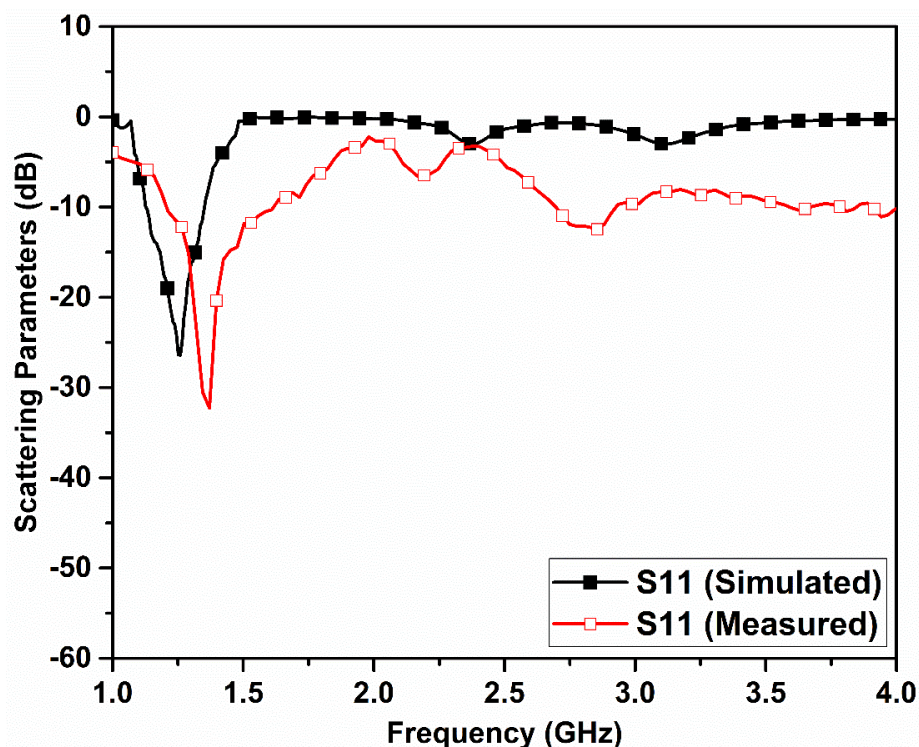


Figure 4.2 (a) Scattering parameters of smaller/inner MPA array

The scattering parameters of the antennas with a resonating frequency of 1.25 GHz and 3.14 GHz for simulated data and 1.37 GHz and 3.06 GHz for measured data. The bandwidth of 28.5 % is obtained in the L band with measured resonant the frequency of 1.37 GHz. For S-band, about 6.9% bandwidth is obtained with the resonant frequency of 3.06 GHz. The measured results (using VNA) are almost in collaboration with simulated data with minute variation only. The cause of the change is due to uncertainty of the dielectric constant delivered by the dielectric producer and that of the dielectric constant used in the simulation. However it does not exactly match with the one provided in the material. Isolation is better 35 dB for L-band and better than 20 dB for S-band (fig. 4.3). It is also observed that measured radiation patterns for L and S-band are in worthy promise with simulated radiation

pattern as exposed in fig. 4.4 (a) ; 4.4 (b) ; 4.5 (a) & 4.5 (b) with realized gain about 5 dBi and 7.16 dBi for L and S-band operation. The cross-polarization in between both the patch antennas was better than 35 dBi for E/H-planes.

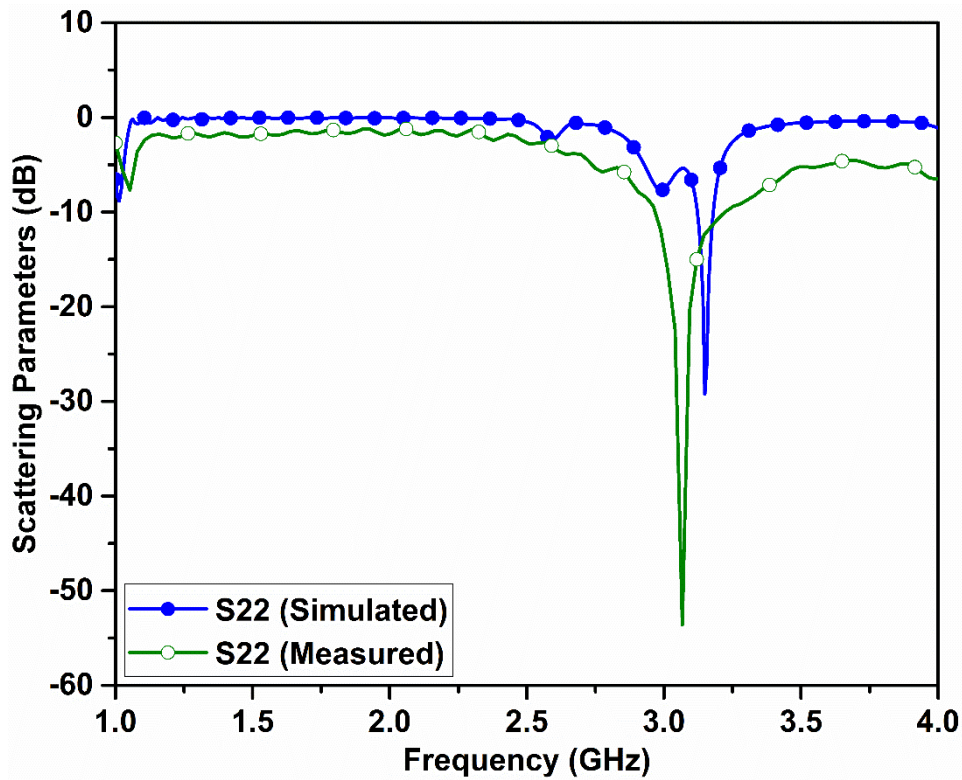


Figure 4.2 (b) Scattering parameters of larger/outer MPA array

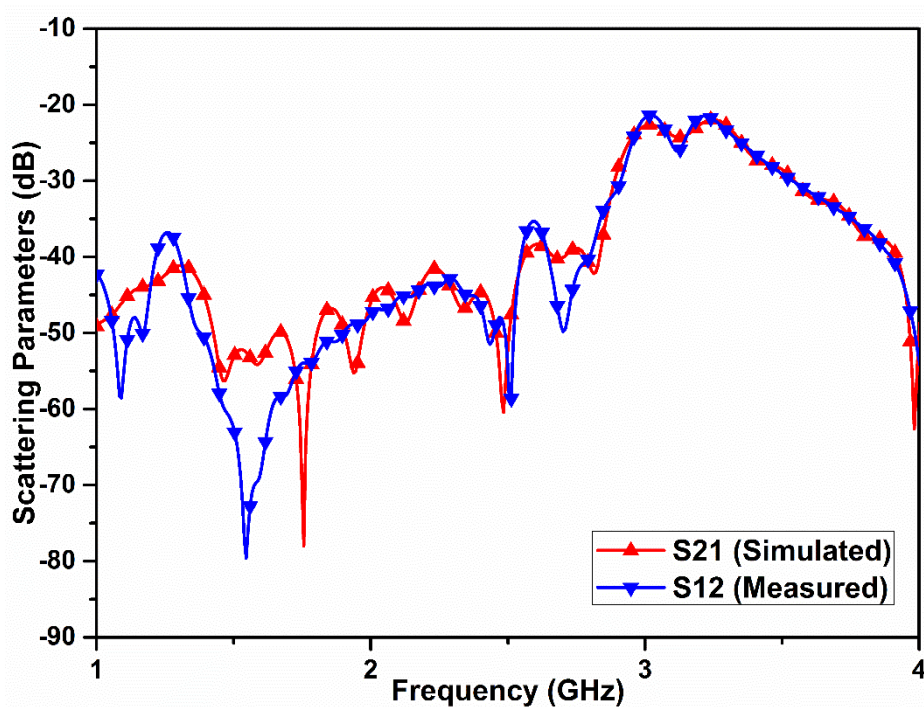


Figure 4.3 Isolation between MPA arrays

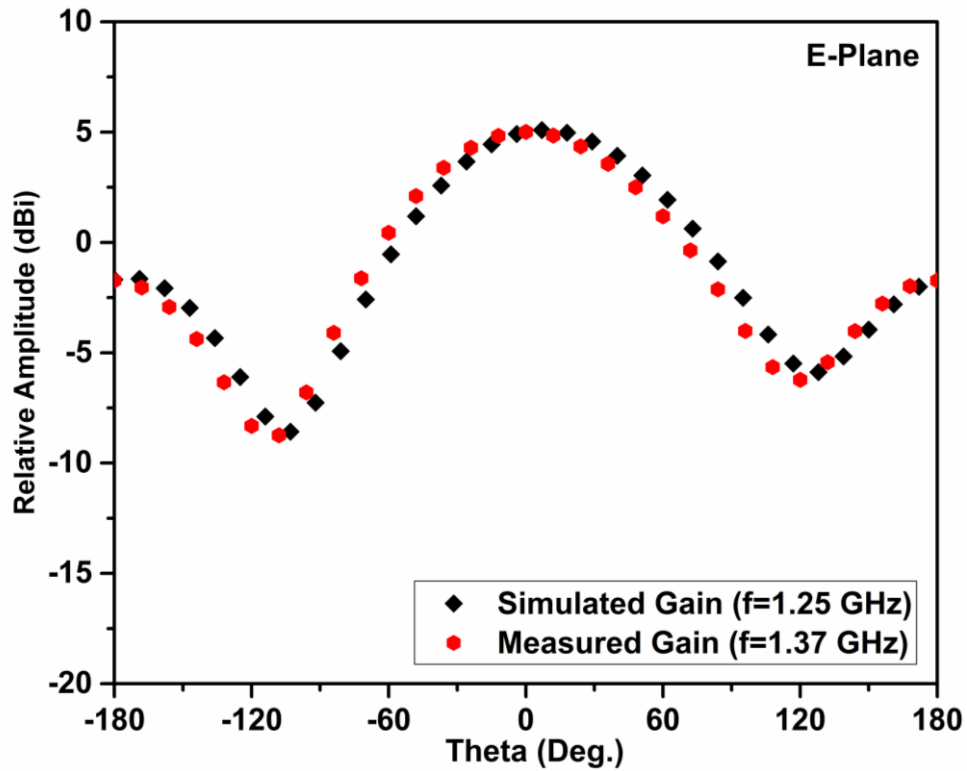


Figure 4.4 (a) Gain for smaller/inner MPA array (E-plane)

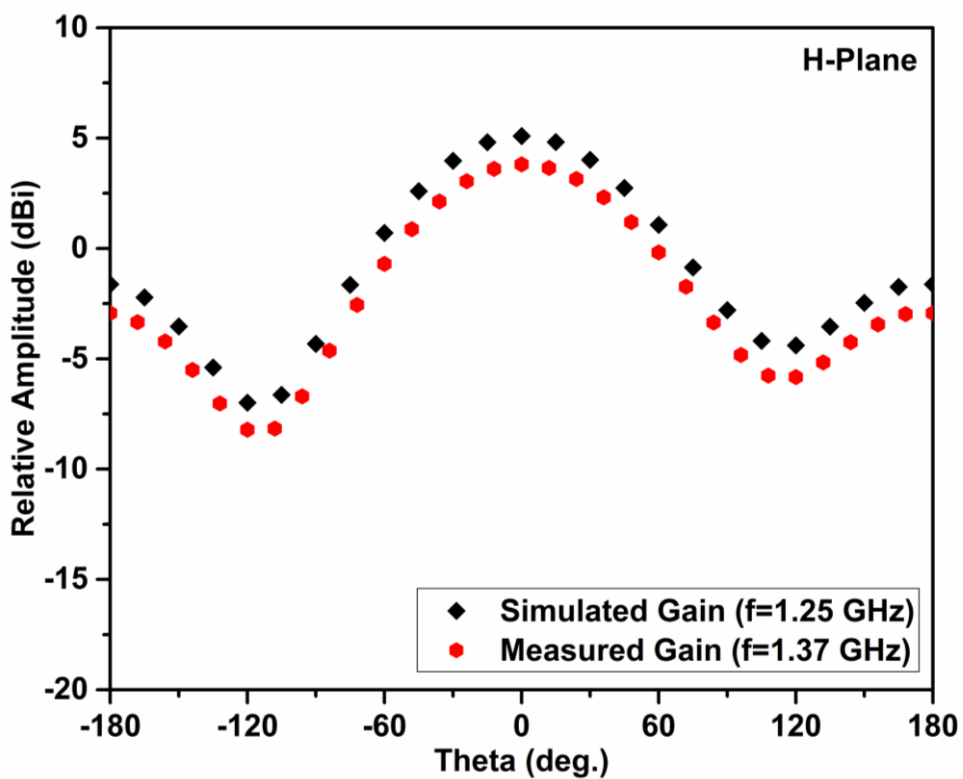


Figure 4.4 (b) Gain for smaller/inner MPA array (H-plane)

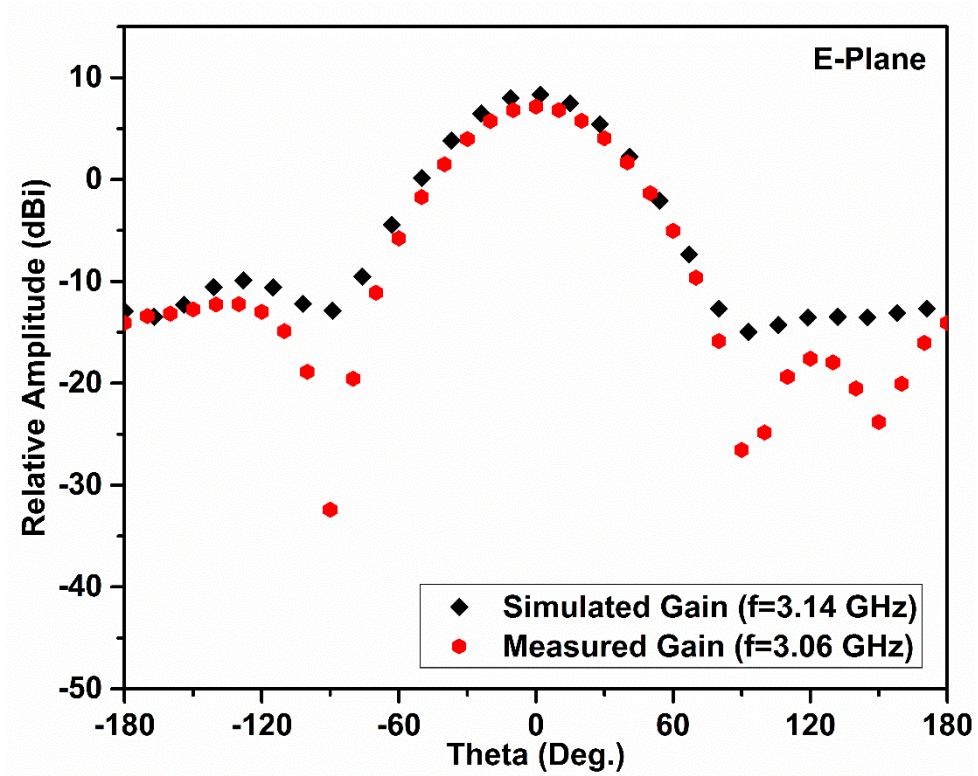


Figure 4.5 (a) Gain for larger/outer MPA array (E-plane)

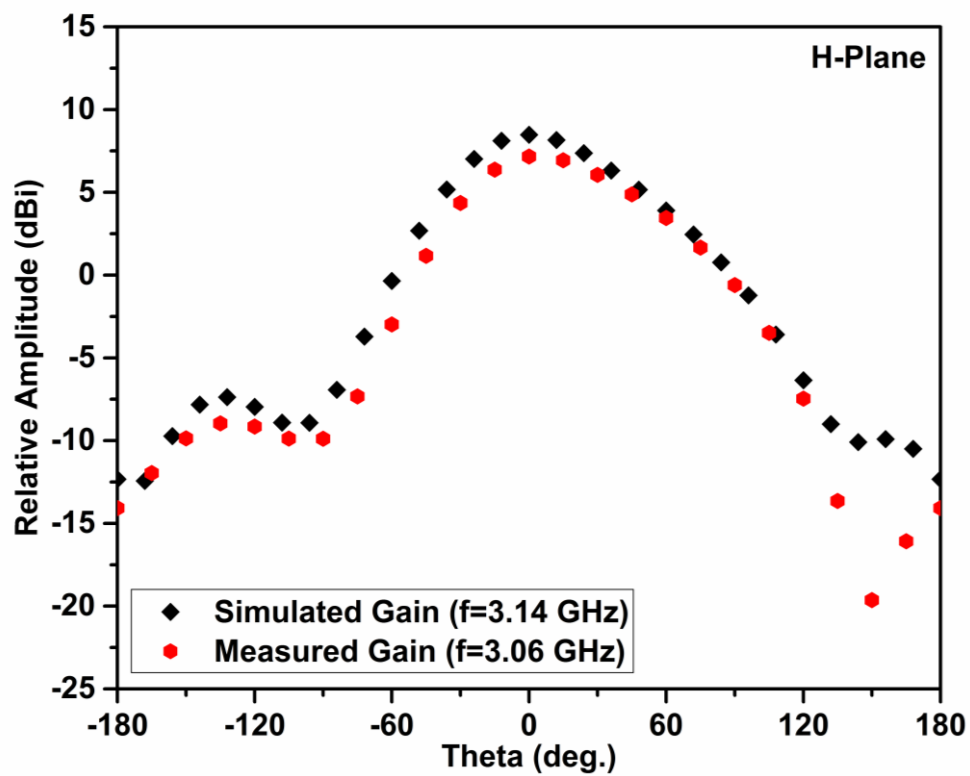


Figure 4.5 (b) Gain for larger/outer MPA array (H-plane)

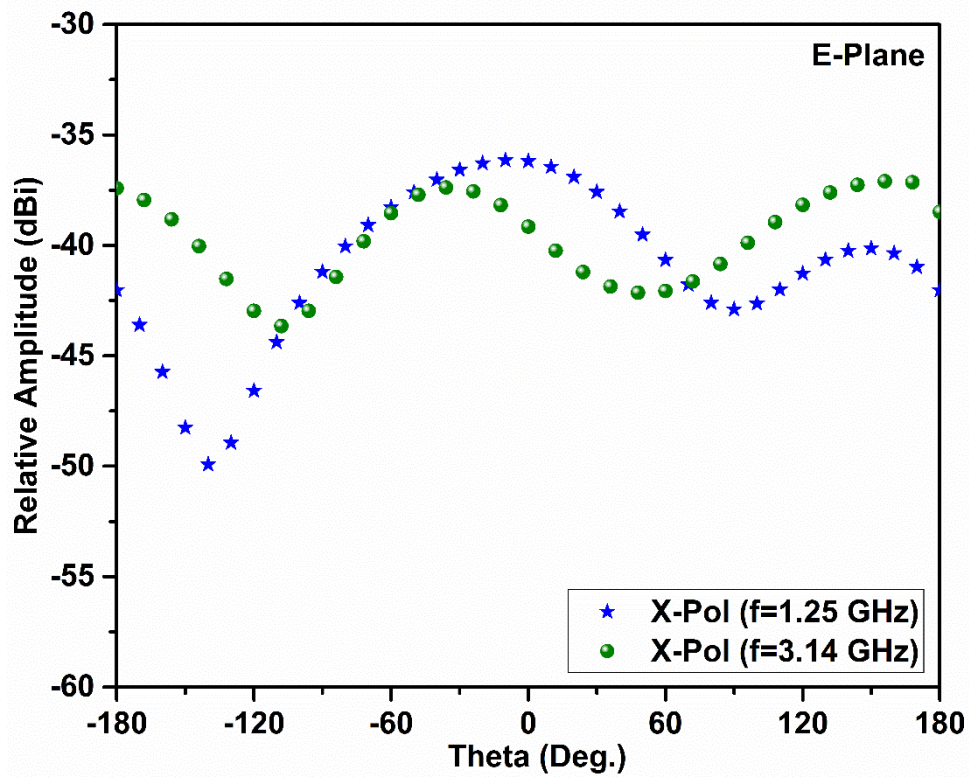


Figure 4.6 (a) Cross-polarization between two antennas (E-plane)

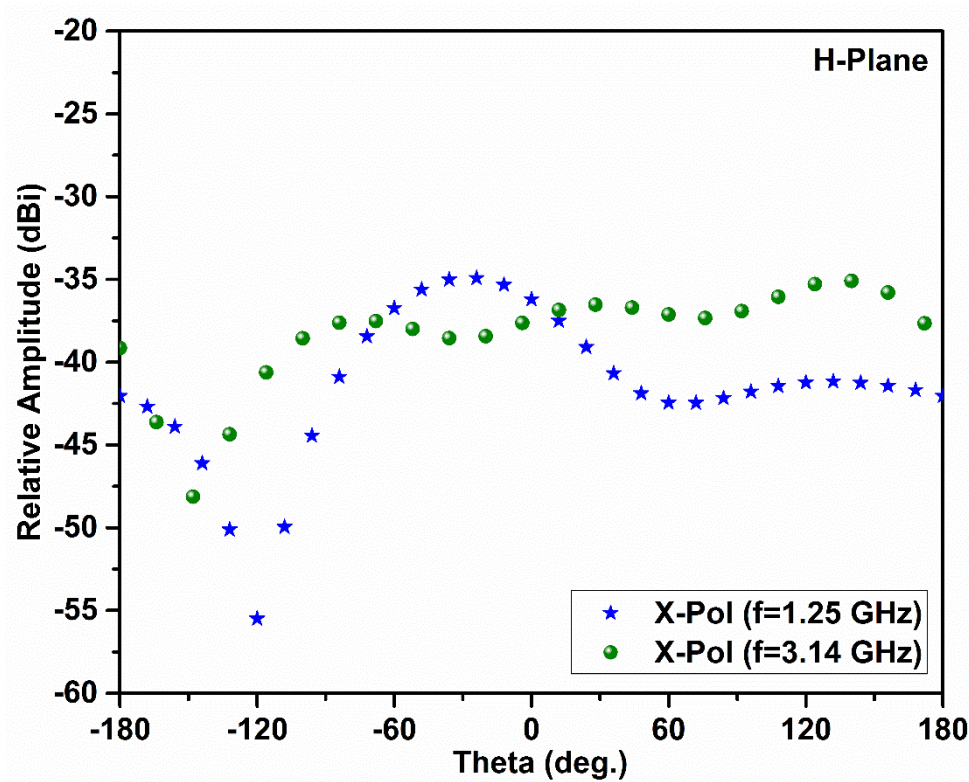


Figure 4.6 (b) Cross-polarization between two antennas (H-plane)

**Table 4.2** Basic parameters obtained from MPA

Parameters		Parameter Values	
		L-Band	S-Band
Resonant Frequency (GHz)	Simulated	1.25	3.14
	Measured	1.79	3.06
Return loss (dB)	Simulated	-26.40	-29.26
	Measured	-32.26	-53.59
Bandwidth (%)	Simulated	4.00	1.91
	Measured	19.23	8.49
Co-Polar (dBi) E-Plane	Simulated	5.01	8.36
	Measured	5.00	7.16
Co-Polar (dBi) H-Plane	Simulated	5.09	8.47
	Measured	3.80	7.16
Cross-Polar (dBi)	E-Plane	-36.19	-39.15
	H-Plane	-36.20	-37.41

### 4.3 Conclusion

Microstrip patch antenna array configuration was successfully designed and analysed for L- & S-band. The designed antenna present bandwidth up to 18% and cross-polarization up to -38 dBi along with isolation better than 25 dB resulting in numerous applications such as devices enabled with Global Positioning System (GPS) along with mobile communication. Both the antennas can be used simultaneously or separately for different application purpose. However, due to adjacent bands, it is highly recommended to use time/frequency multiplexing for the frequency of operations giving better results. The overall structure was designed for the utilization of unallocated or available space. Due to narrow bandwidth, the designed array configuration can be used for application area, where multiple devices are operating at the same time such as “GPS”, etc. The variation of better experimental results than simulated are mostly attributed to the simulation parameters on the space constraint of the simulator.



**CHAPTER 5**  
**CONCLUSION & FUTURE SCOPE**



## 5.1 Conclusion & Future Scope

In this thesis, investigations are carried out using a shared aperture method for different configurations of “Microstrip Patch Antennas” or MPA resonating in L & S-band. Aperture sharing is one of the ways of studying the multifunctionality of the antenna system. A shared aperture MPA comprising “Dollar” was investigated for testing purpose as a preliminary work & to check the feasibility of L & S-band using aperture sharing. The designed antenna has been successfully tested for L & S-band. Two different sized “Dollar” based structures placed beside each other were represented here, both of them resonating in L/S-band simultaneously & separately. The effect of coupling was observed & studied in this chapter. In this chapter a detailed table was also reported for the feed point location of all the structures presented in the thesis work. Calculation of the feed point location of all the structures is also represented using standard equations.

In the continuity of the preliminary work, we have further designed two different configurations comprising horizontally and vertically arranged Y-shapes as described in the 2<sup>nd</sup> Chapter. The basic configuration consists of two Y-shapes placed on the same surface acting as a patch antenna, resonating separately. The effect of placement of Y-shapes (either vertically or horizontally) was observed on different parameters of both the antennas. One main thing about antenna design is that due to the design simplicity, it is easy to design these type of antennas. Due to the presence of two antennas on the same substrate, the design has wide applications. Such as one can use the same antenna for mobile communications as well as satellite communication at the same time.

The influence of the “parasitic” patch element on resonating frequency as well as isolation among two MPA was productively examined & represented in the 2<sup>nd</sup> chapter. The proposed antennas were based on two different configurations. The first configuration was based on “Swastika” shape-based MPA & another configuration were based on notch loaded rotated square shape-based MPA. The effect of the presence of parasitic element on antenna parameters was successfully investigated and represented in “Swastika” shape-based MPA. The basic configuration comprises “Swastika-shape” (L-Band) and “7-shape” (S-Band) based structures placed on the same surface. The effect of coupling was also investigated on the antenna. Another structure based on parasitic elements was designed using notch loaded structure comprising a 2x2 matrix with/having 4 elements placed on to the same surface. Out of 4 elements, two were acting as radiating elements while rest two were substituted as

## **CONCLUSION**

---

“parasitic elements” & all the elements were not associated with each other. Due to the presence of parasitic elements, better isolation was observed.

Another configuration represented in this thesis was based on shorted/notch loaded MPA. Two different configurations were presented here and both the structures are almost alike to each other and resonating in L/S-Bands. It was observed that when we place two patch antennas side-by-side, affecting the working of both the antenna depends upon internal patch width as well as the width of the notch. The overall antennas were designed with less cross-interference & reduced coupling. The designed antenna configurations represent excellent corroboration among simulated & measured data for S-band. Both the MPA represented here are adjacent to each other placed on the same surface.

Finally, an array was designed with the aperture sharing to study the multifunctionality of the system, by using the unallocated space for the design of another antenna. A prototype of an array was successfully fabricated and represented. This prototype array achieves satisfactory measured results which are in agreement with simulated data along with better isolation. The antenna represented here has a smaller aperture when compared with independent antennas and exhibits robust characteristics comparatively. The proposed antenna is having large return loss and enhancement in bandwidth was also observed when compared with previous work. Due to the frequency of operation in L and S-Band, the designed antenna can be used for high-performance wideband communications as well as for wireless communications. Various configuration represented here can be further extended with more than three bands while using aperture sharing.

This thesis has investigated some of the interesting application & design of shared aperture based structure for dual-band applications (i.e. L/S-band) operation with some future scope for a lot of research left in this field. The future scope of the design of aperture is sharing based antennas for L/S-band with reduced dimensions & multiple arrays. The overall dimension parameters can be reduced either using Defected Ground (DGS) Structures or by doing some comprise in dielectric materials as well as port location. Further, the concept can also be used further for triple/multi-band operation while same surface/aperture for multiple antennas. However, due to placement of the resonating elements adjacent to each other, the coupling among resonating elements is affecting the performance of the individual antenna, which can be reduced by using the parasitic elements with appropriate dimensions enclosed to the resonating elements, thus resulting in bandwidth enhancement too.

## **REFERENCES**



## REFERENCES

---

### REFERENCES (CHAPTER 1)

- [1] IEEE Transactions on Antennas and Propagation, vols. AP-17, No. 3, May 1969; AP-22, No. 1, January 1974; and AP-31, No. 6, Part II, November 1983.
- [2] Balanis, C. A. (1997). *Antenna Theory, Analysis & Design*, 3rd Edition, John Wiley and Sons Inc. New York, USA
- [3] Stutzman, W. L., & Thiele, G. A. (1998). *Antenna Theory and Design*, Wiley: New York.
- [4] Deschamps, G. A., “*Microstrip Microwave Antennas*”, Proc. 3rd USAF Symposium on Antennas, 1953.
- [5] Munson, R. E., “*Conformal Microstrip Antennas and Microstrip Phased Arrays*”, IEEE Trans. Antennas Propagation, Vol. 22, pp. 74–78, 1974.
- [6] Kumar, G., & Ray, K.P. (2003). *Broadband Microstrip Antennas*, Artech House, Inc.
- [7] Garg, R., Prakash, B., Inder B., & Apisak I. (2001). *Microstrip Antenna Design Handbook*, ArtechHouse, Inc. ISBN: 0-89006-513-6, Boston.
- [8] Rodney, B. W. (Ed.). (2003). *Microstrip Patch Antennas, A Designer’s Guide*. Kluwer Academic Publishers.
- [9] Axness, T.A., Coffman, R.V., Kopp, B.A., and O’Hawer, K.W., “*Shared Aperture Technology Development*”, Johns Hopkins APL Technical Digest, vol. 17, No. 3 (1996), pp: 285-294.
- [10] Pokuls, R., Uher, J., Pozar. D.M., “*Dual-Frequency and Dual-Polarization Microstrip Antennas for SAR Applications*”, IEEE Transactions on Antennas and Propagation, vol. 46, no. 9, pp: 1289-1296, Sep, 1998.
- [11] Lager, I.E., Coman, C.I., and Ligthart, L.P., “*The Shared Aperture, Sparse Array Antenna Approach to Designing Broadband Array Antennas*”, MSMW’04 Symposium proceedings. Kharkov, Ukraine, vol.1, pp: 91-96. June, 2004.
- [12] Yang, S., and Fathy, A.E., “*Cavity Backed Patch Shared Aperture Antenna Array Approach for Mobile DBS Applications*”, Antennas and Propagation Society international symposium, IEEE. pp: 3959-3962, July, 2006.
- [13] Coman, C.I., Lager, I.E., and Ligthart, L.P., “*Shared Aperture Sparse array antenna for wide band applications*,” 33rd European Microwave Conference, 2003, vol. 2, pp: 515-518.

- 
- [14] Vetharatnam, G., Kuan, C.B., and Teik, C.H., “*Combined Feed Network for a Shared-Aperture Dual-Band Dual-Polarized Array*”, IEEE Antennas and Wireless Propagation Letters, vol. 4, pp: 297-299, Sep., 2005.
- [15] Pozar, D.M., and Targonski, S.D., “*A Shared-Aperture Dual-Band Dual-Polarized Microstrip Array*”, IEEE Transactions on Antennas and Propagation, vol. 49, no. 2, pp:150-157, 2001.
- [16] Vallecchi, A., Biffi, G., Genrili, and Calamia, M., “*Dual-Band Dual Polarization Microstrip Antenna*”, IEEE Antennas and Propagation Society International Symposium, , pp 134-137, DOI: 10.1109/APS.2003.1220139, 2003.
- [17] Vetharatnam, G., Kuan, C.B., and Teik, C.H., “*Combined Feed Network for a Shared-Aperture Dual-Band Dual-Polarized Array*”, IEEE Antennas and Wireless Propagation Letters, vol. 4, pp: 297-299, DOI: 10.1109/LAWP.2005.855636, 2005.
- [18] Zhuo, S.-G., and Chio, T.-H., “*Dual-wideband and Dual-polarized Shared Aperture Antenna*”, Proceedings of ISAP, pp: 798-801, 2012.
- [19] Sharma, D.K., Kulshrestha, S., Chakrabarty, S.B., and Jyoti, R., “*Shared Aperture Dual Band Dual Polarization Microstrip Patch Antenna*”, Microwave and Optical Technology Letters, vol. 55, pp: 917-922, DOI: doi/10.1002/mop.27414, 2013.
- [20] Sun, Z., Esselle, K.P., Zhong, S.-S., and Guo, Y.J., “*Shared-Aperture Dual-Band Dual-Polarization Array Using Sandwiched Stacked Patch*”, Progress In Electromagnetics Research C, vol 52, pp: 183-195, DOI: 10.2528/PIERC14052106, 2014.
- [21] Vetharatnam, G., and Koo, V.C., “*Compact L- & C-Band SAR Antenna*”, Progress In Electromagnetics Research Letters, vol. 8, 105-114, DOI: 10.2528/PIERL09031805, 2009.
- [22] Zhong, S.-S., Sun, Z., Kong, L.-B., Gao, C., Wang, W., and Jin, M.-P., “*Tri-Band Dual-Polarization Shared-Aperture Microstrip Array for SAR Applications*”, IEEE Transactions on Antennas and Propagation, vol. 60, no. 9, pp: 4157-4165, DOI: 10.1109/TAP.2012.2207034, 2012.
- [23] Zhong, S.-S., and Sun, Z., “*Shared-Aperture Multi-Band Dual-Polarized SAR Microstrip Array Design*”, Advancement in Microstrip Antennas with Recent Applications, ISBN 978-953-51-1019-4, DOI: <http://dx.doi.org/10.5772/54666>, 2013.

## REFERENCES

---

- [24] Coman, C.I., Lager, I.E., Ligthart, L.P., “*Shared Aperture Sparse Array Antenna for Wide Band Applications*”, 33rd European Microwave Conference, pp: 515-518, DOI: 10.1109/EUMC.2003.177530, 2003.
- [25] Lager, I.E., Coman, C.I., and Ligthart, L.P., “*The Shared Aperture, Sparse Array Antenna Approach to Designing Broadband Array Antennas*”, MSMW’04 Symposium Proceedings, Kharkov, Ukraine, pp: 91-96, DOI: 10.1109/MSMW.2004.1345794, 2004.
- [26] Yang, S., and Fathy, A.E., “*Cavity-Backed Patch Shared Aperture Antenna Array Approach for Mobile DBS Applications*”, IEEE Antennas and Propagation Society International Symposium, DOI: 10.1109/APS.2006.1711492, 2006.
- [27] Coman, C.I., Lager, I.E., and Ligthart, L.P., “*The Design of Shared Aperture Antennas Consisting of Differently Sized Elements*”, IEEE Transactions on Antennas and Propagations, vol. 54, no. 2, pp: 376-383, DOI: 10.1109/TAP.2005.863382, 2006.
- [28] Chakrabarti, S., “*Development of Shared Aperture Dual Polarized Microstrip Antenna at L-Band*”, IEEE Transaction on Antennas and Propagations, vol. 59, no. 1, pp: 294-297, DOI: 10.1109/TAP.2010.2091249, 2011.
- [29] Gusain, H.S., Raghavan, S., Rao, P.H., “*Shared Aperture Printed Slot Antenna*”, Third International Conference on Computing Communication & Networking Technologies (ICCCNT), DOI: 10.1109/ICCCNT.2012.6395993, 2012.
- [30] Smolders, A.B., Mestrom, R.M.C., Reniers, A.C.F., Geurts, M., “*A Shared Aperture Dual-Frequency Circularly Polarized Microstrip Array Antenna*”, IEEE Antenna and wireless Propagation Letters, vol. 12, pp: 120-123, DOI: 10.1109/LAWP.2013.2242427, 2013.
- [31] Naishadha, K., Li, R.L., Yang, L., Wu, T., Hunsicker, W., and Tentzeris, M., “*A Shared-Aperture Dual –Band Planar Array with Self-Similar Printed Folded Dipoles*”, IEEE Transactions on Antennas and Propagation, vo. 61, no.2, pp: 606-613, DOI: 0.1109/TAP.2012.2216491, 2013.
- [32] Tian, Z., Ouyang, J., and Long, Y., “*A Shared Aperture Millimeter Wave Antenna Using 3D Siw Technology*”, PIERS Proceedings Guangzhou, China, pp: 1812-1816, 2014.
- [33] Chang, L., Yufeng, Wang, Chen, L., Zhang, J., “*Wideband Shared Aperture Antenna Arrays for Mobile Communication System*”, IEEE 16th International Conference on Commnication Technology (ICCT), DOI: 10.1109/ICCT.2015.7399794, 2015.

- [34] M. Meng, et., al., “*Design of a shared-aperture dual-band dual-polarized microstrip antenna*”, 3rd IEEE International symposium on Microwave, Antenna, Propagation and EMC technologies for Wireless Communications, 2009, DOI: 10.1109/MAPE.2009.5355657.
- [35] A.R. Dastkhosh and H.R.D.Oskouei, “*A wideband high-gain dual-polarized slot array patch antenna for WiMax applications in 5.8GHz*”, *International Journal of Antennas and Propagation*, vol. 2012, pp:1-6, doi:10.1155/2012/595290.
- [36] K. Naishadham, R. Lin Li, Li Yang, T. Wu, W. Hunsicker, and M. Tentzeris, “*A Shared-Aperture Dual-Band Planar Array With Self-Similar Printed Folded Dipoles*,” *IEEE Transactions on Antennas and Propagation*, vol. 61, no. 2, February 2013 DOI: 10.1109/TAP.2012.221649.
- [37] S.-G. Zhou, P.-K. Tan, T.H. Chio, “*Wideband, low profile P- and Ku band shared aperture antenna with high isolation and low cross-polarisation*”, *IET Microwaves, Antennas & Propagation*, vol. 7, issue. 4, pp:223-229, 2013, doi: 10.1049/iet-map.2012.0550.
- [38] M. Du, and S. Shuai, “*Shared-aperture antenna and base station*”, US Patent publication No. US10003132B2, 2016.
- [39] P.H. Rao, S. Sujitha, K.T. Selvan., “*A multiband, Multipolarization shared-aperture antenna: Design and evaluation*”, *IEEE Antennas and Propagation Magazine*, vol. 59, issue. 4, pp:26-37, 2017, DOI: 10.1109/MAP.2017.2706654.
- [40] V.K. Kothapudi and V. Kumar, “*A Single Layer S/X-Band series-fed shared aperture antenna for SAR applications*”, *Progress in Electromagnetics Research C*, vol. 76, pp: 207-219, 2017, doi: 10.2528/PIERC17070104.

**REFERENCES (CHAPTER 2)**

- [1] Mandal, D., Kar, R.S., and Bhattacharjee, A.K., “*Input Impedance of Rectangular Microstrip Antennas on Non-Radiating Edges for Different feed sizes*”, Progress In Electromagnetics Research C, vol. 1, pp 191-198, doi:10.2528/PIERC08020104, 2008.
- [2] Ali, I., and Chang, R.Y., “*Design of Dual-Band Microstrip Patch Antenna with Defected Ground Plane for Modern Wireless Application*”, IEEE 82<sup>nd</sup> Vehicular Technology Conference, doi:10.1109/VTCFall.2015.7390887, 2015.
- [3] Ansari, J.A., Yadav, N.P., Mishra, A., Singh, P., Vishvakarma, B.R., “*Analysis of Multilayer Rectangular Patch Antenna for Broadband Operation*”, Wireless Personal Communication, pp: 315-327, DOI: 10.1007/s11277-010-0055-z, 2012.
- [4] Yilmaz, A.E., and Kuzuoglu, M., “*Calculation of Optimized Parameters of Rectangular Microstrip Patch Antenna using Particle Swarm Optimization*”, Microwave and Optical Technology Letters, vol. 49, No. 12, pp: 2905-2907, <https://doi.org/10.1002/mop.22918>, 2007.
- [5] Ansari, J.A., Mishra, A., Yadav, N.P., and Singh, P., “*Dualband Slot Loaded Circular Disk Patch Antenna for WLAN Application*”, International Journal of Microwave and Optical Technology, pp: 124-129, 2010.
- [6] Ansari, J.A., Singh, P., and Dubey, S.K., “*H-Shaped Stacked Patch Antenna for Dual Band Operation*”, Progress In Electromagnetics Research B, Vol.5, pp: 291-302, doi: 10.2528/PIERB08031203, 2008.
- [7] Smolders, A.B., Mestrom, R. M. C., Reniers, A. C. F., and Geurts, M., “*A Shared Aperture Dual-Frequency Circularly Polarized Microstrip Array Antenna*”, IEEE Antennas and Wireless Propagation Letters, vol. 12, DOI: 10.1109/LAWP.2013.2242427, 2013.
- [8] Pozar, D.M., and Targonski, S. D., “*A Shared-Aperture Dual-Band Dual-Polarized Microstrip Array*”, IEEE Transactions on Antennas and Propagation, vol. 49, no. 2, February 2001.
- [9] Zhong, S.-S., and Sun, Z., “*Shared-Aperture Multi-Band Dual-Polarized SAR Microstrip Array Design*”, <http://dx.doi.org/10.5772/54666> InTech publication, March 2013.
- [10] Naishadham, K., Li, R.L., Yang, L., Wu, T., Hunsicker, W., and Tentzeris, M., “*A Shared-Aperture Dual-Band Planar Array with Self-Similar Printed Folded Dipoles*”,

- IEEE Transactions on Antennas and Propagation, vol. 61, no. 2, DOI: 10.1109/TAP.2012.221649, February 2013.
- [11] Coman, C.I., Lager, I. E., and Ligthart, L. P., “*The Design of Shared Aperture Antennas Consisting of Differently Sized Elements*”, IEEE Transactions on Antennas and Propagation, vol. 54, no. 2, DOI: 10.1109/TAP.2005.863382, February 2006.
- [12] Vetharatnam, G., Kuan, C. B., and Teik, C. H., “*Combined feed network for a shared aperture dual-band dual-polarized array*”, IEEE Antennas and Wireless Propagation Letters, vol. 4, pp. 297-299, DOI: 10.1109/LAWP.2005.855636, July 2005
- [13] Pozar, D. M., and Targonski, S. D., “*A shared-aperture dual-band dual-polarized microstrip array*”, IEEE Transactions on Antennas and Propagation, vol. 49, no. 2, pp. 150-157, DOI: 10.1109/8.914255, February 2001.
- [14] Soodmand, S., “*A novel circular shaped dual-band dual-polarized patch antenna and Introducing a new approach for designing combined feed networks*”, Loughborough Antennas & Propagation Conference, Loughborough, UK, pp. 401-404, November 2009.
- [15] Vallecchi, A., Gentili, G. B., and Calamia, M., “*Dual-band dual polarization microstrip antenna*”, IEEE Antennas and Propagation Society International Symposium, Columbus, OH, USA vol. 4, pp. 134-137, June 2003.
- [16] Abdelaziz, A.A., “*Bandwidth Enhancement of Microstrip Antenna*”, Progress In Electromagnetics Research, PIER 63, pp: 311-317, doi: 10.2528/PIER06053001, 2006.
- [17] Au, T.M., and Luk, K.M., “*Effect of parasitic element on the characteristics of Microstrip Antenna*,” IEEE Transaction on Antennas and Propagation, vol. 39 (8), 1247-1251, DOI: 10.1109/8.97366, 1991.
- [18] Sabapathy, T., Jamlos, M.F., Jusoh, M., Jais. M.I., Kamarudin, M.R., “*Gain Enhancement of Circular Patch Antenna using Parasitic Ring*”, IEEE Antennas and Propagation Society International Symposium (APSURSI), pp: 1836-1837, DOI: 10.1109/APS.2013.6711577, 2013.
- [19] Li, L., Zhang, Y., Wang, J., Zhao, W., Liu, S., and Xu, R., “*Bandwidth and gain Enhancement of Patch Antenna with Stacked Parasitic Strips Based on LTCC Technology*”, Hindawi Publishing Corporation, International Journal of Antennas and Propagation, vol 2014 (461423), <http://dx.doi.org/10.1155/2014/461423>, pp: 1-5.
- [20] Raout, R., Talandage, K., “*Bandwidth and Gain Enhancement of Rectangular MSA by using Parasitic Patch and Capacitive Feeding Technique for Wideband Application*”,

## REFERENCES

---

- International Conference on Microwave, Optical and Communication Engineering, IIT Bhubaneswar, India, Dec-2015, pp:393-396.
- [21] Mekki, A.S., Hamidon, M.N., Ismail, A., and Alhawari, A.R.H., “*Gain Enhancement of a Microstrip Patch Antenna Using a Reflecting Layer*”, Hindawi Publishing Corporation, International Journal of Antennas and Propagation, vol. 2015 (975263), DOI: <http://dx.doi.org/10.1155/2015/975263>, pp: 1-7.
- [22] Kumar, A., Gupta, N., and Gautam, P.C., “*Gain and Bandwidth Enhancement Techniques in Microstrip Patch Antennas-A Review*”, International Journal of Computer Applications, vol 148 (7), 2016, pp: 9-14.
- [23] Santiko, A.B., Paramayudha, K., Wahyu, Y., Sumartono, Wijanto, H., “*Design and Realization Multi Layer Parasitic for Gain Enhancement of Microstrip Patch Antenna*”, International Seminar on Intelligent Technology and Its Application, pp: 299-303.
- [24] Peng, L., Mao, J.-Y., Li, X.-F., Jiang, X., and Ruan, C.-L., “*Bandwidth Enhancement of Microstrip Antenna Loaded by Parasitic Zeroth-Order Resonators*”, Microwave and Optical Technology Letters, vol. 59, No. 5, DOI: 10.1002/mop, pp: 1096-1100, 2017.
- [25] Xu, H., Zhou, J., Yu, Z., Zhuang, J., “*Low-Profile Broadband circularly polarized patch antenna with gain enhancement*”, IET Microwave, Antennas & Propagation, col 11(12), pp: 1817-1822, doi: 10.1049/iet-map.2017.0143, 2017.
- [26] Reddy, M.H., Joany, R.M., Reddy, M.J., Sugadev, M., and Logashanmugam, E., “*Bandwidth Enhancement of Microstrip Patch Antenna using Parasitic Patch*”, IEEE International Conference on Smart Technologies and Management for Computing, Communication, Controls, Energy and Materials (ICSTM), pp: 295-298, August 2017.
- [27] Firmansyah, T., Herudin, Suhendar, Wiryadinata, R., Santoso, M.I., Denny, Y.R., Supriyanto, T., “*Bandwidth and Gain Enhancement of MIMO Antenna by Using Ring and Circular Parasitic with Air-Gap Microstrip Structure*”, TELKOMNIKA, vol. 15 (3), DOI: 10.12928/TELKOMNIKA.v15i3.6377, pp: 1155-1163, 2017.
- [28] Toktas, A., Yerlikaya, M., Sabanci, K., Kayabasi, A., Yigit, E., and Tekbas, M., “*Reducing Mutual Coupling for a Square UWB MIMO Antenna using Various Parasitic Structures*”, International Conference on Electrical and Electronics Engineering (ELECO), 2017.
- [29] Malviya, L., Panigrahi, R.K., and Kartikeyan, M.V., “*MIMO antennas with diversity and mutual coupling reduction techniques: a review*”, International Journal of Microwave and Wireless Technologies, doi: 10.1017/S1759078717000538, pp: 1-18, 2017.

- [30] Luo, C., Hong, J., Amin, M., “*Mutual Coupling Reduction for Dual-Band MIMO Antenna with Simple Structure*”, *Radio Engineering*, vol. 26 (1), pp: 51-56, DOI: 10.13164/re.2017.0051, 2017.
- [31] Panda, R.A., Sahana, R., Panda, E.P., Behra, S., “*Mutual Coupling Reduction of Circular Patch Antenna for Multiband Application*”, *International Research Journal of Engineering and Technology (IRJET)*, vol. 05 (01), pp: 1325-1328, 2018.

**REFERENCES (CHAPTER 3)**

- [1] Rafique, U., Khalil, H., and Rehman, S., “*Dual-Band microstrip patch antenna array for 5G mobile communications*”, Progress In Electromagnetics Research Symposium-Fall, Singapore, pp. 55-59. DOI: [10.1109/PIERS-FALL.2017.8293110](https://doi.org/10.1109/PIERS-FALL.2017.8293110), 2017.
- [2] Singh, P., “*Rectangular notch loaded dual band annular ring patch antenna*”, Journal of Microwave, Optoelectronics and Electromagnetic Application, vol. 13, no. 8, p. 85-96. DOI: <http://dx.doi.org/10.1590/S2179-10742014000100007>, 2014.
- [3] Vetharatnam, G., Kuan, B.C., and Teik, H.C., “*Combined feed network or a shared-aperture dual-band dual-polarized Array*”, IEEE Antennas and Wireless Propagations Letters, vol. 4, p. 297-299. DOI: [10.1109/LAWP.2005.855636](https://doi.org/10.1109/LAWP.2005.855636), 2005.
- [4] Sun Z., Esselle, K.P., Zhong, S.-S., and Guo, Y. J., “*Shared-aperture dual-band dual-polarization array using sandwiched stacked patch*”, Progress In Electromagnetics Research, C vol. 52, p. 183-195. DOI: [10.2528/PIERC14052106](https://doi.org/10.2528/PIERC14052106), 2014.
- [5] Zhuo, S.G., and Chio, T.H., “*Dual-wideband, dual-polarized shared aperture antenna with high isolation and low cross-polarization*”, The 10th International Symposium on Antennas, Propagation, and EM Theory, 2012, p. 30-33. DOI: [10.1109/ISAPE.2012.6408694](https://doi.org/10.1109/ISAPE.2012.6408694)
- [6] Sharma, D.K., Kulshrestha, S., Chakrabarty, S.B., Jyoti, R., “*Shared aperture dual-band dual polarization microstrip patch antenna*”, Microwave and Optical Technology Letters, vol. 55 (4), p. 917-922. DOI: <https://doi.org/10.1002/mop.27414>, 2013.
- [7] Vetharatnam, G., and Koo, V.C., “*Compact L- & C-Band SAR Antenna*”, Progress In Electromagnetics Research Letters, vol. 8, p. 105-114. DOI: [10.2528/PIERL09031805](https://doi.org/10.2528/PIERL09031805), 2009.
- [8] Pandey, V.K., and Vishvakarma, B. R., “*Analysis of an E-shaped Patch Antenna*”, Microwave and Optical Technology Letters, vol.49, no.1, <https://doi.org/10.1002/mop.22024>, 2007.
- [9] Ansari, J.A., Dubey, S. K., and Mishra, A., “*Analysis of Half E-Shaped patch for wideband application*”, Microwave and optical technology letters, vol. 51, no.6, <https://doi.org/10.1002/mop.24367>, 2009.
- [10] Ansari, J.A., Singh, P., and Dubey, S.K., Khan, R.U., and Vishvakarma, B. R., “*H-Shaped Stacked Patch Antenna for Dual Band Operation*”, Progress In Electromagnetics Research B, vol.5, pp: 291-302, doi: [10.2528/PIERB08031203](https://doi.org/10.2528/PIERB08031203), 2008.

- [11] Lau, K.L., Kong, K.C., and Luk, K.M., “*Dual-band stacked folded shorted patch antenna*”, *Electronics Letters*, vol. 43, issue 15, pp: 789-790, DOI: 10.1049/el:20070878, 2008.

**REFERENCES (CHAPTER 4)**

- [1] Jordan, R.L., Huneycutt, B. L., and Werner, M., “*The SIR-C/X-SAR synthetic aperture radar system*”, IEEE Trans. Geosci. Remote Sensor, vol. 33, no. 4, pp. 829–839, 1995.
- [2] Stuhr, F., Jordan, R. L., and Werner, M., “*SIR-C/X-SAR: An advanced radar*”, presented at the IEEE Aerospace Applications Conf., Aspen, CO, DOI: 10.1109/AERO.1996.495910, 1996.
- [3] Pozar, D.M., and Targonski, S. D., “*A shared-aperture dual-band dual polarized microstrip array*”, IEEE Trans. Antennas Propagation, vol. 49, no. 2, pp. 150–157, DOI: 10.1109/8.914255, 2001.
- [4] Vetharatnam, G., Kuan, C. B., and Teik, C. H., “*Combined feed network for a shared-aperture dual-band dual-polarized array*”, IEEE Antennas Wireless Propagation Letters, vol. 4, pp. 297–299, DOI: 10.1109/LAWP.2005.855636, 2005.
- [5] Mangenot, C., and Lorenzo, J., “*Dual band dual polarized radiating subarray for synthetic aperture radar*”, IEEE Antennas and Propagation Society International Symposium, vol. 3, pp. 1640–1643, 1999.
- [6] Hsu, S.H., Ren, Y. J., and Chang, K., “*A dual-polarized planar-array antenna for S-band and X-band airborne applications*”, IEEE Antennas and Propagation Magazine, vol. 51, no. 4, pp. 70–78, DOI: 10.1109/MAP.2009.5338685, 2009.
- [7] Pozar, D.M., Schaubert, D. H., Targonski, S. D., and Zawadski, M., “*A dual-band dual-polarized array for spaceborne SAR*”, IEEE Antennas and Propagation Society International Symposium, vol. 4, pp. 2112–2115, DOI: 10.1109/APS.1998.701626, 1998.
- [8] Qu, X., Zhong, S. S., Zhang, Y. M., and Wang, W., “*Design of an S/X dual-band dual-polarised microstrip antenna array for SAR applications*”, IET Microwave Antennas Propagation, vol. 1, no. 2, pp. 513–517, DOI: 10.1049/iet-map:20060232, 2007.
- [9] Gao, G. M., Zhang, Y., Li, A., Zhao, J., and Cheng, H., “*Shared aperture Ku/Ka bands microstrip array feeds for parabolic cylindrical reflector*”, International Conference on Microwave and Millimeter Wave Technology (ICMMT), pp. 1028–1030, DOI: 10.1109/ICMMT.2010.5524822, 2010.
- [10] He, S.H., and Xie, J. D., “*Analysis and design of a novel dual-band array antenna with a low profile for 2400/5800-MHz WLAN systems*”, IEEE Transaction on Antennas Propagation, vol. 58, no. 2, pp. 391–396, 10.1109/TAP.2009.203769, 2010.

- [11] Yue, Y., Zhou, J., “*A Wideband Dual-Polarized Antenna Array for Multifunction Radar*”, IEEE 5th Asia-Pacific Conference on Antennas and Propagation (APCAP), DOI: 10.1109/APCAP.2016.7843259, 2016.
- [12] R. Pokuls, J. Uher, and D. M. Pozar, “*Dual-frequency and dual-polarization microstrip antennas for SAR applications*”, IEEE Trans. Antennas Propag., vol. 46, no. 9, pp. 1289–1296, Sep. 1998.
- [13] X.Qu, S. S. Zhong, Y. M. Zhang, and W.Wang, “*Design of an S/X dualband dual-polarised microstrip antenna array for SAR applications*”, IET Microw. Antennas Propagation, vol. 1, no. 2, pp. 513–517, April 2007.
- [14] N. Llombart, A. Neto, G. Gerini, and P. de Maagt, “*Planar circularly symmetric EBG structures for reducing surface waves in printed antennas*”, IEEE Trans. Antennas Propag., vol. 53, pp. 3210–3218, Oct. 2005.

## LIST OF PUBLICATIONS

### Published:

1. Dhiman. J., Khah, S.K., "Parasitic coupled microstrip antenna using shared aperture technique" *Micro & Nano Letters*, vol. 14, issue 8, pp. 845-847, July 2019, doi: 10.1049/mnl.2018.5768 (SCI/Scopus Indexed).
2. Dhiman. J., Sharma, A., Khah, S.K., "Shared aperture microstrip patch antenna array for L and S-band" *Progress In Electromagnetics Research Letters*, vol. 86, pp. 91-95, 2019, doi:10.2528/PIERL19052905 (ESCI/Scopus Indexed)
3. Dhiman. J., Khah, S.K., "Y-Shaped Microstrip Patch Antennas for L and S Band Using Shared Aperture" published in *Wireless Personal Communications*, 111, 1–8 (2020 doi: 10.1007/s11277-019-06841-w (SCIE/Scopus Indexed)
4. Dhiman, J., Khah, S.K., "Multifunctional shared aperture antenna for L and S band" *Advanced Computational Techniques in Electromagnetics Journal*, vol. 2016, no. 1, pp:1-6, 2016, doi: 10.5899/2016/acte-00204

### Under Review:

1. Dhiman, J., Khah, S.K., "Notch loaded microstrip patch antenna for dual-band (L and S) operation using shared aperture" under review in *Micro & Nano Letters* (SCI/Scopus Indexed)
2. Dhiman, J., Khah, S.K., "A non-conventional patch based shared aperture antenna with parasitic element for L/S band" under review in *Radioengineering*



### **LIST OF CONFERENCE/WORKSHOP/SEMINAR ATTENDED**

1. National Seminar on “Innovations & Challenges in Basic & Applied Sciences (ICBAS-2017)”, held at Maharaja Agrasen University, Atal Shiksha Kunj, Baddi, Solan (HP), India (4th March 2017)
2. “3rd National Conference on Multifunctional Advanced Materials (MAM-2016)” held at Himalayan centre of Excellence in Nanotechnology, Shoolini University (HP), India (11-13 May, 2016), in Association with DRDO, DAE and ISRS.
3. “4th INUP Familiarization Workshop on Nanofabrication Technologies”, held at IIT, Bombay, India (16-18 December 2015)
4. “One Day Workshop on Technical Manuscript Preparation with Latex”, held at Jaypee University of Information Technology, Wagnaghat, Solan (HP), India (29th November 2015)

